

NATIONAL RESEARCH COUNCIL

ADVISORY COMMITTEE
ON TECHNICAL RECOMMENDATIONS FOR CONSTRUCTION

**Guide for the Design and Construction
of Externally Bonded Fibre Reinforced
Inorganic Matrix Systems
for Strengthening Existing Structures**



CNR-DT 215/2018

**Copyright owned
by
The National Research Council**

**No part of this publication may be stored in a retrieval system, or
transmitted in any form or by any means
– electronic, mechanical, recording, or otherwise –
without the prior written permission
of the Italian National Research Council.
The reproduction of this document is permitted
for personal, non-commercial use.**

CONTENTS

1 INTRODUCTION.....	1
1.1 INTRODUCTION TO THE CNR-DT 215/2018 DOCUMENT	1
1.2 PURPOSE OF THE GUIDELINE	3
1.3 SYMBOLS.....	4
2 FRCM MATERIALS FOR STRUCTURAL STRENGTHENING	8
2.1 INTRODUCTION	8
2.2 REVIEW OF SIGNIFICANT APPLICATIONS	9
2.2.1 Applications on masonry structures	9
2.2.1.1 Strengthening of masonry panels.....	9
2.2.1.2 Strengthening of vaults and arches	9
2.2.1.3 Floor and roof ring beams	11
2.2.1.4 Confinement of masonry columns	13
2.2.2 Applications on reinforced concrete structures.....	13
2.2.2.1 Flexural strengthening of beams, columns and floor joists	13
2.2.2.2 Shear strengthening of beams and columns.....	14
2.2.2.3 Confinement of columns.....	15
2.2.2.4 Strengthening of beam-column joints.....	16
2.2.2.5 Shear strengthening of reinforced concrete walls	17
2.2.2.6 Slab strengthening (anti-detachment)	17
2.2.2.7 Infill walls strengthened against overturning.....	18
2.2.2.8 Bridge strengthening.....	19
2.3 MECHANICAL PROPERTIES OF THE STRENGTHENING SYSTEM.....	20
3 BASIC CONCEPTS FOR THE DESIGN OF STRENGTHENING INTERVENTIONS AND SPECIAL DESIGN PROBLEMS.....	22
3.1 MECHANICAL PROPERTIES OF THE STRENGTHENING SYSTEM IN DESIGN AND VERIFICATION PROBLEMS	22
3.2 DESIGN VALUES	23
3.2.1 Verification in the case of fire.....	24
4 STRENGTHENING OF MASONRY STRUCTURES	25
4.1 IN-PLANE STRENGTHENING OF WALLS.....	25
4.1.1 Shear Capacity	25
4.1.2 Combined axial and bending moment capacity	27
4.2 STRENGTHENING OF MASONRY PANELS FOR OUT-OF-PLANE LOADS.....	28
4.3 CROWNING BEAMS IN FRCM-REINFORCED MASONRY.....	29
4.4 CONFINEMENT OF MASONRY COLUMNS UNDER AXIAL COMPRESSION.....	30
4.4.1 Confinement of circular columns.....	31
4.4.2 Confinement of rectangular columns	32
4.5 SIMPLE- AND DOUBLE-CURVATURE STRUCTURES.....	33
4.5.1 Single curvature structures	34
4.5.1.1 Reinforcement identification and assessment through the kinematic approach	34
4.5.1.2 Reinforcement identification and assessment through the static approach.....	35
4.5.2 Barrel vaults	36
4.5.3 Double curvature structures	36
5 STRENGTHENING OF REINFORCED CONCRETE STRUCTURES.....	37
5.1 FLEXURAL STRENGTHENING	37

5.1.1	Ultimate limit state (ULS).....	37
5.1.2	Serviceability limit state (SLS).....	37
5.2	SHEAR STRENGTHENING	38
5.2.1	Effective design strength.....	39
5.3	CONFINEMENT OF REINFORCED CONCRETE COLUMNS SUBJECTED TO CENTRED COMPRESSION	40
5.3.1	Confinement of prismatic cross-section columns	40
6	DETAILING.....	41
7	MAINTENANCE AND REPAIR	43
8	CONTROL.....	44
8.1	CONSTRUCTION CHECKS ON SITE.....	44
8.2	QUALITY CONTROL OF THE STRENGTHENING SYSTEM.....	44
8.2.1	Semi-destructive tests.....	44
8.2.2	Non-destructive tests	45
9	EXPERIMENTAL TESTS ON STRUCTURAL ELEMENTS.....	47
10	REFERENCES	49
11	NUMERICAL EXAMPLES.....	56
11.1	IN-PLANE STRENGTHENING OF MASONRY WALLS.....	56
11.1.1	Shear capacity	56
11.1.2	In-plane combined axial and bending moment capacity.....	58
11.2	STRENGTHENING OF MASONRY PANELS FOR OUT-OF-PLANE LOADS	62
11.3	CONFINEMENT OF MASONRY COLUMNS	70
11.3.1	Example 1.....	70
11.3.2	Example 2.....	72
11.4	STRENGTHENING OF AN RC BEAM	73
11.4.1	Design of the flexural strengthening	73
11.4.2	Design of the shear strengthening	78
11.5	CONFINEMENT OF A REINFORCED CONCRETE COLUMN	79
12	APPENDIX 1: ON THE IN-PLANE AXIAL-MOMENT RESISTANCE CALCULATION.....	81
13	APPENDIX 2: ASSESSMENT OF SOLIDARITY BETWEEN REINFORCEMENT AND STRUCTURE IN THE CASE OF CURVED SUPPORT.....	85

1 INTRODUCTION

1.1 INTRODUCTION TO THE CNR-DT 215/2018 DOCUMENT

The FRCM (Fibre-Reinforced Cementitious Matrix/Mortar) composites are nowadays used in structural rehabilitation interventions, more and more frequently, instead of classic FRP fibre reinforced composites (Fibre Reinforced Polymer), made with long glass, carbon or aramid fibres immersed in polymeric matrices (such as epoxy resins). In international literature the first are also called TRC (Textile Reinforced Concrete), TRM (Textile Reinforced Mortars), FRM (Fabric Reinforced Mortar) or even IMG (Inorganic Matrix-Grid Composites). In the following, since the acronym FRCM has been adopted in already approved Italian ministerial documents, it is preferred to continue using the same acronym.

FRCM composites are the result of coupling nets, made with the same fibres mentioned above, or with others which have appeared more recently on the building materials market, with an inorganic matrix based on lime or cement mortar. Innovative fibres include basalt, PBO (Polyparaphenylene benzobisoxazole) and steel. In particular, this last material, very common in the construction field, is proposed again for use in FRCMs, in a version with highly enhanced mechanical performance, thanks to a particular processing process.

The inorganic matrix has numerous advantages over the organic FRP matrix, especially for applications to masonry structures, given its greater affinity with this type of substrate. At the moment some guidelines are available in the international field for the qualification of FRCMs and for the design of structural reinforcement interventions carried out with such materials. In this connection the US acceptance criteria (ACI 434 - *Acceptance Criteria for Masonry and Concrete Strengthening Using Fiber-Reinforced Cementitious Matrix (FRCM) Composite Systems*, issued by ICC Evaluation Service, 2018) and the design guidelines (RILEM TC 250-CSM & ACI 549 - *Guide to Design and Construction of Externally Bonded Fabric-Reinforced Cementitious Matrix (FRCM) and Steel Reinforced Grout (SRG) Systems for Repair and Strengthening Masonry Structures*, pending approval) can be mentioned.

In recent years, the scientific interest in the innovative applications of FRCMs for structural rehabilitation, on the one hand, and the special nature of the widely varied Italian building heritage on the other, have attracted the interest of numerous researchers operating in the fields of Structural Mechanics, Construction, Structural Rehabilitation and Seismic Engineering.

It is clear that the drafting of an Italian Guideline for the design and construction of strengthening interventions with FRCMs could no longer be postponed; above all, the drafting of a wide ranging document usable for the different types present in the national building heritage, from the masonry to the concrete constructions, as well as for the many FRCM products currently present on the national market that are different in nature of the matrix and the net reinforcement.

The CNR, through its *Advisory Committee on Technical Recommendations for Construction*, promptly felt this need and made efforts to satisfy it by setting up a Working Group in June 2016 with the task of drawing up a *Guideline for the design and construction of externally bonded fibre reinforced inorganic matrix systems for strengthening existing structures*.

In July 2017, the CNR Advisory Committee approved a first draft of this Technical Document on a proposal from the Working Group. Subsequently, the Working Group expanded to include all interested Italian researchers already scientifically committed to the topic, and benefited from the invaluable contribution of the FRCM manufacturers. It was thus possible to draw up the present version of the Technical Document, broader than the initial draft and characterized by more advanced applications and more sophisticated approaches which are at the frontier of current international research on the topic of structural reinforcement with FRCM.

The first draft, mentioned above, is the basis of the Guideline prepared and recently approved (January 2019) by the Italian Ministry of Infrastructure and Transport (MIT) for the identification of procedures for the qualification of FRCMs.

A valid contribution to the drafting of this Guideline was provided by the results of a round robin promoted by the RILEM TC 250-CSM between the laboratories of different European Universities.

This Technical Document has been prepared by a Working Group whose members are:

AIELLO Prof. Maria Antonietta	- Università del Salento
ASCIONE Prof. Luigi	- Università di Salerno
ASSOCOMPOSITI	- Politecnico di Milano
BARATTA Prof. Alessandro	- Università “Federico II”- Napoli
BILOTTA Ing. Antonio	- Università “Federico II”- Napoli
CAMATA Prof. Guido	- Università “G. d’Annunzio” - Chieti-Pescara
BORRI Prof. Antonio	- Università di Perugia
CARLONI Prof. Christian	- Università di Bologna
CAROZZI Arch. Francesca Giulia	- Politecnico di Milano
CASADEI Ing. Paolo	- Kerakoll S.p.A. - Sassuolo (MO)
CLAURE Prof. Guillermo	- Università di Miami, Coral Gables, Florida - USA
CERSOSIMO Ing. Giuseppe	- Interbau S.r.l.- Milano
COSENZA Prof. Edoardo	- Università “Federico II”- Napoli
CORBI Geol. Ileana	- Università “Federico II”- Napoli
CORBI Prof. Ottavia	- Università “Federico II”- Napoli
D’ANTINO Ing. Tommaso	- Politecnico di Milano
de FELICE Prof. Gianmarco	- Università Roma Tre - Roma
DE SANTIS Ing. Stefano	- Università Roma Tre - Roma
DI LUDOVICO Prof. Marco	- Università “Federico II”- Napoli
DI PRISCO Prof. Marco	- Politecnico di Milano
FERRACUTI Prof. Barbara	- Università “Niccolò Cusano” - Roma
FOCACCI Prof. Francesco	- Università eCampus
FRASSINE Prof. Roberto	- Politecnico di Milano
GIACOMIN Ing. Giorgio	- G&P Intech S.r.l. - Altavilla Vicentina (VI)
GREPPI Ing. Roberto	- T.C.S. S.r.l. - Montichiari (BS)
LA MENDOLA Prof. Lidia	- Università di Palermo
LIGNOLA Prof. Gian Piero	- Università “Federico II”- Napoli
MANTEGAZZA Dott. Giovanni	- Mahac S.r.l., Technical Manager &Co-Founder - Milano
MAZZOTTI Prof. Claudio	- Università di Bologna
MONTALBANO Ing. Antonino	- Sika Italia S.p.a. - Milano
MORANDINI Ing. Giulio	- Mapei S.p.a. - Milano
NANNI Prof. Antonio	- Università di Miami, Miami, Florida
NERILLI Ing. Francesca	- Università “Niccolò Cusano” – Roma
NICOLETTI Ing. Andrea	- BASF Construction Chemical Italia S.p.A., Treviso
NIGRO Prof. Emidio	- Università “Federico II”- Napoli
OCCHIUZZI Prof. Antonio	- CNR-ITC, San Giuliano Milanese
PECCE Prof. Maria Rosaria	- Università del Sannio - Benevento
PELLEGRINO Prof. Carlo	- Università di Padova
POGGI Prof. Carlo	- Politecnico di Milano
PROTA Prof. Andrea	- Università “Federico II”- Napoli
REALFONZO Prof. Roberto	- Università di Salerno
ROSATI Prof. Luciano	- Università “Federico II”- Napoli

SACCO Prof. Elio - Università “Federico II”- Napoli
SAVOIA Prof. Marco - Università di Bologna
ZAMPA Ing. Andrea - Fibre Net S.r.l. - Udine

Coordinator:
ASCIONE Prof. Luigi

Technical Secretariat:
LIGNOLA Prof. Gian Piero

This Technical Document has been approved by the *Advisory Committee on Technical Recommendation for Construction* as a draft version on 23/10/2018 and submitted for public hearing. At the conclusion of the public hearing, with the resulting modifications, it was approved in a definitive version on 06.02.2019 by the *Advisory Committee on Technical Recommendations for Construction*, composed as follows:

ANGOTTI Prof. Franco	- Università di Firenze
AURICCHIO Prof. Ferdinando	- Università di Pavia
ASCIONE Prof. Luigi	- Università di Salerno
BARATTA Prof. Alessandro	- Università “Federico II” – Napoli
COSENZA Prof. Edoardo	- Università “Federico II” – Napoli
DI PRISCO Prof. Marco	- Politecnico di Milano
LAGOMARSINO Prof. Sergio	- Università di Genova
MACERI Prof. Franco, Presidente	- Università “Tor Vergata” – Roma
MANCINI Prof. Giuseppe	- Politecnico di Torino
MAZZOLANI Prof. Federico Massimo	- Università “Federico II” – Napoli
OCCHIUZZI Prof. Antonio	- Consiglio Nazionale delle Ricerche, ITC
PINTO Prof. Paolo Emilio	- Università “La Sapienza” – Roma
POGGI Prof. Carlo	- Politecnico di Milano
PROTA Prof. Andrea	- Università “Federico II” – Napoli
ROYER CARFAGNI Prof. Gianni	- Università di Parma
SAVOIA Prof. Marco	- Università di Bologna
SCARPELLI Prof. Giuseppe	- Università Politecnica delle Marche
SOLARI Prof. Giovanni	- Università di Genova
URBANO Prof. Carlo	- Politecnico di Milano
ZANON Prof. Paolo	- Università di Trento

The same Committee has approved the English version on the 6th of February 2020.

1.2 PURPOSE OF THE GUIDELINE

The purpose of this guideline is to provide, within the framework of the Italian regulations, a document for the design and construction of externally bonded FRP systems for strengthening existing structures. A guideline, by definition is not a binding regulation, but merely represents an aid for practitioners interested in the field of the strengthening with FRCMs. Nevertheless, the responsibility remains with the user of this guide.

The following topics will be addressed:

- FRCM materials

- Review of significant applications
- Basic concepts of reinforcement with FRCCM and special problems
- Reinforcement of masonry structures
- Reinforcement of RC structures
- Construction details
- Maintenance and repair
- Control and monitoring
- Experimental tests on structural models
- Literature references
- Worked examples

The Guideline also contains the following Appendices:

- **Appendix 1**, Calculation of the ultimate resistant moment (combined axial and bending) in the plane
- **Appendix 2**, Assessment of solidarity between reinforcement and structure in the case of curved support

1.3 SYMBOLS

The meaning of the main symbols utilized in this Guideline are as follows.

General notations

- $(.)_c$ Value of quantity $(.)$ for concrete
- $(.)_{cc}$ Value of quantity $(.)$ for confined concrete
- $(.)_d$ Design value of quantity $(.)$
- $(.)_f$ Value of quantity $(.)$ referred to the fibre (or grid) itself
- $(.)_k$ Characteristic value of quantity $(.)$
- $(.)_m$ Value of quantity $(.)$ for masonry
- $(.)_{mat}$ Value of quantity $(.)$ referred to the matrix
- $(.)_{mc}$ Value of quantity $(.)$ for confined masonry
- $(.)_R$ Value of quantity $(.)$ as resistance
- $(.)_s$ Value of quantity $(.)$ for steel
- $(.)_S$ Value of quantity $(.)$ as stress

Uppercase Roman letters

- A_m Cross-sectional area of confined masonry column
- A_c Cross-sectional area of confined concrete column, without steel reinforcement
- A_s Area of steel reinforcement
- A_f Area of dry fibre
- E_f Young's modulus of elasticity of dry fibre
- E_1 Young's modulus of elasticity of uncracked FRCCM
- E_m Young's modulus of elasticity of masonry
- D Diameter of circular columns, or diagonal of rectangular/square cross sections
- H Length of masonry panel (height of cross section)

L_{max}	Maximum anchoring length
M_{Rd}	Design flexural capacity of strengthened member
M_{Sd}	Factored moment
M_{0d}	Design flexural capacity before strengthening
M_{1d}	Design flexural capacity after strengthening
$N_{Rcc,d}$	Design axial capacity of confined concrete member
$N_{Rmc,d}$	Design axial capacity of confined masonry member
N_{Sd}	Factored axial force
N_o	Axial force to assess simple- and double-curvature structures
N_m	Compressive force on masonry
N_f	Tensile force in strengthening system
FC	Confidence factor
F_m	Resultant of compressive force on masonry, calculated with <i>stress-block</i>
F_f	Resultant of tensile force transferred by reinforcement
$V_{t,R}$	In-plane shear capacity of strengthened masonry
V_{Rd}	Shear capacity of concrete member
$V_{Rd,c}$	Shear capacity limited by compressed concrete
$V_{Rd,f}$	FRCM contribution to the shear capacity
$V_{Rd,m}$	Out-of-plane shear capacity of strengthened masonry
$V_{Rd,s}$	Steel contribution to the shear capacity
$V_{t,f}$	FRCM contribution to the shear capacity $V_{t,R}$
V_t	Un-Reinforced masonry contribution to the shear capacity $V_{t,R}$
$V_{t,c}$	Diagonal crushing threshold of masonry
X_d	Design value of generic property
X_k	Characteristic value of generic property

Lowercase Roman letters

t	Thickness of masonry panel
t_{mat}	Thickness of FRCM matrix
t_f	Equivalent thickness of FRCM provided by manufacturer
t_{2f}	$= 2 \cdot t_f$ when reinforcement is applied on both sides of member
t_{vf}	Equivalent thickness of fibres parallel to shear force
n_f	Total number of FRCM layers
b, h	Dimensions of confined member cross section
b_f	Dimension of FRCM in the bending plane
b', h'	Dimensions of confined member cross section, minus rounding corners
d	Effective height of section
d_f	Distance between the extreme compressed masonry and the extreme FRCM under tension
f_{ccd}	Design strength of confined concrete
f_{cd}	Design concrete compressive strength
f_{fed}	Effective design strength of reinforcement
f_1	Confining lateral pressure

$f_{1,eff}$	Effective confining pressure
$f_{c,mat}$	Characteristic compressive strength of the matrix
f_{mcd}	Design compressive strength of FRCM-confined masonry
f_{md}	Design compressive strength of unconfined masonry
f_{vd}	Design shear strength of masonry
f_{yd}	Design yield strength of steel reinforcement
g_m	Masonry density in kg/m ³ (confinement)
h_w	Height of the beam web
k_H	Coefficient of efficiency in the horizontal direction (confinement)
k_{mat}	Dimensionless coefficient to account for inorganic matrix (confinement)
k'	Dimensionless coefficient for strength increment (confinement)
i	Spacing of connectors
l_{ed}	Effective anchoring length
l	Length of connectors
ℓ	Height of masonry panel
ℓ_f	Design dimension of FRCM for shear
y_n	Distance from extreme compression fibre to neutral axis
p_f	Spacing of reinforcements
$\bar{q}_{u,f}$	Stress limit for dry fibre to apply simplified method in Table 4.1
r_c	Corner rounding radius
r	Curvature radius for simple- and double-curvature structures

Lowercase Greek letters

γ_m	Partial factor for materials and products
γ_{rt}	Partial factor to assess simple- and double-curvature structures
γ_{Rd}	Partial factor for resistance models
$\varepsilon_{lim,conv}$	Conventional strain limit (end condition)
$\sigma_{lim,conv}$	Conventional stress limit (end condition)
α	Amplification coefficient for substrate debonding and/or fibre/matrix intermediate slip
α_1, α_2	Strength increment coefficient (confinement)
α_3, α_4	Strength increment coefficient (confinement)
α_t	Coefficient to account for reduced tensile strength of fibres when stressed in shear
$\varepsilon_{lim,conv}^{(\alpha)}$	Conventional strain limit (intermediate condition)
$\sigma_{lim,conv}^{(\alpha)}$	Conventional stress limit (intermediate condition)
ε_u	Ultimate tensile strain of FRCM
σ_u	Ultimate tensile stress of FRCM
σ_o	Normal stress
σ_{max}	Maximum interface stress to assess simple- and double-curvature structures
σ_r	Stress orthogonal to interface to assess simple- and double-curvature structures
τ_{0d}	Design shear strength of masonry
τ_r	Interface shear stress to assess simple- and double-curvature structures

σ_{r0}	Debonding interface capacity to assess simple- and double-curvature structures
σ_r	Minimum tensile capacity to assess simple- and double-curvature structures
ϵ_{uf}	Ultimate tensile strain of dry fibres
$\sigma_{u,f}$	Ultimate tensile stress of dry fibres
η	Conversion factor
η_a	Environmental conversion factor
θ	Shear crack angle with respect to longitudinal axis of members
β	Fibre angle with respect to longitudinal axis of members
β_o	Reductive coefficient to assess simple- and double-curvature structures
σ_{fd}	Design strength of FRCM
ϵ_{fd}	Design strain of FRCM
$\epsilon_{fd,rid}$	Reduced design strain of FRCM reinforcement for confined members
ϵ_{mu}	Ultimate compressive strain of masonry
$\bar{\epsilon}_m$	Ultimate compressive strain of masonry with linear behaviour
ρ_{mat}	Matrix reinforcement ratio (confinement)

2 FRCM MATERIALS FOR STRUCTURAL STRENGTHENING

2.1 INTRODUCTION

FRCM materials – hereinafter also referred to as FRCM strengthening systems or, more simply, FRCM systems or also FRCM reinforcements are obtained by using reinforcement grids made of aramid, basalt, carbon, PBO and glass bundles/yarns or by using unidirectional high-strength steel cords; in particular, steel yarns are used in the form of small strands in order to obtain corrugated surfaces which promote bonding between the reinforcement and matrix. In the following, in order to refer to the strengthening grids, the terms “fabrics” or “textiles”, which are commonly used, will also be indifferently adopted.

Grids and strands are combined with inorganic matrices, made for example with lime- or cement-based binders, with the possible addition of additives. In the case of organic additives, it is recommended that the organic component does not exceed 10% by weight of the inorganic binder. In fact, it should be kept in mind that as the overall percentage of organic components increases the FRCM system can undergo a degradation of permeability, durability and fire behaviour properties.

In general, FRCM strengthening systems, in the case of a single-ply fabric application, have a thickness ranging between 5 and 15 mm, excluding the levelling of the substrate. In the case of multiple plies, thickness increases, but it is usually not greater than 30 mm. The net distance between the lateral surfaces of the bundles/yarns or strands, along the directions in which they are developed, does not usually exceed 2 times the thickness of the mortar and in any case it cannot be greater than 30 mm.

The high strength-to-weight ratio of FRCM systems makes it possible to enhance the mechanical performance of the strengthened structural element, essentially being able to withstand the tensile stresses without increasing its mass or significantly changing its stiffness.

In general FRCM reinforcements demonstrate good chemical-physical compatibility with masonry and concrete substrates and a certain degree of vapour permeability; moreover, they can be prepared and applied in a simple way by using basically traditional procedures, even on wet surfaces. Due to their mechanical properties, FRCM reinforcements are specifically indicated for applications requiring limited deformations, as typically occurs for strengthening of masonry.

The following paragraphs explain the design rules related to the main structural applications for which predictive models widely shared by the technical and scientific community, both nationally and internationally, are available.

Further applications shall necessarily be supported by in-depth preliminary investigations performed in laboratory on full scale structural elements and by numerical verifications.

For the aspects related to identification and qualification of the system, as well as for those related to durability, transport, storage, handling, use, see the documentation produced for the CE marking or the Technical Assessment Certificates (CVT) and the compulsory installation manuals for these materials, according to the Guideline recently approved by the Italian Ministry of Infrastructures and Transportation (MIT – January 2019) and entitled: *Linea Guida per la identificazione, la qualificazione ed il controllo di accettazione di compositi fibrorinforzati a matrice inorganica (FRCM) da utilizzarsi per il consolidamento strutturale di costruzioni esistenti*. It deals with the same types of strengthening systems covered by this document, and limits use, for glass fibre grids, to AR (*Alkali Resistant*) fibres only.

In the remainder of the document, the terms “dry fabric” or “dry textile” will refer to fabric/textile not embedded inside the inorganic matrix, thus including coated or pre-impregnated fabrics or grids, according to the MIT Guideline.

The unified approach proposed in the document makes it possible to apply the same rules to the wide range of FRCM materials, differing in their types of strengthening grids and matrixes, available in the Italian market together with the considerable variety of supports present in the national

building heritage. The common design approach represents a particular aspect of the document and the main difficulty encountered in its drafting, something which has already happened in the implementation of the qualification guideline.

It will be responsibility of the technicians in charge of design and construction supervision to choose, from the systems available in the market, the most suitable type of reinforcement for the specific application, taking into account the matrix and grid properties.

Finally, for the aspects related to acceptance criteria at the construction site, the reader can refer to the current technical regulations and to the previously introduced MIT Guideline.

2.2 REVIEW OF SIGNIFICANT APPLICATIONS

Some significant applications related to strengthening of masonry and RC structures with FRCM systems are reported below (Figures 2.1 – 2.22). They introduce the reader to the wide range of possible effective applications that can be developed with this type of system.

2.2.1 Applications on masonry structures

2.2.1.1 Strengthening of masonry panels

The shear and combined axial and bending moment capacity of a masonry wall can be increased by applying a FRCM strengthening system on wall surfaces and by adopting a continuous or discontinuous layout.



Figure 2.1 – Strengthening of masonry walls with basalt fibre grids.

2.2.1.2 Strengthening of vaults and arches

Vaults and masonry arches can be strengthened by applying FRCMs to both their extrados and intrados. In both cases, the aim is to compensate the lack of tensile capacity of the masonry structure preventing the opening of macro-cracks.

The layout of the reinforcement can be continuous or discontinuous and can be connected to the surrounding walls and to the vault itself by adhesion and also with special connectors.

When possible, this type of reinforcement is generally combined with the construction of small stiffening masonry walls at the extrados and with the insertion of steel ties.



Figure 2.2 – Extradotal strengthening of a single-leaf vault with extensive application of basalt fibre grid and hydraulic lime mortar.



Figure 2.3 – Application of unidirectional galvanized steel fibre strips and mortar for the extradotal strengthening of masonry vaults.



(a)



(b)

Figure 2.4 – (a) Intradoxal strengthening of a barrel vault trough application of ultra-high strength unidirectional galvanized steel fibre strips together with natural hydraulic lime mortar; (b) Extra-doxal strengthening of cross vaults by applying ultra-high strength unidirectional galvanized steel fibre strips together with hydraulic lime mortar.



Figure 2.5 – Intradoxal strengthening of a masonry vault with AR glass fibre grid and mortar.

2.2.1.3 Floor and roof ring beams

In order to increase the collapse multipliers associated with overturning mechanisms of wall macro-elements an external ring element made of fabric sheets encircling the building can be built. It is also possible to construct ring beams at the roof level made of masonry reinforced by composite fabric inserted inside the bed mortar joints.



Figure 2.6 – Floor ring beams built with PBO and steel fabrics.



Figure 2.7 – Roof ring beams built with steel fabrics.

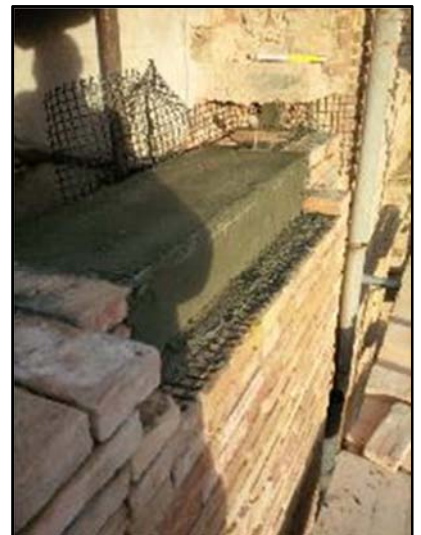


Figure 2.8 – Roof ring beams built with AR glass fibre grids.

2.2.1.4 Confinement of masonry columns

Wrapping of elements subjected to uniaxial compression or to compression and minimal bending makes it possible to increase the ductility of the element and to increase its load-bearing capacity. The layout of the wrapping can be continuous or discontinuous.



Figure 2.9 – Confinement of masonry column with AR glass fibre grid.

2.2.2 Applications on reinforced concrete structures

2.2.2.1 Flexural strengthening of beams, columns and floor joists

Flexural strengthening is achieved by applying fabric strips to the side of the element subject to tensile stresses. Using this method the deflection under service loads can be reduced, although often not very substantially, and crack openings can be limited.



Figure 2.10 – Flexural strengthening of a beam and of a column with PBO fibre grid.



Figure 2.11 – Beam flexural strengthening with ultra-high strength unidirectional galvanized steel fibre strips and cementitious mortar.

2.2.2.2 Shear strengthening of beams and columns

Shear strengthening is achieved by applying fabric strips to the lateral surfaces of the element to be strengthened. The reinforcement can be continuous, with the application of each fabric sheet adjacent to the previous one, or discontinuous, interspersing the strengthening strips with empty spaces. Furthermore, the element can be reinforced by completely wrapping the cross-section or with U-jacketing and possibly using connectors.



Figure 2.12 – Shear strengthening of a beam with PBO fibre grid.

2.2.2.3 Confinement of columns

As for masonry, wrapping of elements subjected to uniaxial compression or to compression and small bending allows the ductility of the element and its load-bearing capacity to be increased. Wrapping can have a continuous or a discontinuous layout.



Figure 2.13 – Confinement of a column by means of ultra-high strength unidirectional galvanized steel fibre strips and cementitious mortar.



Figure 2.14 – Confinement of a column with unidirectional galvanized steel fibre strips and mortar.

2.2.2.4 Strengthening of beam-column joints

The ductility of beam-columns joints can be increased by continuously wrapping the extremities of the elements connected in the joint.



Figure 2.15 – Strengthening of beam-columns joints.



Figure 2.16 – Strengthening of beam-columns joints with unidirectional galvanized steel fibre strips and mortar.

2.2.2.5 Shear strengthening of reinforced concrete walls



Figure 2.17 – Shear strengthening of reinforced concrete walls.

2.2.2.6 Slab strengthening (anti-detachment)



Figure 2.18 – Slab strengthening (anti-detachment).



Figure 2.19 – Slab reinforcement (anti-detachment) with AR glass fibre grid and mortar.

2.2.2.7 Infill walls strengthened against overturning

Infill walls can be connected to the structural reinforced concrete frame by applying the strengthening grid to the infill wall and connecting it to the frame with anchors, or by applying textile sheets between the frame and the infill wall.



Figure 2.20 – Strengthening of walls against overturning with a FRCM system made of glass grid, mortar, adhesion promoter and glass fibre connectors.



Figure 2.21 – Overturning protection of infill walls with different types of grids and anchors.

2.2.2.8 Bridge strengthening



Figure 2.22 – Intradoxal strengthening of a concrete arch bridge with PBO grids.

2.3 MECHANICAL PROPERTIES OF THE STRENGTHENING SYSTEM

The typical stress-strain behaviour of a FRCM system subject to uniaxial tensile force can be described by considering three consecutive branches (Figure 2.23), corresponding, respectively, to the uncracked phase (Stage A), to the crack development phase (Stage B) and to the fully cracked phase (Stage C).

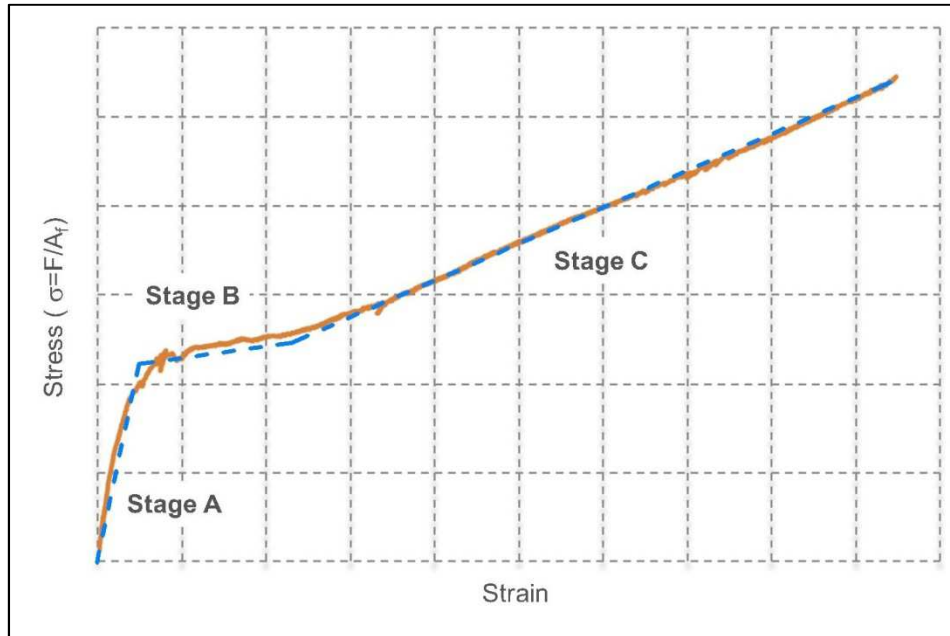


Figure 2.23 – Typical constitutive law of a FRCM coupon subject to uniaxial tensile test (A_f area of dry fabric/textile).

This diagram is not sufficient to characterize the mechanical behaviour of an FRCM system because a number of different failure modes may occur related to the reinforcement in a strengthened structural element as a result of substrate-strengthening system interaction; they are listed below and described in Figure 2.24:

- A. debonding with cohesive failure within the substrate of the reinforcement;
- B. debonding at the matrix-to-support interface;
- C. debonding at the matrix-to-textile interface;
- D. slippage of the textile within the matrix;
- E. slippage of the textile and cracking of the outer layer of mortar;
- F. tensile failure of the textile.

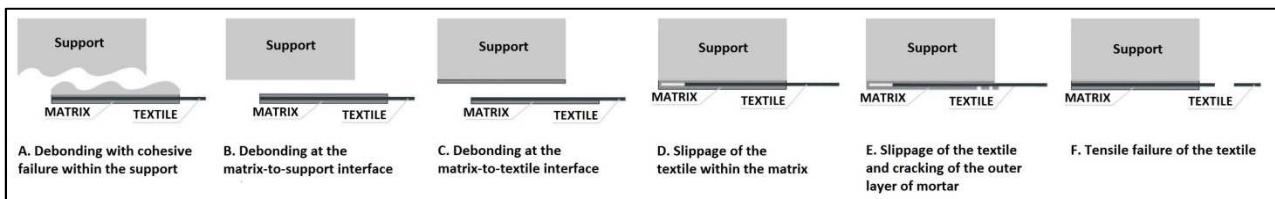


Figure 2.24 – Failure modes.

For this reason, mechanical characterization shall also include, in addition to the tensile test of the FRCM system and of the dry textile, the bond test and possibly any other appropriate tests depending on the specific characteristics of the system.

According to the present Guideline, FRCM strengthening systems have to be characterized such that the following mechanical properties can be used:

- a) conventional stress limit, $\sigma_{\text{lim,conv}}$ (characteristic value), conventional strain limit, $\varepsilon_{\text{lim,conv}}$, as defined further below (both properties depend on the substrate);
- b) tensile stiffness of the sample in the stage A, if detectable (E_f , mean value);
- c) ultimate tensile stress σ_u (characteristic value) and ultimate tensile strain ε_u (mean value) of the FRCM composite at failure;
- d) ultimate tensile stress, $\sigma_{u,f}$ (characteristic value) of the dry textile (failure);
- e) elastic modulus E_f of the dry textile (mean value);
- f) ultimate tensile strain, $\varepsilon_{u,f}$, of the dry textile ($\varepsilon_{u,f} = \sigma_{u,f} / E_f$);
- g) compressive strength of the matrix/mortar, $f_{c,\text{mat}}$, intended as characteristic or nominal (the latter assumed as characteristic).

The definition of the above qualification parameters represents an original contribution of the members of two working groups, from CNR and MIT, achieved through a structured work of progressive refinement and also making use of the results from a *Round Robin Test* activity carried out by the laboratories of different European Universities, promoted by RILEM TC 250-CSM.

Stresses are conventionally referred to the cross-sectional area of the dry textile (A_f), regardless of the presence of the matrix/mortar.

The equivalent fibre thickness of the FRCM system, t_f , provided by the Manufacturer (technical datasheet) is defined as follows: the equivalent fibre thickness of a composite grid along the direction of the weft (warp) is the ratio between the density of the yarns/strands only in the direction of the weft (warp) and the specific weight of the fibres which constitute the weft (warp).

In the case of a grid having the same number and the same type of yarns/strands along the weft and warp directions, the equivalent fibre thickness will be the same along those two directions. In other cases, the equivalent thickness is different depending on whether the direction along the weft or the warp is considered.

3 BASIC CONCEPTS FOR THE DESIGN OF STRENGTHENING INTERVENTIONS AND SPECIAL DESIGN PROBLEMS

3.1 MECHANICAL PROPERTIES OF THE STRENGTHENING SYSTEM IN DESIGN AND VERIFICATION PROBLEMS

The conventional stress limit $\sigma_{\text{lim,conv}}$ represents the bond strength of a specific FRCM system and is evaluated by means of bond tests, performed on FRCM reinforcements applied to conventional substrates. As such it then depends on the type of substrate and corresponds to the characteristic value of the peaks of the applied tensile force registered during the tests (refer to the Italian Guideline for the identification, qualification and acceptance control of FRCM strengthening systems, published by the Italian Ministry of Infrastructure and Transport (MIT)). The conventional strain limit is defined as $\varepsilon_{\text{lim,conv}} = \sigma_{\text{lim,conv}} / E_f$ (Figure 3.1).

The use of the conventional strain limit and of the corresponding conventional stress limit makes it possible to design strengthening interventions by means of FRCM systems without performing a specific verification concerning the failure modes related to debonding or to slippage of the textile within the matrix, typically at the end of the reinforcement. This verification is, however, necessary when these failure modes can take place. This situation usually occurs when the maximum stress in the FRCM system is located at its extremities, for instance in interventions involving the flexural strengthening of beams or panels, especially when subjected to seismic action, or shear strengthening of reinforced concrete beams.

Failure due to the debonding or to slippage of the textile within the matrix, occurring at the extremities of the FRCM reinforcement, is prevented if the FRCM system can be extended up to a significant distance from the cross-section with maximum tensile stress, for instance, in strengthening of masonry walls subject to out-of-plane loads or when FRCM systems are applied at the intrados of reinforced concrete beams to increase their flexural capacity with respect to dead loads.

That being said, for the purposes of this Guideline, the conventional limit values $\varepsilon_{\text{lim,conv}}$ and $\sigma_{\text{lim,conv}}$ represent the parameters to be adopted in the verifications of failure mechanisms located at the extremities of the FRCM system.

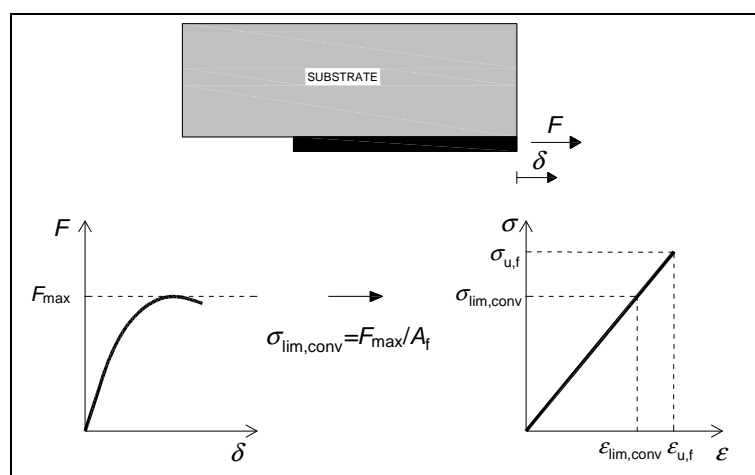


Figure 3.1- Determination of $\sigma_{\text{lim,conv}}$ and $\varepsilon_{\text{lim,conv}}$.

If the above mentioned failure modes due to the debonding or to the slippage of the textile within the matrix, are located instead in intermediate zones, i.e., along the reinforced element (not at its ex-

tremities), the tensile failure of the textile occurs for strain values significantly higher than the conventional strain limit.

In this case, the values of the parameters to be adopted in the verifications governed by debonding or slippage, but located in intermediate zones, are $\varepsilon_{\text{lim,conv}}^{(\alpha)} = \alpha \cdot \varepsilon_{\text{lim,conv}}$ and $\sigma_{\text{lim,conv}}^{(\alpha)} = E_f \cdot \varepsilon_{\text{lim,conv}}^{(\alpha)}$.

The amplification coefficient α can be taken as equal to 1.5 for all the FRCM strengthening systems, except for those in which the point corresponding to the conventional stress limit $\sigma_{\text{lim,conv}}$ falls within Stage A of the stress-strain diagram above. For these FRCM systems a value of 1.0 shall be assumed for the amplification coefficient α .

Higher values of the coefficient α , i.e. greater than 1.5 or 1.0 respectively, can be considered, but they shall be supported by suitable experimental tests on structural members, as described in § 9.

In any case, the value of $\sigma_{\text{lim,conv}}^{(\alpha)}$ shall be smaller than σ_u or at least equal to it. The partial safety factors and conversion factors, mentioned in the following Section, shall be applied to the above mentioned values.

In the situations governed by the tensile strength of the textile rather than by the debonding of the FRCM system or by the slippage of the textile within the matrix, the values of the parameters to be adopted in design problems are the ultimate strain of the dry textile and the corresponding ultimate stress, $\varepsilon_{u,f}$ and $\sigma_{u,f}$. Partial safety factors and conversion factors, described in the following Section, shall be applied to these values as well.

In some specific applications presented in the following chapters, such as the confinement, the proposed predictive formula, obtained from test databases, have been calibrated on the basis of the ultimate strain of the dry textile, which is the qualification parameter often used by researchers to present their results.

3.2 DESIGN VALUES

The design value, X_d , of a generic strength or strain property of a FRCM strengthening system can be expressed as follows:

$$X_d = \eta \cdot \frac{X_k}{\gamma_m} \tag{3.1}$$

where η is a suitable conversion factor accounting for special design problems, X_k is the characteristic value of the property, and γ_m is the corresponding partial factor.

The latter is equal to 1.5 for Ultimate Limit States (ULS) and to 1.0 for Serviceability Limit States (SLS). For the verifications concerning Ultimate Limit States, the effects of environmental factors shall be taken into account. In the absence of more specific data, the values of η_a given in Table 3.1 shall be attributed to the conversion factor η , independently of the characteristics of the textile.

Exposure conditions	η_a
Internal	0.90
External	0.80
Aggressive environment	0.70

Table 3.1 – Environmental conversion factors.

Higher values, up to 1.0, may be used if supported by specific laboratory tests performed by the Manufacturer according to the general principles mentioned in § 9, also taking account of the cracking of the matrix.

As far as the verifications concerning Serviceability Limit States, to be carried out for interventions on reinforced concrete structures, are concerned, the static fatigue phenomenon shall be taken into account, as prescribed in § 5.1.2.

3.2.1 Verification in the case of fire

In the event of a fire, the strengthened structure shall be verified without the reinforcing system. The actions have to be determined with reference to the quasi-permanent combination, and the capacity of the structural members shall be evaluated with unitary partial factors for materials.

4 STRENGTHENING OF MASONRY STRUCTURES

Strengthening of masonry structures is one of the most important applications for FRCC systems. These systems can be extended to the entire surface of the walls or applied in strips, having enough width to limit the tangential stress at the masonry - reinforcement interface.

Safety checks can be conducted at the ultimate limit state only, as indicated below.

Usually, the increase of design capacity of an element strengthened with FRCC should not be more than 50% compared to the unreinforced counterpart. This limitation does not apply to seismic actions.

4.1 IN-PLANE STRENGTHENING OF WALLS

FRCC systems can be adopted to improve the in-plane load bearing capacity of walls. In the case of masonry with poor mechanical properties, such as for example cavity walls, it is necessary to combine the FRCC strengthening interventions with other types of operations in order to preserve the structure of the wall and to allow for appropriate stress transfer to the FRCC.

The following paragraphs provide indications for the design and/or checks of strengthening interventions on walls loaded in their planes in shear or bending.

4.1.1 Shear Capacity

In order to increase the in-plane shear capacity of masonry walls, it is preferable to arrange FRCC reinforcements symmetrically on both sides, and usually extended to the entire surface with the fibres preferably in both the vertical and horizontal directions. For the design of the shear strengthening, the area of the fibres arranged parallel to the shear force only is considered; however, to ensure the effectiveness of such interventions, also after cracking, it is advisable to apply fibres in the orthogonal direction.

The shear capacity of the strengthened wall ($V_{t,R}$) is calculated as the sum of the contribution of unreinforced masonry (V_t), evaluated according to building codes for unreinforced masonry failing under tension, and the contribution of the reinforcement ($V_{t,f}$).

The latter contribution is evaluated according to:

$$V_{t,f} = \frac{1}{\gamma_{Rd}} \cdot n_f \cdot t_{vf} \cdot \ell_f \cdot \alpha_t \cdot \varepsilon_{td} \cdot E_f \cdot \quad (4.1a)$$

where:

- γ_{Rd} is a partial safety factor equal to 2, according to current knowledge;
- n_f is the total number of reinforcement layers arranged on the sides of the wall;
- t_{vf} is the equivalent thickness of a layer of the fibres arranged in the direction parallel to the shear force;
- ℓ_f is the design dimension of the reinforcement measured orthogonally to the shear force, and in any case it cannot be assumed as longer than the dimension H of the wall (Figure 4.1).

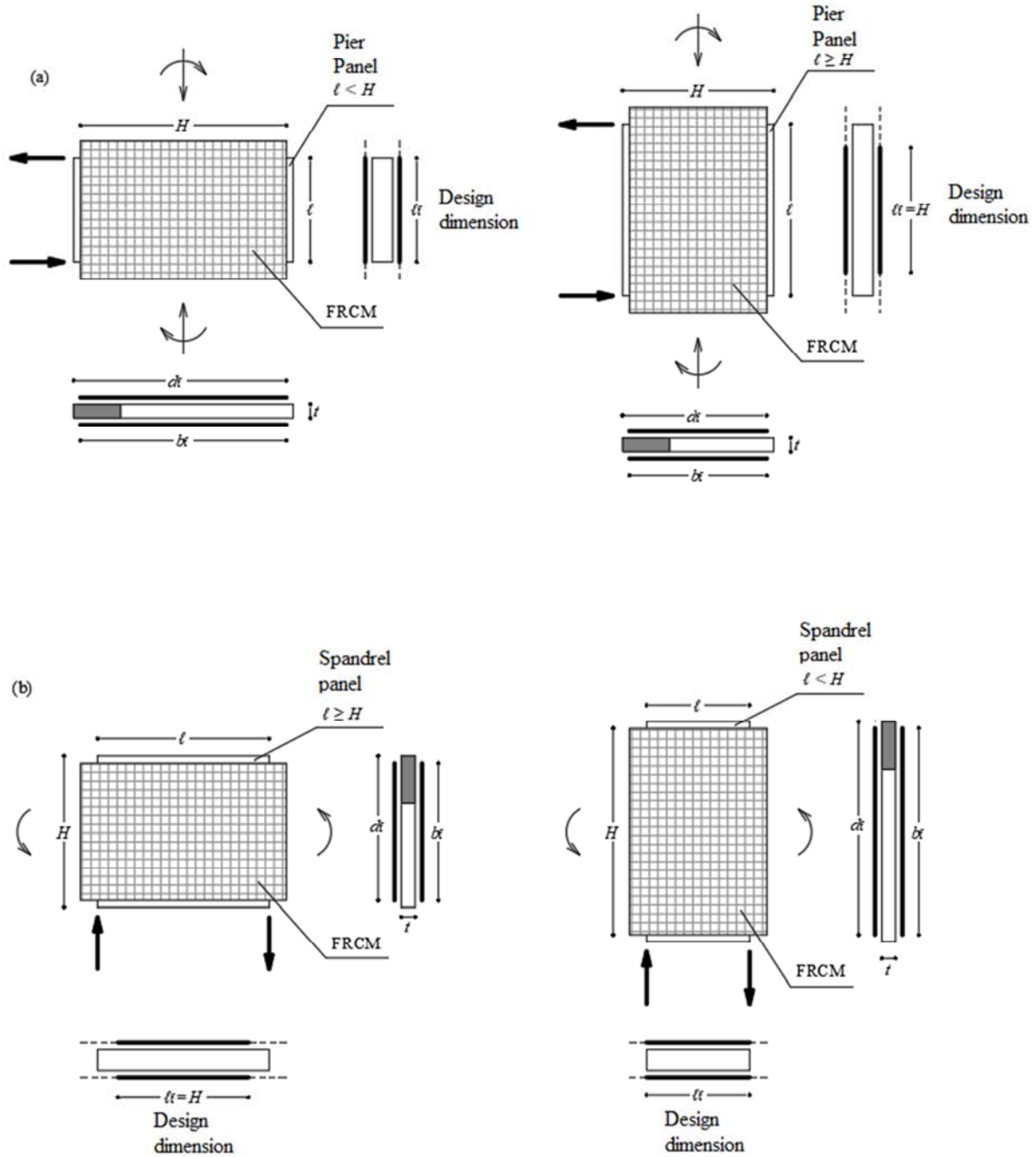


Figure 4.1 - FRCM in-plane strengthening of panels: (a) strengthening of pier panel; (b) strengthening of spandrel panel.

The product $n_f \cdot t_{vf} \cdot \ell_f$ represents the area of the equivalent cross section of reinforcement effective in shear, in the direction parallel to the shear force, which intersects a shear crack inclined at 45° . Hence the limit $\ell_f \leq H$.

The value of ε_{fd} is derived from $\varepsilon_{lim,conv}^{(\alpha)}$ through (3.1). The coefficient α_f takes into account the reduced tensile strength of the fibres when stressed in shear. Without experimental results, it can be assumed equal to 0.80.

With a strengthening system applied on one side only of the wall, the shear contribution shall be reduced by at least 30% and connectors shall be applied to fix the reinforcement to the wall.

If fibres orthogonal to the direction of shear are effectively anchored, it should be also checked that the shear force does not exceed the following diagonal crushing value for masonry:

$$V_{t,c} = 0.25 \cdot f_{md} \cdot t \cdot d_f, \quad (4.1b)$$

where:

- t is the thickness of the wall;
- f_{md} is the design compressive strength of the masonry;
- d_f is the distance between the extreme compressed masonry and the extreme FRCM under tension (fibre direction orthogonal to the shear force - Figure 4.1).

In (4.1b) the properties of unreinforced masonry only are given since it is assumed that the FRCM does not contribute to the compressive strength of masonry.

In a simplified way, the strengthened masonry capacity can be calculated by multiplying the average shear stress capacity of unreinforced masonry without normal stresses by appropriate multiplicative coefficients. Such coefficients can be used only in the case of masonry having thicknesses lower than 400 mm, in the case of reinforcements arranged symmetrically over the entire surface of the two sides of the walls and ensuring that $\sigma_{u,f} t_f \geq \bar{q}_{u,f}$; coefficients are given in Table 4.1.

Masonry Type	Corrective coefficient	$\bar{q}_{u,f}$ (N/mm)
Masonry in disorganized stones (pebbles, or erratic/irregular stones)	1.5	44.60
Masonry in rough-hewn stone, with faces of inhomogeneous thickness	1.5	44.60
Masonry in split stones, well laid	2.0	32.20
Masonry in soft stone (tuff, macco, etc.)	2.0	44.60
Masonry in squared stony blocks	1.2	44.60
Masonry in bricks and lime mortar	1.7	24.50
Masonry in half-full bricks with cement mortar	1.3	44.60

Table 4.1 - Corrective coefficients of the mechanical properties of strengthened masonry.

The values given in Table 4.1 have been taken from tests carried out in the laboratory, without taking into account the exposure conditions referred to in Table 3.1. Therefore the results obtained from the tests shall be suitably reduced, by multiplying by the factor η_a in Table 3.1, corresponding to the appropriate exposure condition.

When such reductions lead to corrective coefficients close to unity, higher increments can be achieved with the use of (4.1a) or with the results of a suitable experimental programme, conducted as specified in § 9.

4.1.2 Combined axial and bending moment capacity

In order to increase the in-plane flexural capacity of wall panels, FRCM strengthening is possible with fibres applied along the direction of the axis of the structural element. The strengthening is preferably applied on both sides of the panel, usually covering almost the entire surface (Figure

4.1). This strengthening arrangement increases the flexural capacity of a wall section only if properly anchored. Strengthening that has been extended by at least 300 mm, starting from the verification section or connected to the masonry by means of suitable devices, is considered properly anchored. The flexural capacity associated with an assigned compression axial, $M_{Rd}(N_{sd})$, can be calculated assuming the following:

- Plane sections remain plane;
- Perfect bonding exists between FRCM and concrete.

The masonry constitutive law σ – ε for uniaxial stress state can be summarized as follows:

- tensile stress: negligible;
- compression: linear behaviour up to both the design strength f_{md} and design strain $\bar{\varepsilon}_m$; design strength equal to f_{md} for strain between $\bar{\varepsilon}_m \leq \varepsilon \leq \varepsilon_{mu}$ and zero strength for strain larger than the ultimate strength, ε_{mu} .

Unless experimental data are available, the masonry ultimate design strain, is equal to 3.5‰. The strengthening constitutive law σ – ε for tensile stresses is linear elastic up to the limit strain ε_{fd} obtained from 3.1 from the conventional strain limit $\varepsilon_{lim,conv}^{(\alpha)}$ in the case of failure mechanisms due to intermediate debonding or from the conventional strain limit $\varepsilon_{lim,conv}$ in the case of end debonding. The strengthening modulus of elasticity is E_f as defined in section 2 (dry fabric). The strengthening does not exhibit any stiffness or compressive strength. Then, if the neutral axis cuts the strengthening section, this is subdivided by the neutral axis into two parts, one of which is tensile and one of which is non-reactive.

The masonry panel flexural capacity is verified when the following relationship is satisfied:

$$M_{Sd} \leq M_{Rd} \quad (4.2)$$

where M_{Sd} and M_{Rd} are design moments and the flexural capacity of the strengthened member, respectively. M_{Rd} is evaluated considering the design axial force associated with M_{Sd} .

The distance of the extreme section, where there is FRCM strengthening, from the edges of the strengthening panel, shall be at least equal to the above indicated anchorage length (see also § 6), unless suitable anchoring devices are provided.

Appendix 1 shows the equations for calculating $M_{Rd}(N_{sd})$ for different failure mechanisms.

4.2 STRENGTHENING OF MASONRY PANELS FOR OUT-OF-PLANE LOADS

An FRCM strengthening system is often used to improve the out of plane of masonry panel capacity, typically in the case of seismic actions.

With reference to a unit strip of masonry panel, flexural safety of the strengthening masonry panel is achieved, both in the (typical) vertical direction and in the horizontal direction, if Equation (4.2) is satisfied, where M_{Sd} and M_{Rd} are the applied bending moment and the flexural capacity related to the unit strip, respectively.

The design flexural capacity, M_{Rd} , of the strengthened masonry section may be determined as a function of the mechanical characteristics of masonry and FRCM, the thickness, t , of the masonry panel and the applied axial force corresponding to M_{Sd} . The masonry panel subjected to out-of-plane loads is generally characterized by a maximum bending moment at the centre of the panel and

negligible forces at the end sections. Therefore, in this case there is no end debonding failure mechanism and the maximum strengthening strain is significantly higher.

The design flexural capacity, M_{Rd} , can be calculated assuming the hypotheses referred to in Section 4.1.2 with the following Equation:

$$M_{Rd} = M_{0d} + \frac{1}{\gamma_{Rd}} \cdot (M_{1d} - M_{0d}), \quad (4.3)$$

where M_{0d} is the design bending moment of the unstrengthened masonry section, M_{1d} the design bending moment of the strengthened masonry section and γ_{Rd} is a partial factor for resistance models which, given the current state of knowledge, is assumed equal to 2 .

It is necessary to check that the shear force design action, V_{sd} , does not exceed the shear capacity:

$$V_{Rd,m} = 1 \cdot y_n \cdot f_{vd}, \quad (4.4)$$

where f_{vd} is the design shear strength of the unstrengthened masonry as per the building code, equal to the ratio of the sum of the compressive forces and the area between extreme compression member and neutral axis, y_n .

The flexural capacity of the strengthened section is calculated considering the design strain, ε_{fd} , obtained from 3.1 starting from the conventional strain limit $\varepsilon_{lim,conv}^{(a)}$ in the case of failure mechanisms due to intermediate debonding or from the conventional strain limit $\varepsilon_{lim,conv}$ in the case of end debonding. This strain should be multiplied by the modulus of elasticity E_f ($\varepsilon_{fd} \cdot E_f = \sigma_{fd}$). The contribution of the FRCM under compression should not be considered.

The distance of the extreme section, where the FRCM strengthening is required, from the edges of the strengthening panel shall be at least equal to the above indicated anchorage length (see also § 6), unless suitable anchoring devices are provided.

4.3 CROWNING BEAMS IN FRCM-REINFORCED MASONRY

Crowning beams in FRCM-reinforced masonry are built to provide the structure with a box-type behaviour and prevent, or delay, the onset of out-of-plane overturning collapse mechanisms. Crowning beams are built with clay bricks or stone units and are reinforced by installing FRCM systems in the horizontal joints of mortar (Figures 2.7 and 2.8). Fabric is installed in a number of layers to provide the crowning beam with adequate tensile and bending strength, with negligible effects on the stiffness of the masonry. The width of the crowning beam should preferably be equal to the thickness of the masonry wall and the FRCM reinforcement should have the same width as well.

The tensile strength of a FRCM-reinforced crowning beam, having height H and width b , can be estimated as follows:

$$N_{t,Rd} = n_f \cdot t_f \cdot b_f \cdot \alpha \cdot \varepsilon_{fd} \cdot E_f \quad (4.5)$$

where:

- n_f : is the number of FRCM layers;

- b_f : is the width of the FRCM system installed in the horizontal joints of mortar, equal to the width of the crowing beam;
- $\varepsilon_{fd} \cdot E_f = \sigma_{fd}$.

The product: $n_f \cdot t_f \cdot b_f$ corresponds to the equivalent cross-sectional area of the FRCM reinforcement installed in the crowing beam. The value of the design tensile strain ε_{fd} is obtained from $\varepsilon_{lim,conv}^{(\alpha)}$ using Eq. (3.1). The provisions on anchorage, already mentioned in the previous sections, apply.

The tensile strength of the crowing beam can be taken into account in the assessment of local collapse mechanisms, provided that an overlap length equal to the width of the crowing beam, with a minimum of 300mm, is ensured at the connections or at corners between orthogonal walls. When possible, anchorage techniques that are proven to be effective by experimental evidence (§ 9) should be applied. Moreover, vertical connectors should ensure that the load is transferred between the crowing beam and the underlying masonry.

The ultimate flexural strength of the FRCM-reinforced crowing beam under external loads, directed either out of the plane or in the plane of the wall, can be estimated under the same assumptions of §4.2. For assessment purposes, failure takes place when either the FRCM design strain (ε_{fd}) or the ultimate compressive strain (ε_{m}) of masonry in the horizontal direction is reached. Once the neutral axis depth is calculated through the translation equilibrium equation for the relevant failure mode, the ultimate flexural strength of the crowing beam can be calculated on the basis of the above-mentioned assumptions.

4.4 CONFINEMENT OF MASONRY COLUMNS UNDER AXIAL COMPRESSION

Masonry members subjected mainly to axial compression forces can be confined with FRCM by installing a continuous wrapping of composite with inorganic matrix in which the fibres are oriented mainly orthogonally to the axis of the column. In this way, the external wrap limits the transversal expansion inducing a favourable state of triaxial compression. It is recommended to overlap one fourth of the circumferential length/perimeter of the section or 300 mm, whichever is greater, with the fabric mesh. Reference can be made to § 6 when steel meshes are adopted.

Confinement techniques are feasible for both damaged or deteriorated members and intact members with a view to the static or seismic enhancement of the structure. FRCM confinement shall cover the entire external surface of the member to be reinforced.

Verification of the confined member subjected to centred axial compression consists of checking the following limitation:

$$N_{Sd} \leq N_{Rmc,d} \quad (4.6)$$

where N_{Sd} is the design value of the axial force (to be evaluated, for the different predictable load combinations, as prescribed by the current Code) and $N_{Rmc,d}$ the design value of the axial capacity of the confined member.

The design axial capacity $N_{Rmc,d}$, is defined as follows:

$$N_{Rmc,d} = A_m \cdot f_{mcd} \geq A_m \cdot f_{md} \quad (4.7)$$

where the symbol A_m represents the area of the cross section of the confined member, f_{md} is the compressive strength of unconfined masonry and f_{mcd} is the design value of the compressive strength of confined masonry.

The compressive strength of a confined member, f_{mcd} , can be obtained by defining the confinement pressure f_1 which is limited by the mechanical performance of the matrix which if damaged affects the efficacy of its interaction with the fibres. The compressive strength is therefore defined once a reduced confinement pressure $f_{1,eff}$, denoted as “effective confinement pressure”, is evaluated. Its value depends also on the characteristics of the masonry column:

$$f_{mcd} = f_{md} \cdot \left[1 + k' \cdot \left(\frac{f_{1,eff}}{f_{md}} \right)^{\alpha_1} \right] \quad (4.8)$$

where k' is a coefficient (dimensionless) of strength increase and α_1 is an exponent, which can be assumed equal to 0.5 in the absence of reliable experimental results.

The value of the coefficient k' can be established on the basis of experimental results obtained on masonry specimens with characteristics similar to those of the member to be confined. Alternatively, the following formula can be adopted:

$$k' = \alpha_2 \cdot \left(\frac{g_m}{1000} \right)^{\alpha_3}, \quad (4.9)$$

where g_m is the masonry mass density expressed in kg/m^3 and α_2 and α_3 are coefficients which can be assumed prudently equal to 1.0, if experimental results are not available to justify different assumptions.

4.4.1 Confinement of circular columns

For the case of circular columns with diameter D , confined with n_f strengthening layers, with equivalent thickness of the fibres in the direction orthogonal to the axis of the member, t_f , and $f_{c,mat}$ representing the characteristic compressive strength of the inorganic matrix, the effective confinement pressure, $f_{1,eff}$, can be calculated as:

$$f_{1,eff} = k_H \cdot f_1, \quad (4.10)$$

$$f_1 = \frac{2 \cdot n_f \cdot t_f \cdot E_f \cdot \varepsilon_{ud,rid}}{D} \quad (4.11)$$

where f_1 is the confinement pressure, k_H the horizontal efficiency coefficient, to be assumed equal to 1 for circular columns with continuous wrapping, and $\varepsilon_{ud,rid}$ the design strain of the composite FRCM which can be assumed equal to:

$$\varepsilon_{ud,rid} = \min \left(k_{mat} \cdot \eta_a \cdot \frac{\varepsilon_{uf}}{\gamma_m}; 0.004 \right), \quad (4.12)$$

with:

$$k_{\text{mat}} = \alpha_4 \left(\rho_{\text{mat}} \cdot \frac{f_{c,\text{mat}}}{f_{\text{md}}} \right)^2 \leq 1, \quad (4.13)$$

$$\rho_{\text{mat}} = \frac{4 \cdot t_{\text{mat}}}{D}, \quad (4.14)$$

where t_{mat} is the overall thickness of the FRCM and k_{mat} the dimensionless coefficient of confinement efficiency which takes account of the presence of the inorganic matrix.

In the absence of experimental results able to justify various assumptions, the coefficient α_4 can be assumed equal to 1.81.

4.4.2 Confinement of rectangular columns

Only moderate increases in axial compressive strength can be achieved with FRCM confinement of elements with square or rectangular cross section. Applications of this type should be carefully examined and analysed.

In the absence of adequate experimental tests which prove the efficacy, the effect of external confinement is neglected for rectangular sections (Figure 4.2) with shape ratio $b/h > 2$ where b is the greater and h the lower size of the section.

Before applying the FRCM system the corners of the cross section should be smoothed in order to prevent dangerous localized stress concentrations which could lead the system to a premature failure.

The corner radius shall respect the following condition:

$$r_c \geq 20\text{mm} \quad (4.15)$$

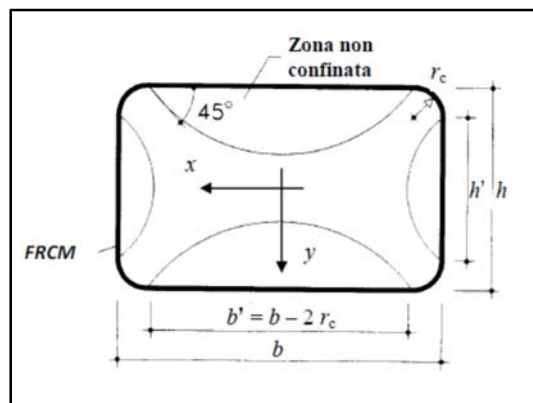


Figure 4.2 – Confinement of rectangular columns.

For the case of columns confined with steel meshes, the above expedient on the corner radius mentioned above can be neglected, as reported at § 6. The folding device to be adopted shall be reported on the installation manual provided by the Manufacturer.

The formulations already introduced for circular sections can be utilized, with the following changes:

$$k_H = 1 - \frac{b'^2 + h'^2}{3 \cdot A_m}, \quad A_m = b \cdot h \quad (4.16)$$

$$D = \text{diagonal length of the square or rectangular cross section} \quad (4.17)$$

4.5 SIMPLE- AND DOUBLE-CURVATURE STRUCTURES

The application of reinforcing FRCM systems is able to improve the behaviour of simple and double curvature structures, counteracting the triggering of possible collapse mechanisms.

A principle that shall be kept in mind when reinforcing structural elements with FRCM technology is that these materials, unlike other reinforcement systems, can have some significant tensile ductility properties related to the presence of the semi-ductile segment of the constitutive traction bond (Figure 2.23, Stage B), provided that this segment has a non-negligible extension, as will be clarified in the following. Therefore by coupling the ductile reinforcement to a material in which the elongation is due to the detachment between two interfaces, the resulting element is endowed with the same ductility characteristic as the reinforcement, provided that this is able to withstand the related effort without losing solidarity with the wall support. The opportunity of conferring a ductile behaviour to the system at the structural level results in an increase in the resistant capacity and in an overall qualitative improvement, bearing in mind the need for a reliable model for checking the integrity of the reinforcement and the reinforcement-structure connection.

In order not to compromise the ductility of the structure, the solidarity of the reinforcement to the wall support shall be verified with reference to the maximum tensile effort that can be applied to the reinforcement and evaluated with reference to the value of the stress that determines the transition from stage A to stage B (semi-ductile part) of the diagram in Figure 2.23.

This (characteristic) stress is not included among the qualification parameters listed in the Italian Ministry Guideline. However, it can easily be obtained from the results of the qualification tests and for preliminary evaluations it can be approximated by

$$\sigma_o = \sigma_{uf} / \beta_o \quad (\beta_o = 1.8 \div 2.2). \quad (4.18)$$

In order to assess the bond to the supporting material a force equal to $N_o = \sigma_o \cdot A_f$ should be considered applied on both sides of the reinforcement, where A_f is the total area of the dry net and σ_o is the characteristic value of the above mentioned stress.

In the case of a curved surface, the curvature produces a debonding stress σ_{r0} (Figure 4.3) at the interface between the reinforcement and the masonry, and between the net and the matrix, which shall be smaller than the minimum tensile strength σ_{rt} between the strength of the matrix and of the support, whence it is necessary to check that:

$$\sigma_{ro} = \frac{N_o}{rb} \leq \frac{\sigma_{rt}}{\gamma_{rt}}, \quad (4.19)$$

where σ_{rt} is a characteristic value and γ_{rt} is a partial factor that is suitably assumed equal to 1.5.

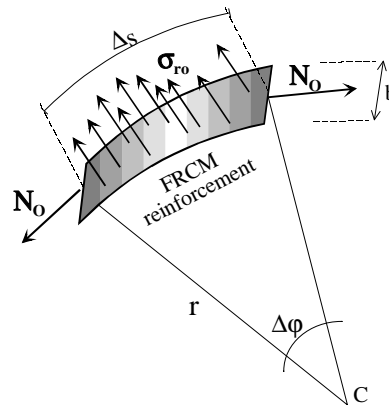


Figure 4.3 - Reinforcement element applied to the intrados and radial debonding stress.

After expression 4.19 has been verified, the capacity of the reinforcement shall be checked in relation to the applied loads. With reference to the equilibrium of an arch element, for the interface between the reinforcement and the wall element, it shall be verified that the following expression holds true (see Chapter 13, Appendix 2):

$$\sigma_{\max} = \frac{\sigma_r}{2} + \sqrt{\frac{\sigma_r^2}{4} + \tau^2} \leq \frac{\sigma_{rt}}{\gamma_{rt}}, \quad (4.20)$$

where:

- τ_r is the active shear stress at the interface
- σ_r is the active normal stress at the interface.

4.5.1 Single curvature structures

The static capacity of masonry structures can be analysed with equal efficacy both through the examination of possible collapse modes (kinematic approach) and through the search for admissible equilibrium paths (static approach). It should be noted that, if the two procedures are implemented with all the necessary accuracy, the results obtained are absolutely equivalent. The case is different if one of the procedures or both are applied by an approximate or incomplete procedure, since, in this case, the static method always produces a result on the safe side and therefore it is completely reliable, while the kinematic method is more delicate because it produces results with some cost to safety, unless the reference kinematics are very carefully selected.

4.5.1.1 Reinforcement identification and assessment through the kinematic approach

The collapse of single-curved structural systems can be traced to the formation of unilateral hinges due to the limited tensile strength of the masonry, causing the trigger of a kinematic mechanism.

Since the unilateral hinges do not produce energy dissipation in the absence of tensile strength, this mechanism results in a collapse of the structure if the work developed by the acting loads is larger than zero.

The collapse condition, which occurs when the work of the acting loads is larger than zero, can be evaluated on the basis of the displacements inferred from diagrams constructed using the theory of kinematic chains.

If the degree of safety with respect to kinematic collapse is not adequate, it is possible to counteract the formation of the most dangerous kinematic mechanisms by arranging reinforcements of FRCM material over the intrados or extrados in such a position as to prevent the free opening of the unilateral hinges involved. In this way the possibility of forming the most dangerous kinematics remains limited, with a consequent increase in the degree of safety.

Taking for granted the reliability of the bond between reinforcement and structure, if reinforcement hinges are activated, for each hinge a work equal to the limit force value N_0 times the relative displacement between the edges of the slot associated with the hinge will be considered, provided that the semi-ductile part B has an extension such as to allow the FRCM reinforcement to undergo the competent elongation remaining in stage B. The occurrence of this circumstance is a necessary condition for the applicability of the kinematic approach.

4.5.1.2 Reinforcement identification and assessment through the static approach

An alternative to the method explained in the previous subsection consists of verifying the capacity of the structure to balance the applied loads without violating the resistant properties of the material of which it is made. For structures with a simple curvature, such as single- or multi-span arches, or even vaults similar to a sequence of arches that are somehow collaborating with each other, such as for example barrel vaults, reference can be made to an equivalent isostatic system in which the internal forces depend on a number of hyperstatic interactions appropriately chosen, according to the established methods of the Theory of Structures.

Considering that the tensile strength of masonry has been assumed to be null, the structure can tolerate the applied loads without collapsing if it is possible to graduate the hyperstatic forces so that the resultant of the stresses falls within the cross section of the structure (arch, piers, etc.), or if the curve of the pressures, built as the funicular curve of active loads and reactive forces, is everywhere inside the profile of the structure.

If by contrast the above mentioned stability test yields a negative result, then after identifying any "non-admissible" line of pressures, the stability of the structure can be ensured by applying the reinforcement at the intrados and/or extrados in order to cover the entire extension of the arch along which the pressure line runs out from the boundary of the structure.

After the reinforcement has been arranged and the admissibility of the pressure line is recovered, it remains to be verified that the masonry and the reinforcement are able to safely tolerate the respective efforts.

For this purpose it is necessary to identify the most stressed sections, such as the one corresponding to the position where the distance of the pressure line from the middle line of the structure is maximum; this cross section is stressed by eccentric compression and shear force as shown in Figure 4.4, where N is the normal force in the checking pattern, and T is the associated shear force; N_m is the result of compressions in the masonry while N_f is the tensile stress in the reinforcement.

The relevant checks will be carried out according to the methods and criteria set out in paragraph 4.2 integrated with what is illustrated in Appendix 1, Chapter 12.

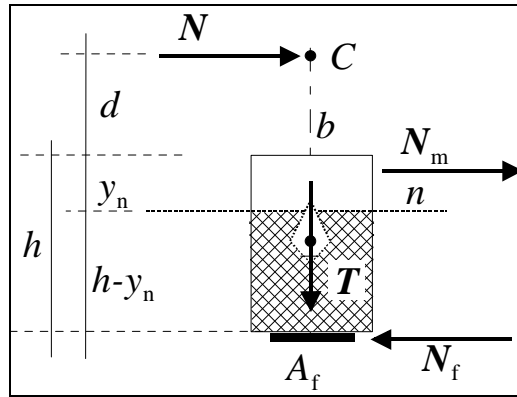


Figure 4.4 – Test cross-section.

4.5.2 Barrel vaults

Simple curvature structures, such as barrel vaults, can be regarded as consisting of a sequence of parallel arches, and therefore can be reinforced and verified in the same way as described in the previous paragraphs. In order to secure the compactness of the structural system it is appropriate also to arrange longitudinal reinforcements along the direction of the generators of the vault. The density of the reinforcement shall be adequate to preserve the spread of the reinforcing effect over all the masonry constituting the vault, and therefore it is appropriate to proportion the distance p_f between the reinforcements to the dimensions of the vault, according to the following relationship:

$$p_f \leq 3t + b_f, \quad (4.21)$$

where:

- t is the vault thickness,
- b_f is the width of the applied reinforcements.

4.5.3 Double curvature structures

The characterization of the collapse of double-curvature structures in general involves kinematic mechanisms that cannot be identified in a simple manner; for this reason it is preferable to evaluate the benefit of the reinforcement by checking the admissibility of equilibrium stress fields in terms of stresses and/or of internal forces.

Masonry vault statics, for which it is always prudent to assume that the material cannot withstand tension, can be studied by identifying a pressure membrane that plays the same role as the pressure line in the case of single-curvature structures.

5 STRENGTHENING OF REINFORCED CONCRETE STRUCTURES

In this section, bending and shear strengthening of reinforced concrete (RC) members, as well as confinement of mainly axially loaded RC members, are examined. The formulas provided, based on current knowledge, will be used only to strengthen members against quasi-static vertical (gravitational) loads. The structural members subjected to seismic actions should be verified without accounting for the presence of the strengthening, according to the current building code; the member capacity shall be computed assuming unit values of the material partial safety factors.

For applications where debonding failure is expected, the mean concrete compressive strength shall not be lower than 15 N/mm^2 .

The increase in the capacity of the strengthened member cannot be higher than 50% of the capacity of the non-strengthened member.

5.1 FLEXURAL STRENGTHENING

Formulas to verify the flexural strengthening both at the serviceability and ultimate limit states are provided in this section.

5.1.1 Ultimate limit state (ULS)

Flexural design at the ULS of FRCM strengthened members requires that:

$$M_{Sd} \leq M_{Rd} \quad (5.1)$$

where M_{Sd} and M_{Rd} are the member flexural capacity and factored ultimate bending moment, respectively.

The flexural capacity, M_{Rd} , of the strengthened member can be expressed as a function of the mechanical properties of concrete, pre-existing steel reinforcing bars, and FRCM composite, assuming the following hypotheses:

- (i) plane sections remain plane;
- (ii) perfect bond between the FRCM composite and concrete.

The maximum compressive strain of concrete shall not exceed 0.0035.

The resisting bending moment is calculated considering it as the limiting strain ε_{fd} obtained by Eq. (3.1). The contribution of the compressed FRCM can be ignored.

The FRCM strengthening shall also be verified with respect to end debonding failure or slippage of the fibres within the matrix. The latter phenomenon is assumed to exist if, without the presence of proper mechanical anchorages, the composite tensile stress in the cross-section where the strengthening is first needed to increase the resisting bending moment is lower than $\sigma_{fd} = E_f \cdot \varepsilon_{fd}$. This value of σ_{fd} is calculated using Eq. (3.1) without applying any amplifying coefficient to $\varepsilon_{lim,conv}$. The distance between the FRCM end and the section where it is first needed shall be at least equal to the anchorage length (see § 6). To evaluate the stress in the fibres, which shall be lower than σ_{fd} , the translation of the bending moment diagram could be taken into account.

5.1.2 Serviceability limit state (SLS)

Under the service loads, the stress in the tensile steel bars shall not exceed 80% of the associated

steel design tensile strength.

Furthermore, to account for the effect of long-term loads and unless further detailed analyses are available, the maximum tensile stress in the FRCM should not exceed the values provided in Table 5.1 for the different types of fibre.

Type of fibre					
UHTSS	AR Glass	Aramid	Basalt	Carbon	PBO
$0.55 \sigma_{u,f}$	$0.20 \sigma_{u,f}$	$0.30 \sigma_{u,f}$	$0.20 \sigma_{u,f}$	$0.55 \sigma_{u,f}$	$0.30 \sigma_{u,f}$

Table 5.1 – Upper bound limit of the FRCM tensile stress for long-term loads.

5.2 SHEAR STRENGTHENING

The shear strength of the FRCM strengthened member can be computed as:

$$V_{Rd} = \min \{ V_{Rd,s} + V_{Rd,f}, V_{Rd,c} \} \quad (5.2)$$

where $V_{Rd,c}$, $V_{Rd,s}$, and $V_{Rd,f}$ are the concrete, steel, and FRCM contributions to the shear capacity, respectively. Steel and concrete shear contributions shall be calculated according to the current building code, whereas the FRCM contribution shall be computed as follows.

In the case of U- or fully-wrapped FRCM configurations, $V_{Rd,f}$ can be estimated according to the Mörsh truss as:

$$V_{Rd,f} = \frac{1}{\gamma_{Rd}} \cdot 0.9 \cdot d \cdot f_{fed} \cdot 2 \cdot t_f \cdot (\cot \theta + \cot \beta) \cdot \frac{b_f}{p_f} \cdot \sin^2 \beta, \quad (5.3)$$

where:

- d is the distance from the extreme compression fibre to the centroid of tension steel reinforcement,
- θ is the inclination angle, with respect to the longitudinal axis of the element, of the main shear crack. For the sake of simplicity, θ can be evaluated neglecting the presence of the FRCM strengthening,
- β is the inclination angle, with respect to the longitudinal axis of the element, of the FRCM fibres,
- f_{fed} is the effective design strength of the FRP shear reinforcement, computed as explained in the following,
- t_f is the textile equivalent thickness,
- b_f and p_f are the width and the spacing of FRCM strips, measured orthogonal to the direction of the fibres ($b_f / p_f = 1.0$ when FRCM strips are placed adjacent to one another), respectively,
- γ_{Rd} is a model partial safety factor that can be assumed equal to 1.5.

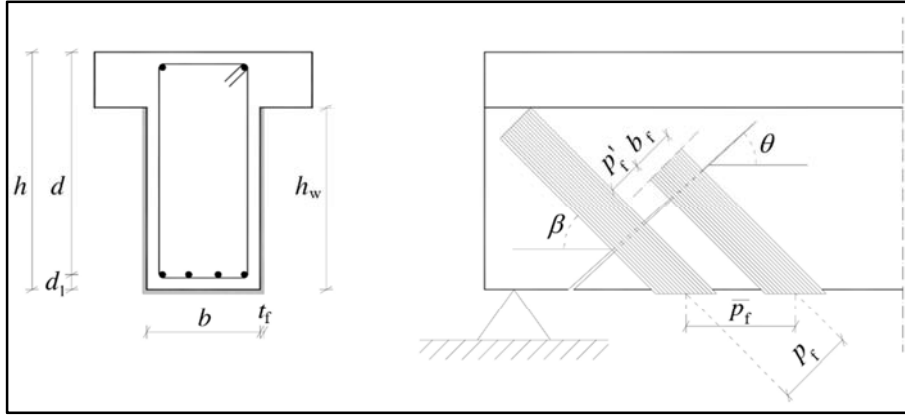


Figure 5.1 – Notation for the shear strengthening using FRP strips.

5.2.1 Effective design strength

Unless the FRCM stresses across the shear cracks are evaluated in detail, the following simplified procedure can be adopted. This procedure is based on the definition of an “effective stress” f_{fed} in the FRCM strengthening, which is the average tensile stress in the composite spanning the main shear crack at shear failure of the strengthened member. If the shear failure of the FRCM strengthened member is associated with FRCM debonding or slippage of the fibres within the matrix, the effective stress f_{fed} shall be evaluated according to the results of bond tests and, in particular, to $\sigma_{\text{lim,conv}}$. Otherwise, the value of f_{fed} could be evaluated on the basis of the FRCM tensile strength $\sigma_{\text{u,f}}$ by proper experimental testing.

In the case of a U-wrapped FRCM strengthening on a rectangular or T cross-section, the effective design strength f_{fed} is:

$$f_{\text{fed}} = \begin{cases} \sigma_{\text{fd}} \frac{L_{\text{max}}}{l_{\text{ed}}} \left(1 - \frac{1}{3} \frac{L_{\text{max}}}{l_{\text{ed}}} \right) & \text{se } L_{\text{max}} \leq l_{\text{ed}} \\ \sigma_{\text{fd}} \left(1 - \frac{1}{3} \frac{l_{\text{ed}}}{L_{\text{max}}} \right) & \text{se } L_{\text{max}} > l_{\text{ed}} \end{cases} \quad (5.4)$$

where:

- $L_{\text{max}} = \frac{\min\{0.9 \cdot d, h_w\}}{\sin \beta}$
- σ_{fd} is the FRCM design tensile strength (obtained based on $\sigma_{\text{lim,conv}}$ or $\sigma_{\text{u,f}}$),
- l_{ed} is the effective anchorage length, equal to 300 mm unless proper measurements are available;
- h_w is the cross-section web height, which shall be entirely covered by the U-wrapped FRCM, i.e. the FRCM shall not have a height lower than h_w .

For some FRCM composites, the matrix-fibre interface material law shows the presence of a residual interface shear stress. This stress remains approximately constant for high values of matrix-fibre slip and its contribution could be significant. Recent studies show how this contribution can be taken into account (see § 10, References).

5.3 CONFINEMENT OF REINFORCED CONCRETE COLUMNS SUBJECTED TO CENTRED COMPRESSION

Reinforced concrete columns under pure compression, both circular and rectangular or square, confined with FRCM can be verified following the same rules already detailed for masonry columns, except for the variants listed below.

The design value of the axial capacity, $N_{Rcc,d}$, is defined as follows:

$$N_{Rcc,d} = A_c \cdot f_{ccd} + A_s \cdot f_{yd}, \quad (5.5)$$

where A_c is the net area of concrete, A_s the steel reinforcement area, f_{ccd} the design compression strength of the confined concrete, f_{yd} the design yielding strength of the steel reinforcement.

The design compression strength of the confined concrete, f_{ccd} , can be calculated as follows:

$$\frac{f_{ccd}}{f_{cd}} = 1 + 2.6 \cdot \left(\frac{f_{l,eff}}{f_{cd}} \right)^{2/3}, \quad (5.6)$$

where:

- f_{cd} is the design compression strength of the unconfined concrete,
- $f_{l,eff}$ is the effective confining pressure.

The coefficient k_{mat} in case of reinforced concrete columns can be assumed as:

$$k_{mat} = 0.217 \cdot \left(\rho_{mat} \cdot \frac{f_{c,mat}}{f_{cd}} \right)^{3/2} \leq 1. \quad (5.7)$$

5.3.1 Confinement of prismatic cross-section columns

Confinement by means of FRCM for square or rectangular reinforced concrete elements follows the same rules provided for masonry columns, except for the variant listed below:

$$k_H = 1 - \frac{b'^2 + h'^2}{3 \cdot A_c}, \quad A_c = b \cdot h. \quad (5.8)$$

6 DETAILING

The construction details for an FRCM strengthening system depend on the geometry of the structure, the nature and consistency of the support and the stress level that the structure is subjected to. The worker shall carefully follow the instructions in the installation manual that the manufacturer is required to provide together with the strengthening system.

Since FRCM systems are qualified in reference to conventional substrates, it is recommended, especially for structurally significant works, to perform bond tests on the specific substrate to be strengthened. The tests can be conducted according to the MIT Guidelines.

In particular, the failure mechanisms of debonding from substrate and of extraction of the fibres from the matrix can be prevented/delayed observing the following detailing rules:

- In all cases where the FRCM strengthening system has to be applied around edges, such edges shall be appropriately rounded and the radius of curvature of the rounding should be at least 20 mm. Such rounding may not be needed for steel fibres, also according to the manufacturer's declaration, unless supported by specific laboratory tests. The bending device that shall be used to make the bends should be indicated also in the installation manual.
- An adequate anchorage length shall be provided, beyond the end section in which the FRCM system is required. Without more accurate investigations, it should be at least 300 mm.
- Adequate overlapping of reinforcement grids is required, following the instructions in the installation manual. Normally, in confinement interventions, the overlapping length of the fibres shall be at least one quarter of the circumference/perimeter of the cross section and never less than 300 mm. Special indications, supported by adequate experiments, shall be provided in the installation manual for confinement interventions with steel fibres. Given the stiffness of such fibres, overlapping should be able to prevent debonding phenomena.
- In the other types of interventions, though not recommended, overlapping lengths lower than 300 mm are possible, if qualified by the Manufacturer when the CVT is handed over.
- With multiple layers, the overlaps shall be appropriately offset. Offsets should not be less than half the thickness of the system, with a minimum of 300 mm.

In confinement interventions, due to the axial stiffness of the FRCM jacket, in order to prevent debonding from the support, it may be desirable to provide a joint/gap between the wrapping and the structure.

The use of connectors can be useful or even mandatory, with the following detailing rules.

- If the FRCM system is applied on one side only of the panel, it is mandatory to use connectors of such a length as to penetrate inside the outermost layer of the wall (Figure 6.1).

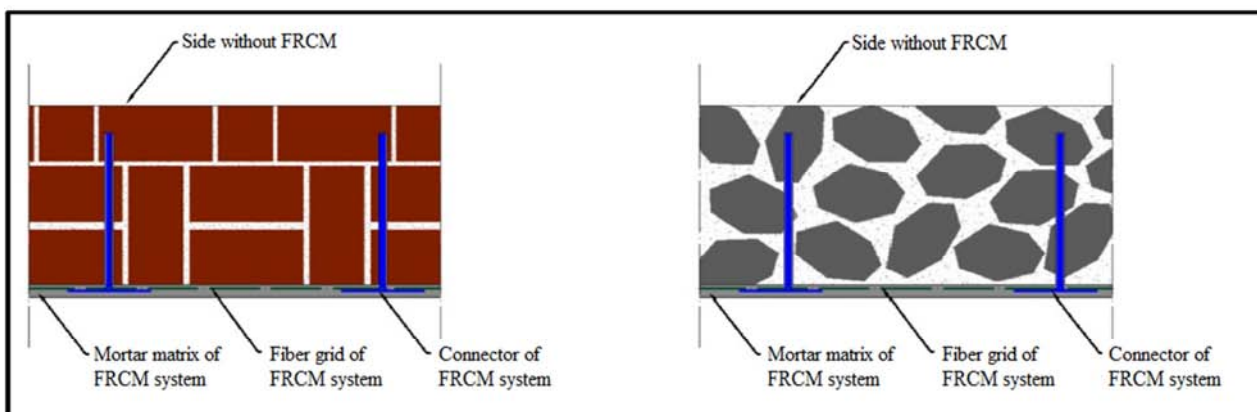


Figure 6.1 - Connectors penetrating inside the first layer of the wall.

- In the case of applications on two sides of cavity walls or with disconnected leaves, it is mandatory that the connectors pass through the leaves.
- In the case of panels having $t \leq 400$ mm with FRCM and with the use of connectors, a distance between the connectors of $i \geq 3t$ and never higher than 1600 mm is recommended; at the wall intersections connectors with $l = 3t$ are recommended.
- In the case of panels having $t > 400$ mm, a distance between the connectors of $i \geq 2t$ and never higher than 2000 mm is recommended; at the wall intersections staggered connectors with $l = 3t$ are recommended (Figure 6.2).

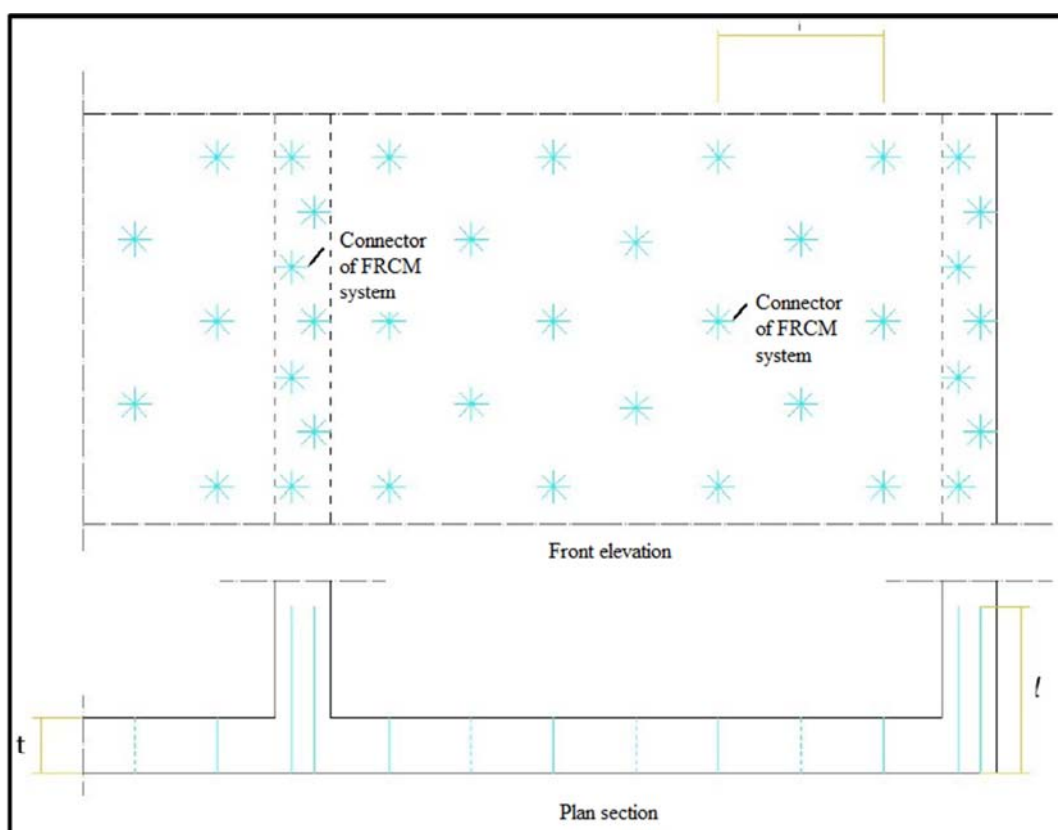


Figure 6.2 – Layout of connectors at walls intersections.

7 MAINTENANCE AND REPAIR

Repair intervention with FRCM should be monitored over time with periodic testing; the frequency depends on the conditions of exposure and possibility of inspection. On such occasions any damage shall be detected, along with the causes and possible remedies. Attention should be paid to detachments, cracking, chromatic variations or other anomalies of the FRCM system. Besides the visual inspections, acoustic tests can also be useful, as well as sonic investigations (recommended if the system has a reduced thickness), and thermographic tests induced by artificial heat. These tests are needed particularly in the case of interventions with FRCM with regularization of the substrate.

Repairs depend on the reason of the damage as well as the type of FRCM and the type and extent of the damage. Potential repairs should be reported in the *installation, repair and maintenance manual*. If these indications are missing, it is advisable to agree with the manufacturer of the FRCM system on the choice of repair intervention and the materials to be used. In addition to the interventions, it is appropriate to provide suggestions to prevent the same phenomena from occurring in the future.

In the case of rebuilding the protective surfaces (plasters), it is necessary to inspect the FRCM strengthening system to check any structural damage following the removal of the protective surface.

8 CONTROL

The strengthening system shall be checked both for the acceptance of the products on site and to verify the quality of the installation of the system. Once the strengthening interventions have been completed it is necessary to carry out an assessment for the purposes of final inspection and subsequently for its possible monitoring over time. In both cases it is possible to use both destructive tests and partially destructive tests. The tests shall be performed by qualified personnel.

If the specific strengthening configuration allows, as for example in the case of applications in winding, or in the presence of suitable anchoring devices, some checks on the substrate may be omitted.

8.1 CONSTRUCTION CHECKS ON SITE

FRCM strengthening systems shall be subjected to a series of on-site inspections to ensure an adequate level of mechanical and physical characteristics and correspondence with requirements from the design engineer.

On-site acceptance checks are carried out by destructive tests on specimens. For the number and type of tests, reference can be made to the Italian Ministerial Guidelines, entitled *Linea Guida per la identificazione, la qualificazione ed il controllo di accettazione di compositi fibrorinforzati a matrice inorganica (FRCM) da utilizzarsi per il consolidamento strutturale di costruzioni esistenti*.

8.2 QUALITY CONTROL OF THE STRENGTHENING SYSTEM

The quality of the strengthening system can be checked by semi-destructive or non-destructive tests. In particular, the semi-destructive tests are mainly considered as purely indicative for the mechanical characterization of the strengthening system. Potential defects in the installation can be detected by non-destructive tests.

The type and number of tests to be performed shall be commensurate with the significance of the interventions, evaluating the incidence of the tested areas in relation to the size of the structure.

In particular, constructions with important public or strategic functions deserve greater attention, also in regard to use by Civil Protection during an emergency.

While planning semi-destructive control tests, it is good practice to provide additional reinforcement zones ("trials") in selected parts of the structure. These areas should be selected with dimensions larger than 500 x 200 mm². The trials shall be conducted at the same time as the interventions, with the same materials and construction techniques, where their removal does not affect the failure mechanisms, taking care that they are exposed to the same environmental conditions of the main reinforcement. If more than one trial is prepared, they shall be uniformly distributed throughout the overall interventions.

8.2.1 Semi-destructive tests

Shear tearing tests can be conducted not only on trial specimens but also on non-critical areas of the interventions, one every 30m² of application for r.c. structures, and a test every 50m² for masonry. However, there shall be at least 3 per type of homogeneous test considered as significant when determining the control programme.

Shear tearing tests. This test is useful for the assessment of the quality of the application and of the preparation of the support. One method to perform the test is described below. The test takes place at a free edge of the structure where the reinforcement is applied (Figure 8.1). The availability of an appropriate free portion of composite material (i.e. not mortared) is required, in connection with the installed FRCM material. It is advisable to impregnate the free part of the reinforcement with epoxy

resin; after curing, a sliding action from the restraining the device at the edge of the substrate should be applied.

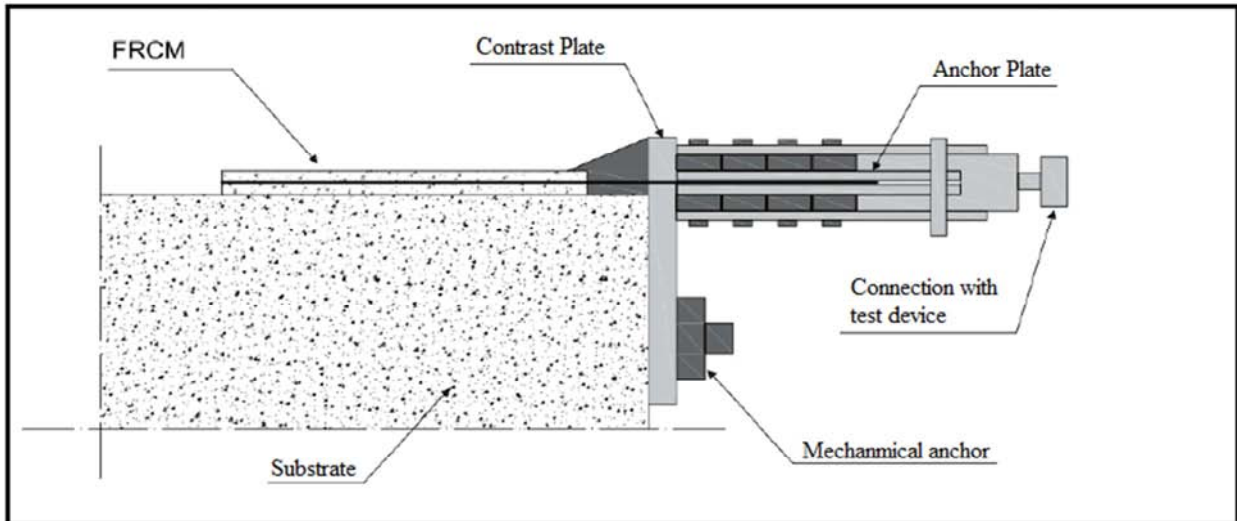


Figure 8.1 – Shear tearing test on site.

The anchoring length of FRCM shall be not less than 300 mm.

The quality of application and surface preparation are considered acceptable if at least 80% of the tests (at least two out of three in the case of three tests only) provide a traction force not lower than 85% of the value of the maximum design force, obtained from the conventional limit strain multiplied by the area of the tested dry fibre grid.

Pull-off tests (Figure 8.2) can be performed, but their interpretation may not be completely reliable in terms of the quality and capacity of the reinforcement, due to the many possible combinations between the quality of the support and the mortar for the matrix.

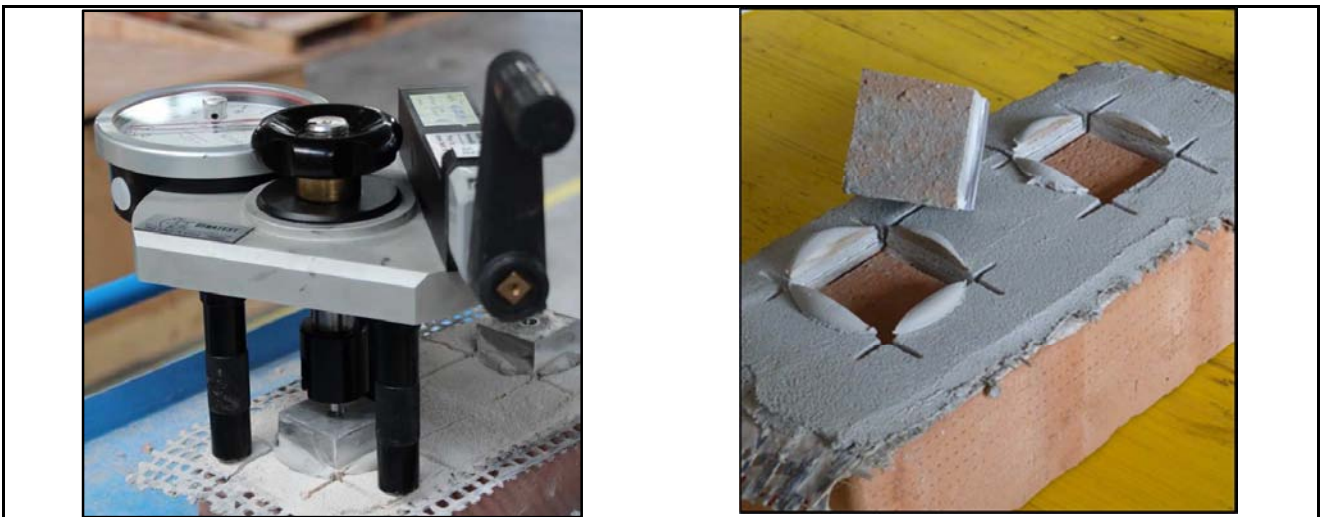


Figure 8.2 – Pull-off test.

8.2.2 Non-destructive tests

The quality of the reinforcement installation can be controlled by semi-destructive tests; particular attention or more in-depth investigations are necessary at the occurrence of any defects in the appli-

cation with an equivalent diameter of 10 cm for widespread application or 5 cm in critical areas (anchoring, overlapping, etc.). The interventions are not approved if there are defects in application covering at least 20% of the surface in each structural element.

The most common non-destructive tests are described below:

Stimulated acoustic tests. They are based on the different oscillatory behaviour of the reinforcing layer with or without adhesion to the substrate. In its most rudimentary version, the test may be performed by a technician hammering the composite surface and listening to the sound of the impact. More objective results may be obtained with automated systems. It should be noted that these tests may not give significant results for detecting defects where the strengthening system is very thick.

Thermographic tests induced by artificial heat. These may be limited in their effectiveness with reinforcing materials characterized by high thermal conductivity (carbon or steel fibres). The heat developed during the test shall not damage the FRCM system. High mortar thicknesses could limit the capacity.

9 EXPERIMENTAL TESTS ON STRUCTURAL ELEMENTS

In the case of applications different from those indicated in paragraphs 3 and 4 of this document, the design of the interventions shall be accompanied by tests to be conducted according to the provisions in clause 4.5.12 "*Design integrated by tests and verification by tests*" of the current Italian Building Code and the procedures illustrated in the Appendix D of UNI EN 1990. Such tests can be done in two ways:

- Experimentation of general nature carried out by the Manufacturer to allow applications beyond the scope of the paragraphs mentioned and made available to design engineers. The experimental/analytical document that comes from that programme shall be valid at least nationally, and point out limits in terms of type and amount of reinforcement, mechanical/geometrical class of structural elements that can be strengthened and the thresholds in terms of increase in load bearing capacity or feasible deformation. It is the responsibility of the design engineer to verify the correct interpretation of the tests conducted and applicability of the results obtained by the manufacturer to the design case.
- *One-off* experimentation required by the design engineer (or by the Works Director) for the approval of a specific project. The manufacturer is not necessarily involved. The testing programme is reduced as the values of many of the parameters such as those encountered in the real specific application can be assumed.

As stated in paragraph 4.5.12 of the Italian Building Code, the strength and efficiency of the interventions shall be measured through tests on samples of adequate size. The results of the tests, carried out on appropriate samples, should be treated with the statistical analysis methods, so as to obtain meaningful parameters such as mean and standard deviation and, when possible, an asymmetry factor of the distribution, so as to characterize a probabilistic model descriptor of the quantities investigated (considered as aleatory variables).

Regarding the details and complete operating methods for design assisted by tests, which can be found in Appendix D of UNI EN 1990, the following aspects are underlined (the variability of the parameters should be explored in the case of experimentation of general nature conducted by the manufacturer):

- Tests on structural elements strengthened with FRCM are to be considered according to the details in clause d) of Paragraph D3 (Types of tests), and in particular "*tests to reduce the uncertainties in the parameters used in the strength models; for example, tests on structural elements or assemblies of structural elements*". Therefore, clause (2) of the aforementioned paragraph states that "*The design values to be used in the tests should be derived, where possible, from the test results by applying consolidated statistical techniques. See D5 to D8*".
- Paragraph D4 (Test planning) indicates the method for setting and defining the purposes of the experimental programme; in particular, the samples and the test method shall reproduce conditions close to those of real-world applications as far as possible in terms of materials (of the structural element and reinforcement), of the load application mode and size of the specimens in order to reduce the onset of different failure modes due to scale effects as much as possible. In addition, the properties of the basic materials used in the tests shall be specified with adequate details and be similar as far as possible to those of the materials in real applications.
- The procedure shall first of all lead to determining a capacity model for the application under test, and refer to the type of structural element to be strengthened, it shall be able to reproduce the results of the experimental tests with good reliability, possibly introducing assumptions erring toward greater safety.
- The steps to follow in order to formulate and calibrate a capacity model based on a predetermined number of variables (mechanical or geometrical parameters) that are statistically inde-

pendent and defined by a Gaussian or log-normal function, based on a sufficient number of experimental test results, are explained in Paragraph D8 of the aforementioned UNI EN 1990. All the most significant factors dependent on the variables shall be explored, and for each selected combination of parameters at least two tests shall be carried out (or preferably three tests in order to reduce the experimental uncertainties). In the calibration of the capacity model, the values actually measured on prototypes shall be used as input parameters. For each selected combination of parameters, the average of the experimental results shall not be lower than the value predicted by the model.

- The two potential methods for deriving the design values from the experimental results are described in Paragraph D5 (Derivation of the design values) of the aforementioned UNI EN 1990. Typically, in the usual situations, method (a) is applicable *"estimating a characteristic value, which is then divided by a partial factor and possibly multiplied, if necessary, by an explicit conversion factor (see D7.2 and D8.2)"*.

The criteria for obtaining the characteristic values and partial factors related to the specific capacity model are illustrated in paragraph D6 (General principles for statistical evaluations) and detailed in paragraph D8 (Statistical determination of capacity models).

In the case of comprehensive experimental programmes, it is possible to simplify the approach proposed in the above paragraphs, by determining the coefficient of variation of the experimental results (required to derive characteristic values) for only one or more of the parameter combinations, and applying this coefficient uniformly for any parameter combination. This procedure can be used as long as the failure mode is similar throughout the variability range of the parameters considered. The minimum number of tests required to estimate the coefficient of variation is 5.

10 REFERENCES

Materials

- Tensile and bond tests

Bilotta A, Ceroni F, Lignola GP, Prota A. Use of DIC technique for investigating the behaviour of FRCM materials for strengthening masonry elements. *Compos Part B* 2017; 129:251-270

Bilotta A, Ceroni F, Nigro E, Pecce M. Experimental tests on FRCM strengthening systems for tuff masonry elements. *Constr Build Mater* 2017, 138:114-133

Carozzi FG, Milani G, Poggi C. Mechanical properties and numerical modeling of Fabric Reinforced Cementitious Matrix (FRCM) systems for strengthening of masonry structures. *Compos Struct* 2014;107:711-725.

Carozzi FG, Poggi C. Mechanical properties and debonding strength of Fabric Reinforced Cementitious Matrix (FRCM) systems for masonry strengthening. *Compos Part B* 2015;70:215-230.

D'Antino T, Carloni C, Sneed LH, Pellegrino C. Matrix-fiber bond behavior in PBO FRCM composites: A fracture mechanics approach. *Eng Fract Mech* 2014;117:94-111.

D'Ambrisi A, Feo L, Focacci F. Experimental analysis on bond between PBO-FRCM strengthening materials and concrete. *Compos Part B* 2013;44(1):524-532.

D'Ambrisi A, Feo L, Focacci F. Experimental and analytical investigation on bond between Carbon-FRCM materials and masonry. *Compos Part B* 2013;46:15-20.

D'Antino T, Papanicolaou C. Mechanical characterization of textile reinforced inorganic-matrix composites. *Compos Part B* 2017;127:78-91.

de Felice G, De Santis S, Garmendia L, Ghiassi B, Larrinaga P, Lourenço PB, Oliveira DV, Paolacci F, Papanicolaou CG. Mortar-based systems for externally bonded strengthening of masonry. *Mater Struct* 2014;47(12):2021-2037.

De Santis S, de Felice G. Steel reinforced grout systems for the strengthening of masonry structures. *Composite Structures*, 2015;134:533-548.

Donnini J, Corinaldesi V, Nanni A. Mechanical properties of FRCM using carbon fabrics with different coating treatments. *Compos Part B* 2016; 88; 220-228.

Razavizadeh A, Ghiassi B, Oliveira DV. Bond behavior of SRG-strengthened masonry units: Testing and numerical modeling. *Constr Build Mater* 2014;64:387-397.

Sneed LH, D'Antino T, Carloni C, Pellegrino C. A comparison of the bond behavior of PBO-FRCM composites determined by double-lap and single-lap shear tests. *Cement and concrete composites* 2015; 64; 37-48.

- Round Robin Test Rilem TC 250-CSM

Caggegi C, Carozzi FG, De Santis S, Fabbrocino F, Focacci F, Hojdis L, Lanoye E, Zuccarino L. Experimental analysis on tensile and bond properties of PBO and Aramid fabric reinforced cementitious matrix for strengthening masonry structures. *Compos Part B* 2017;127:175-195.

Carozzi FG, Bellini A, D'Antino T, de Felice G, Focacci F, Hojdys L, Laghi L, Lanoye E, Micelli F, Panizza M, Poggi C. Experimental investigation of tensile and bond properties of Carbon-FRCM composites for strengthening masonry elements. *Compos Part B*. 2017, 128:100-119

De Santis S, Carozzi FG, de Felice G, Poggi C. Test methods for Textile Reinforced Mortar systems. *Compos Part B*, 2017;127:121-132.

De Santis S, Ceroni F, de Felice G, Fagone M, Ghiassi B, Kwiecień A, Lignola GP, Morganti M, Santandrea M, Valluzzi MR, Viskovic A. Round Robin Test on tensile and bond behaviour of Steel Reinforced Grout systems. *Compos Part B* 2017;127:100-120.

Leone M, Aiello MA, Balsamo A, Carozzi FG, Ceroni F, Corradi M, Gams M, Garbin E, Gattesco N, Krajewski P, Mazzoti C, Oliveira DV, Papanicolaou CG, Ranocchiali G., Roscini F, Saenger D. Glass fabric reinforced cementitious matrix: Tensile properties and bond performance on masonry substrate. *Compos Part B* 2017;127:196-214.

Lignola GP, Caggegi C, Ceroni F, De Santis S, Krajewski P, Lourenço PB, Morganti M, Papanicolaou C, Pellegrino C, Prota A, Zuccarino L. Performance assessment of basalt FRCM for retrofit applications on masonry. *Compos Part B* 2017;128:1-18.

- **Qualification and test methods**

Arboleda D, Carozzi F, Nanni A, Poggi C. Testing Procedures for the Uniaxial Tensile Characterization of Fabric-Reinforced Cementitious Matrix Composites. *Compos Struct* 2015;04015063.

Ascione L, de Felice G, De Santis S. A qualification method for externally bonded Fibre Reinforced Cementitious Matrix (FRCM) strengthening systems. *Compos Part B*, 2015,78:497-506.

de Felice G, Aiello MA, Caggegi C, Ceroni F, De Santis S, Garbin E, Gattesco N, Hojdys Ł, Krajewski P, Kwiecień A, Leone M, Lignola GP, Mazzotti C, Oliveira D, Papanicolaou C, Poggi C, Triantafillou T, Valluzzi MR, Viskovic A. Recommendation of RILEM TC 250-CSM: Test method for Textile Reinforced Mortar to substrate bond characterization. *Materials and Structures* 2018;51(4):95.

In-plane wall strengthening

Babaeidarabad S, De Caso F, Nanni A. URM walls strengthened with fabric-reinforced cementitious matrix composite subjected to diagonal compression. *Journal of Composites for Construction*, 2014.18.

Balsamo A, Asprone D, Iovinella I, Maddaloni G, Menna C, Prota A, Ceroni F, Zinno A. Effectiveness of inorganic matrix-grid composites for strengthening masonry walls. *Proceeding of 16th IB2MAC - International Brick and Block Masonry Conference, Padova, Italy, June 2016.*

Balsamo A, Di Ludovico M, Prota A, Manfredi G. Masonry Walls Strengthened with Innovative Composites. *Proceedings of the 10th International Research Symposium on Fiber Reinforced Polymer Reinforcement for Concrete Structures FRPRCS ACI SP-275, Tampa, Florida, USA, April 2-4, 2011, ACI SP-275-44. (ISBN: 0-87031-412-2).*

Balsamo A, Iovinella I, Di Ludovico M, Prota A. Masonry reinforcement with IMG composites: Experimental investigation, *Key Engineering Materials*, 4th International Conference on Mechanics of Masonry Structures Strengthened with Composite Materials, MuRiCO 2014; Ravenna; Italy; 9-11 September 2014; Code 109316, Volume 624, 2015, Pages 275-282.

- Balsamo A, Iovinella I, Morandini G. FRG strengthening systems for masonry building. Proceeding of NZSEE Conference, Auckland, 21-23 March 2014.
- Baratta A, Corbi I. Topology optimization for reinforcement of no-tension structure, *J. Acta Mechanica*, 2014, 225,:663 – 678.
- Borri A, Corradi M, Sisti R, Buratti C, Belloni E, Moretti E. Masonry wall panels retrofitted with thermal-insulating GFRP-reinforced jacketing. *Mater Struct* 2016, 49: 3957.
- Brignola S, Frumento S, Lagomarsino S, Podestà S. Identification of shear parameters of masonry panels through the in-situ diagonal compression test. *Int J Arch Heritage* 2009, 3:52–73.
- Calderini C, Cattari S, Lagomarsino S. The use of the diagonal compression test to identify the shear mechanical parameters of masonry. *Constr Build Mater* 2010; 24:677–85.
- Cascardi A, Micelli F, Aiello MA. Analytical model based on artificial neural network for masonry shear walls strengthened with FRM systems, *Compos Part B*, 2016, 95:252-263.
- Corbi I. FRP reinforcement of masonry panels by means of C-fibre strips. *Compos Part B*, 2013, 478:348-356.
- Corbi I, Corbi O. Analysis of bi-dimensional solids with internal unilateral constraint coupled to structural elements with different degree of connection, *J. Acta Mechanica*, 2017, 228(2): 607-616.
- Corradi M, Borri A, Castori G, Sisti R. Shear strengthening of wall panels through jacketing with cement mortar reinforced by GFRP grids. *Compos Part B*, 2014, 64:33–42.
- Faella C, Martinelli E, Nigro E, Paciello S. Shear capacity of masonry walls externally strengthened by a cement-based composite material: An experimental campaign. *Constr Build Mater*, 2010, 24:84–93.
- Gattesco N, Dudine A. Efficacia di una tecnica di rinforzo per murature con intonaco in GFRP. Proceeding of National Conference "sulla Sicurezza e Conservazione nel recupero dei beni colpiti dal sisma: Strategie e tecniche di ricostruzione ad un anno dal terremoto abruzzese", vol. 1, p. 251-260, IUAV, Venezia, 8-9 aprile 2010.
- Lignola GP, Bilotta A, Ceroni F. Assessment of the effect of FRCM materials on the behaviour of masonry walls by means of FE models. *Eng Struct*, 2019, 184:145-157.
- Lignola GP, Prota A, Manfredi G. Nonlinear Analyses Of Tuff Masonry Walls Strengthened With Cementitious Matrix–Grid Composites. *Journal of Composites for Construction*, 2009, 13(4):243-251.
- Lignola GP, Prota A, Manfredi G. Numerical investigation on the influence of FRP retrofit layout and geometry on the in-plane behavior of masonry walls. *Journal of Composites for Construction*, 2012, 16(6):712-723.
- Menna C, Asprone D, Durante M, Zinno A, Balsamo A, Prota A. Structural behaviour of masonry panels strengthened with an innovative hemp fibre composite grid. *Constr Build Mater*, 2015, 100:111–121.
- Micelli F, Sciolti MS, Leone M, Aiello MA, Dudine A. Shear behaviour of Fiber Reinforced Mortar strengthened masonry walls built with limestone blocks and hydraulic mortar. In: *Brick and Block Masonry – Trends, Innovations and Challenges – Modena*, da Porto & Valluzzi (Eds) 2016 Taylor & Francis Group, London, ISBN 978-1-138-02999-6.
- Parisi F, Iovinella I, Balsamo A, Augenti N, Prota A. In-plane behaviour of tuff masonry strengthened with inorganic matrix–grid composites. *Compos Part B*, 2013, 45(1):1657–1666.

Prota A, Marcari G, Fabbrocino G, Manfredi G, Aldea C. Experimental in-plane behavior of tuff masonry strengthened with cementitious matrix-grid composites; *Journal of Composites for Construction*, 2006, 10(3):223-233.

Prota A, Manfredi G, Nardone F. Assessment of design formulas for in-plane FRP strengthening of masonry walls. *Journal of Composites for Construction*, 2008, 12(6):643–649.

Out-of-plane wall strengthening

Babaeidarabad S, De Caso F, Nanni A. Out-of-Plane Behavior of URM Walls Strengthened with Fabric-Reinforced Cementitious Matrix Composite, *Journal of Composites for Construction*, 2014a, 18(4), Art. 04013057.

Babaeidarabad S, Loreto G, Arboleda D, Nanni A. FRCM-Strengthened CMU Masonry Walls Subjected to Out-of-Plane Load, *The Masonry Society Journal*, 2014b, 32(1):69-81.

Baratta A, Corbi I, Corbi O. Bounds on the Elastic Brittle solution in bodies reinforced with FRP/FRCM composite provisions, *Compos Part B*, 2015, 68:230-236.

Baratta A, Corbi O. Closed-form solutions for FRP strengthening of masonry vaults, *J. Computers and Structures*, 2015, 147: 244-249.

Baratta A, Corbi O. An approach to the positioning of FRP provisions in vaulted masonry structures, *Compos Part B*, 2013, 53:334 – 341.

Baratta A, Corbi O. Stress Analysis of Masonry Vaults and Static Efficacy of FRP Repairs. *Intern. Journal of Solids and Structures*, 2007, 44(24): 8028-80

Bellini A, Incerti A, Bovo M, Mazzotti C. Effectiveness of FRCM reinforcement applied to masonry walls subject to axial force and out-of-plane loads evaluated by experimental and numerical studies, *International Journal of Architectural Heritage*, 2017a, 12(3):376-394

Bernat-Maso E, Escrig C, Aranha CA, Gil L. Experimental assessment of Textile Reinforced Sprayed Mortar strengthening system for brickwork wallettes, *Constr Build Mater*, 2014, 50:226-236.

Carozzi FG, Colombi P, Poggi C. Fabric reinforced cementitious matrix (FRCM) system for strengthening of masonry elements subjected to out-of-plane loads, *Advanced Composites in Construction (ACIC 2015) - Proceedings of the 7th Biennial Conference on Advanced Composites In Construction*, University of Cambridge, Cambridge, UK, 2015 September 9-11, pp. 182-188.

Corbi I, Corbi O. Combinational optimization for shaping discrete tensile boost elements in continuum structures; *J. Acta Mechanica*, 2018, 229 (9): 3575–3584.

D'Antino T, Carozzi FG, Colombi P, Poggi C. Out-of-plane maximum resisting bending moment of masonry walls strengthened with FRCM composites. *Composite Structures*, 2018, 202:881-896.

D'Ambra C, Lignola GP, Prota A, Sacco E, Fabbrocino F. Experimental performance of FRCM retrofit on out-of-plane behaviour of clay brick walls. *Compos Part B*, 2018, 148:198-206.

Fabbrocino F, Ramaglia G, Lignola GP, Prota A. Ductility-based incremental analysis of curved masonry structures". *Engineering Failure Analysis*, 2019, 97:653-675.

Harajli M, Elkhatib H, San-Jose T. Static and cyclic out-of-plane response of masonry walls strengthened using textile-mortar system, *Journal of materials in civil engineering*, 2010, 22(11):1171-1180.

Papanicolaou CG, Trinantafillou TC. Papathanasiou, M.; Karlos, K, Textile reinforced mortar (TRM) versus FRP as strengthening material of URM walls: out- of- plane cyclic loading, *Materials and Structures*, 2008, 41(1):143-157.

Papanicolaou CG, Trinantafillou TC, Lekka M. Externally bonded grids as strengthening and seismic retrofitting materials of masonry panels, *Constr Build Mater*, 2011, 25(2):504-515.

Ramaglia G, Lignola GP, Fabbrocino F, Prota A. Numerical investigation of masonry strengthened with composites. *Polymers*, 2018, 10 (3), art. no. 334.

Valluzzi MR, Da Porto F, Garbin E, Panizza M. Out-of-plane behavior of infill masonry panels strengthened with composite materials, *Mater Struct* 2014, 47(12):2131-2145.

Confinement

Balsamo A, Cascardi A, Di Ludovico M, Aiello MA, Morandini G. Analytical study on the effectiveness of the FRCM-confinement of masonry columns. In: *Construction Pathology, Rehabilitation Technology and Heritage Management* May 15-18, 2018. Cáceres, Spain.

Carlioni C, Mazzotti C, Savoia M, Subramaniam KV. Confinement of Masonry Columns with PBO FRCM Composites. *Key Engineering Materials*, 2014, 624.

Cascardi A, Aiello MA, Triantafillou T. Analysis-oriented model for concrete and masonry confined with fiber reinforced mortar. *Mater Struct*, 2017, 50(4):202.

Cascardi A, Longo F, Micelli F, Aiello MA. Compressive strength of confined column with Fiber Reinforced Mortar (FRM): New design-oriented-models. *Constr Build Mater*, 2017, 156:387-401.

Cascardi A, Micelli F, Aiello MA. FRCM-confined masonry columns: experimental investigation on the effect of the inorganic matrix properties. *Constr Build Mater*, 2018, 186:811-825.

Di Ludovico M, Fusco E, Prota A, Manfredi G. Experimental behavior of masonry columns confined using advanced materials. In *The 14th world conference on earthquake engineering*. 2008

Fossetti M, Minafò G. Strengthening of Masonry Columns with BFRCM or with Steel Wires: An Experimental Study. *Fibers*, 2016, 4(2):15.

Incerti A, Vasiliu A, Ferracuti B, Mazzotti C. Uni-Axial compressive tests on masonry columns confined by FRP and FRCM. In *Proc. of the 12th International Symposium on Fiber Reinforced Polymers for Reinforced Concrete Structures & The 5th Asia-Pacific Conference on Fiber Reinforced Polymers in Structures*, Joint Conference, Nanjing, China, 14–16 December 2015.

Maddaloni G, Cascardi A, Balsamo A, Di Ludovico M, Micelli F, Aiello MA, Prota A. Confinement of Full-Scale Masonry Columns with FRCM Systems. In *Key Engineering Materials*, 2017, 747:374-381.

Mezrea PE, Yilmaz IA, Ispir M, Binbir E, Bal IE, Ilki A. External Jacketing of Unreinforced Historical Masonry Piers with Open-Grid Basalt-Reinforced Mortar. *Journal of Composites for Construction*, 2016, 21(3), 04016110.

Minafò G, La Mendola L. Experimental investigation on the effect of mortar grade on the compressive behaviour of FRCM confined masonry columns. *Compos Part B*, 2018, 146:1-12.

Ombres L. Confinement effectiveness in eccentrically loaded masonry columns strengthened by Fiber Reinforced Cementitious Matrix (FRCM) jackets. In *Key Engineering Materials* 2015, 624:551-558.

Ombres L, Verre S. Masonry columns strengthened with Steel Fabric Reinforced Cementitious Matrix (S-FRCM) jackets: experimental and numerical analysis. *Measurement*, 2018, 127:238-245.

Santandrea M, Quartarone G, Carloni C, Gu XL. Confinement of Masonry Columns with Steel and Basalt FRCM Composites. In *Key Engineering Materials*, 2017, 747:342-349.

Sneed LH, Carloni C, Baietti G, Fraioli G. Confinement of Clay Masonry Columns with SRG. In *Key Engineering Materials*, 2017, 747: 350-357.

Witzany J, Zigler R. Stress State Analysis and Failure Mechanisms of Masonry Columns Reinforced with FRP under Concentric Compressive Load. *Polymers*, 2016, 8(5):176.

Yilmaz I, Mezrea P, Ispir M, Binbir E, Bal IE, Ilki A. External Confinement of Brick Masonry Columns with Open-Grid Basalt Reinforced Mortar. In *Proceedings of the Fourth Asia-Pacific Conference on FRP in Structures (APFIS 2013)*, Melbourne, Australia (pp. 11-13).

Flexural strengthening of r.c. members

Babaeidarabad S, Loreto G, Nanni A. Flexural strengthening of RC beams with an externally bonded fabric-reinforced cementitious matrix. *Journal of Composites for Construction*, 18(5):1-12.

Bencardino F, Carloni C, Condello A, Focacci F, Napoli A, Realfonzo R. Flexural behavior of RC members strengthened with FRCM: State-of-the-art and predictive formulas. *Compos Part B*, 2018, 148:132-148.

Carloni C, Bournas DA, Carozzi FC, D'Antino T, Fava G, Focacci F, Giacomini G, Mantegazza G, Pellegrino C, Perinelli C, Poggi C. Fiber reinforced composites with cementitious (inorganic) matrix. In *Design procedures for the use of composites in strengthening of reinforced concrete structures, State-of-the-Art Report of the RILEM Technical Committee 234-DUC*, Springer, 2016:349-92.

D'Ambrisi A, Focacci F. Flexural strengthening of RC beams with cement based composites. *Journal of Composites for Construction*, 2011, 15(2):707-20.

Hashemi S, Al-Mahaidi R. Experimental and finite element analysis of flexural behavior of FRP-strengthened RC beams using cement-based adhesives. *Constr Build Mater*, 2012, 26:268-73.

Ombres L. Flexural analysis of reinforced concrete beams strengthened with a cement based high strength composite material. *Composite Structures*, 2011, 94(1):143-55.

Pellegrino C, D'Antino T. Experimental behavior of existing precast prestressed reinforced concrete elements strengthened with cementitious composites. *Compos Part B*, 2013, 55:31-40.

Sneed LH, Verre S, Carloni C, Ombres L. Flexural behavior of RC beams strengthened with steel-FRCM composite. *Eng Struct*, 2016, 127:686-99.

Shear strengthening of r.c. members

Carloni C, Bournas DA, Carozzi FC, D'Antino T, Fava G, Focacci F, Giacomini G, Mantegazza G, Pellegrino C, Perinelli C, Poggi C. Fiber reinforced composites with cementitious (inorganic) matrix. In *Design procedures for the use of composites in strengthening of reinforced concrete structures, State-of-the-Art Report of the RILEM Technical Committee 234-DUC*, Springer, 2016:349-92.

Chen JF, Teng JG. Shear capacity of FRP-strengthened RC beams: FRP debonding. *Constr Build Mater* 2003;17(1):27-41.

D'Antino T, Focacci F, Sneed LH, Pellegrino C. Shear Strength Model for RC Beams with U-Wrapped FRCM Composites. *Journal of Composites for Construction*. Vol 24, No 1. 04019057:1-12.

Gonzalez-Libreros JH, Pellegrino C, D'Antino T, Sneed LH. Evaluation of external transversal reinforcement strains of RC beams strengthened in shear with FRCM composites, In Proc of the 8th biennial Conference on Advanced Composites in Construction (ACIC 2017), Sheffield, UK, September 2017.

Gonzalez-Libreros JH, Sabau C, Sneed LH, Pellegrino C, Sas G. State of Research on Shear Strengthening of RC Beams Using FRCM Composites. *Constr Build Mater* 2017;149:444-458.

Gonzalez-Libreros JH, Sneed LH, D'Antino T, Pellegrino C. Behavior of RC beams strengthened in shear with FRP and FRCM composites. *Eng Struct* 2017;150:830–42.

Monti G, Liotta MA. Test and design equations for FRP-strengthening in shear, *Constr Build Mater* 2007;21:799-809.

Sneed LH, D'Antino T, Focacci F, Gonzalez-Libreros J, Pellegrino C. Contribution of Externally Bonded FRCM to the Shear Strength of RC Beams – A Mechanical Model. October 14, 2018, ACI Fall 2018 Convention, Las Vegas, NV.

11 NUMERICAL EXAMPLES

Some numerical examples are provided with the aim of helping the reader apply the design provisions offered in the previous paragraphs. Symbols have been already defined.

11.1 IN-PLANE STRENGTHENING OF MASONRY WALLS

11.1.1 Shear capacity

Brick Masonry

A masonry pier panel is assumed under external environmental exposure, made of solid clay bricks, having thickness $t = 250$ mm, height $\ell = 2$ m e length $H = 1$ m loaded in-plane in shear. A glass FRCM system is assumed having conventional limit stress $\varepsilon_{\text{lim,conv}} \cdot E_f = 1000$ MPa and dry equivalent thickness of the grid $t_f = 0.025$ mm, balanced with fibres aligned with horizontal and vertical directions of the panel, fully covering the wall sides ($\ell_f = H$).

The minimum shear capacity of unreinforced masonry (V_t), evaluated according to Italian Building Code (*NTC - Circolare n. 7 del 21 gennaio 2019 - 8.7.1.16*) is:

$$V_t = H \cdot t \cdot \frac{1.5\tau_{0d}}{p} \sqrt{1 + \frac{\sigma_0}{1.5\tau_{0d}}} = 1000 \cdot 250 \cdot \frac{1.5 \cdot 0.05}{1.5} \sqrt{1 + \frac{0.5}{1.5 \cdot 0.05}} = 34.6 \text{ kN},$$

assuming a shear stress capacity $\tau_{0d} = 0.05$ MPa and a stress $\sigma_0 = 0.5$ MPa due to gravity loads and corrective coefficient p of stresses in the cross section is equal to its maximum value 1.5 in this case.

The shear strength of reinforced wall ($v_{t,R}$) is the sum of the unreinforced masonry contribution (V_t) and FRCM contribution ($v_{t,f}$):

$$V_{t,f} = 0.5 \cdot n_f \cdot t_{VF} \cdot \ell_f \cdot \alpha_t \cdot \varepsilon_{fd} \cdot E_f = 0.5 \cdot 2 \cdot 0.025 \cdot 1000 \cdot 0.8 \cdot 800 = 16.0 \text{ kN},$$

where:

- $n_f = 2$ is the total number of the reinforcing layers arranged at the sides of the wall (one on each side);
- $t_{VF} = 0.025$ mm is the equivalent thickness of a single layer of the FRCM system, t_f of the fibres in horizontal direction.
- $\varepsilon_{fd} = \eta \frac{\varepsilon_{\text{lim,conv}}^{(\alpha)}}{\gamma_m} = 0.8 \frac{1.5 \cdot 1000 / E_f}{1.5} = \frac{800}{E_f}$ is derived from $\varepsilon_{\text{lim,conv}}^{(\alpha)}$.

The shear capacity of the strengthened wall is thus obtained:

$$V_{t,R} = 34.6 \text{ kN} + 16.0 \text{ kN} = 50.6 \text{ kN}.$$

Lastly the shear capacity is checked to ensure that it is lower than the shear force inducing the diagonal crushing of the masonry:

$$V_{t,c} = 0.25 \cdot f_{md} \cdot t \cdot d_f = 0.25 \cdot 2.5 \cdot 250 \cdot 1000 = 156.25 \text{ kN},$$

where $f_{md} = 2.5 \text{ MPa}$ is the design compressive strength of brick masonry.

Note: using the corrective coefficients from Table 4.1 ($0.8 \cdot 1.7$) it is $V_{t,R} = 41.3 \text{ kN}$.

Tuff Masonry

A masonry pier panel is assumed under internal environmental exposure, made of tuff stone, having thickness $t = 400 \text{ mm}$, height $\ell = 2 \text{ m}$ e length $H = 1 \text{ m}$ loaded in-plane in shear. A glass FRCM system is assumed having conventional limit stress $\varepsilon_{lim,conv} \cdot E_f = 1000 \text{ MPa}$ and dry equivalent thickness of the grid $t_f = 0.025 \text{ mm}$, balanced with fibres aligned with horizontal and vertical directions of the panel, fully covering the wall sides ($\ell_f = H$).

The minimum shear capacity of unreinforced masonry (V_t), evaluated according to Italian Building Code (*NTC - Circolare n. 7 del 21 gennaio 2019 - 8.7.1.16*) is:

$$V_t = H \cdot t \cdot \frac{1.5\tau_{0d}}{p} \sqrt{1 + \frac{\sigma_0}{1.5\tau_{0d}}} = 1000 \cdot 400 \cdot \frac{1.5 \cdot 0.02}{1.5} \sqrt{1 + \frac{0.3}{1.5 \cdot 0.02}} = 26.5 \text{ kN},$$

assuming a shear stress capacity $\tau_{0d} = 0.02 \text{ MPa}$ and a stress $\sigma_0 = 0.3 \text{ MPa}$ due to gravity load and corrective coefficient p of stresses in the cross section is equal to its maximum value 1.5 in this case.

The shear strength of the reinforced wall ($V_{t,R}$) is the sum of the unreinforced masonry contribution (V_t) and FRCM contribution ($V_{t,f}$):

$$V_{t,f} = 0.5 \cdot n_f \cdot t_{vf} \cdot \ell_f \cdot \alpha_t \cdot \varepsilon_{fd} \cdot E_f = 0.5 \cdot 2 \cdot 0.025 \cdot 1000 \cdot 0.8 \cdot 900 = 18.0 \text{ kN},$$

where:

- $n_f = 2$ is the total number of the reinforcing layers arranged at the sides of the wall (one on each side);
- $t_{vf} = 0.025 \text{ mm}$ is the equivalent thickness of a single layer of the FRCM system, t_f of the fibres in horizontal direction.
- $\varepsilon_{fd} = \eta \frac{\varepsilon_{lim,conv}^{(\alpha)}}{\gamma_m} = 0.9 \frac{1.5 \cdot 1000 / E_f}{1.5} = \frac{900}{E_f}$ derived from $\varepsilon_{lim,conv}^{(\alpha)}$.

The shear capacity of the strengthened wall is thus obtained:

$$V_{t,R} = 26.5 \text{ kN} + 18 \text{ kN} = 44.5 \text{ kN}_t.$$

Lastly the shear capacity is checked to ensure that it is lower than the shear force inducing the diagonal crushing of the masonry:

$$V_{t,c} = 0.25 \cdot f_{md} \cdot t \cdot d_f = 0.25 \cdot 1.5 \cdot 400 \cdot 1000 = 150 \text{ kN},$$

where $f_{md} = 1.5 \text{ MPa}$ is the design compressive strength of tuff masonry.

Note: using the corrective coefficients from Table 4.1 ($0.9 \cdot 2.0$) it is $V_{t,R} = 36.9$ kN.

11.1.2 In-plane combined axial and bending moment capacity

A masonry panel characterized by a transversal section having high $H = 1500$ mm and thickness $t = 280$ mm is considered (Figure 11.1).

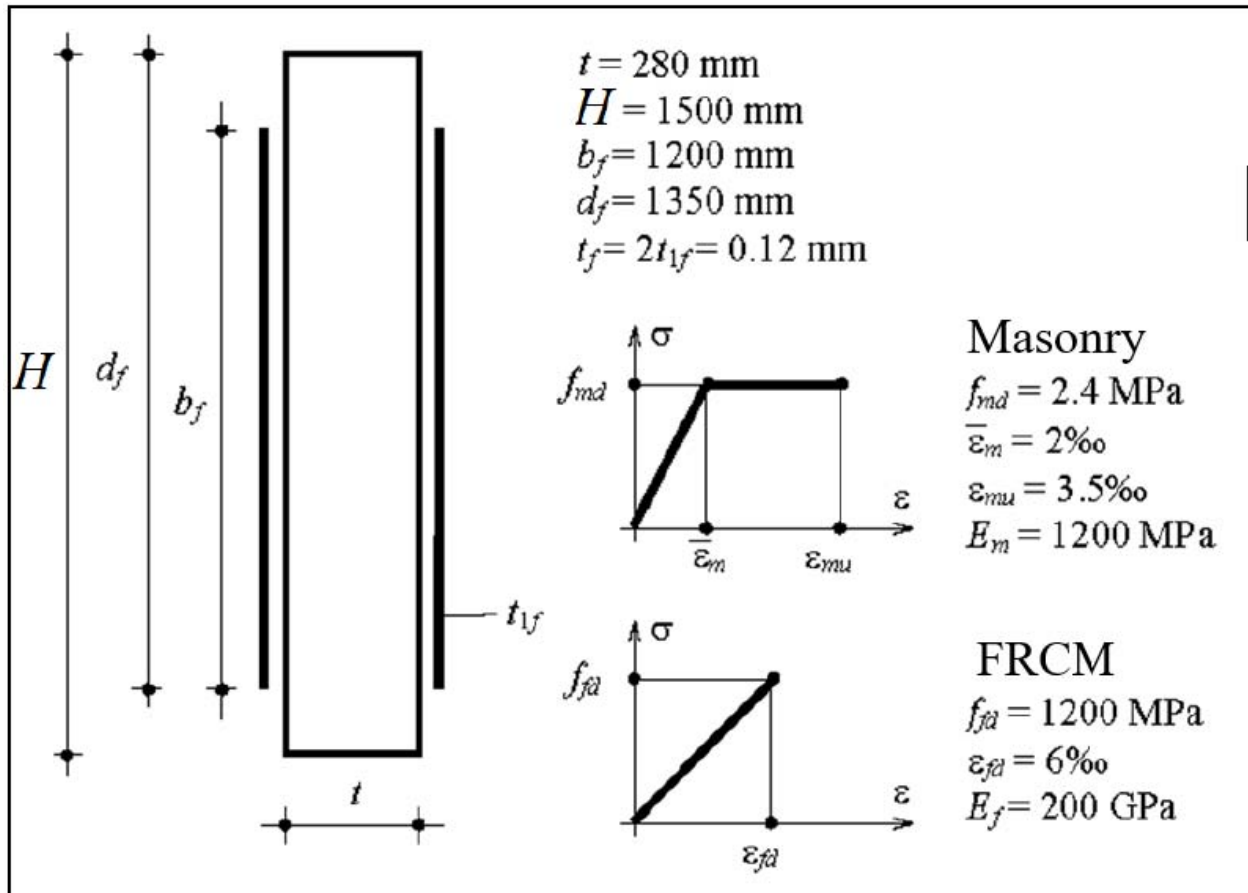


Figure 11.1 – Section geometry and strengthening characteristics.

A strengthening with an equivalent thickness $t_f = 0.06$ mm is applied on each side of the panel so that the strengthening thickness for the in-plane bending action is $t_{2f} = 2t_f = 0.12$ mm. Strengthening is characterized by the design strain $\epsilon_{fd} = 6\text{‰}$ and the elastic modulus $E_f = 200$ GPa. It is extended up to 150 mm by the edges of the panel, so that $d_f = 1500 - 150 = 1350$ mm (Figure 11.1).

The masonry is characterized by compressive strength $f_{md} = 2.4$ MPa and elastic modulus $E_m = 1200$ MPa. Therefore, $\bar{\epsilon}_m = f_{md}/E_m = 2\text{‰}$. $\epsilon_{mu} = 3.5\text{‰}$ is assumed (Figure 11.1).

The design flexural capacity of the section associated to an axial load $N = 150$ kN is to be calculated.

Considering the constitutive law of Figure 11.1 for the masonry under compression, the design flexural capacity of the un-strengthened section is given by the following:

$$M_{Rd0}(N) = f_{md} \frac{tx}{2} \cdot \left[H(1-k) - y_n(1-k)^2 + k \left(\frac{H}{2} - y_n + \frac{2}{3}ky_n \right) \right] = 94.87 \text{ kNm},$$

where $k = \bar{\varepsilon}_m / \varepsilon_{mu} = 0.571$ and:

$$y_n = \frac{2N}{f_{md}} \cdot \frac{\varepsilon_{mu}}{2\varepsilon_{mu} - \bar{\varepsilon}_m} = 312.5 \text{ mm}$$

is the distance from extreme compression fibre to neutral axis.

It is assumed that flexural failure of the strengthened section initially occurs when the ultimate strain of the masonry under compression is reached.

In line with this assumption, the distance from extreme compression fibre to neutral axis is calculated with the Equation (A1.2) as follows:

$$y_n = \frac{N - E_f t_{2f} d_f \varepsilon_{mu} + \sqrt{N^2 + E_f t_{2f} d_f \varepsilon_{mu} \left[(2-k) t d_f f_{md} - 2N \right]}}{t f_{md} (2-k) - E_f t_{2f} \varepsilon_{mu}} = 461.9 \text{ mm}.$$

The strengthening maximum strain is therefore the following:

$$\varepsilon_f = \frac{\varepsilon_{mu}}{y_n} (d_f - y_n) = 6.7\%.$$

This value is greater than the strengthening design strain. Therefore, the section failure occurs when the strengthening design strain is reached. It is assumed that, in the failure condition, the maximum masonry strain is greater than $\bar{\varepsilon}_m$. In line with this assumption, the distance from extreme compression fibre to neutral axis is calculated with the Equation (A1.6) as follows:

$$y_n = \frac{2N + t \xi f_{md} d_f + E_f t_{2f} d_f \varepsilon_{fd}}{t f_{md} (2 + \xi) + E_f t_{2f} \varepsilon_{fd}} = 465.5 \text{ mm},$$

where $\xi = \bar{\varepsilon}_m / \varepsilon_{fd} = 0.33$. The masonry maximum strain is:

$$\varepsilon_m = \frac{\varepsilon_{fd}}{d_f - y_n} y_n = 3.16\% ,$$

and the value obtained confirms the assumption previously made ($\varepsilon_m > \bar{\varepsilon}_m$).

Finally, the design bending moment is calculated with (A1.3) as follows:

$$M_{Rd}(N) = \frac{t f_{md}}{12} \left[2d_f y_n \xi (2\xi + 3) + 3H \left[y_n (2 + \xi) - \xi d_f \right] - 2y_n^2 (\xi^2 + 3 + 3\xi) - 2\xi^2 d_f^2 \right] + \varepsilon_{fd} E_f t_{2f} \frac{d_f - y_n}{12} (2y_n + 4d_f - 3H) = 143.3 \text{ kNm}.$$

Figure 11.2 shows the comparison between the strength domain $M_{Rd0}(N)$ of the un-strengthened section and the strength domain $M_{Rd}(N)$ of the strengthened section.

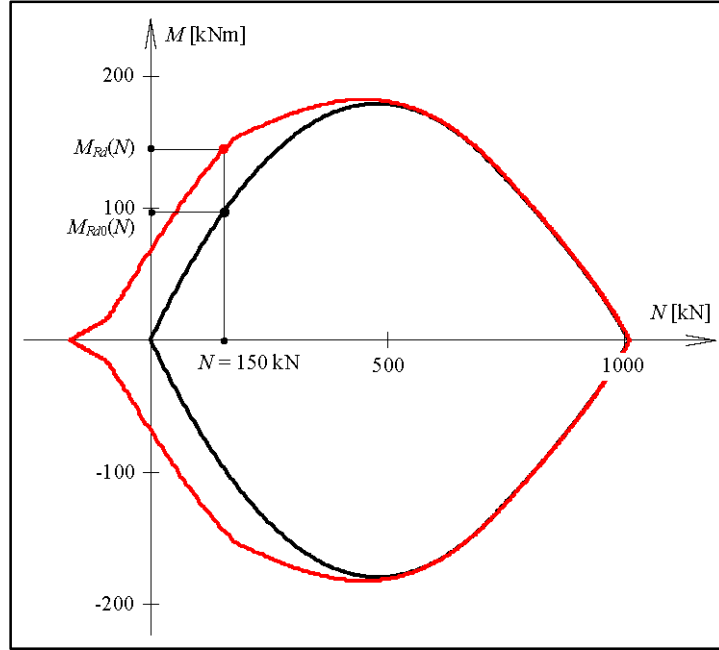


Figure 11.2 - Strength domains of the strengthened and un-strengthened sections. The domains are calculated considering the masonry constitutive law of Figure 11.1.

If the compressive stress diagram is assumed to be rectangular with a uniform compressive stress of $\alpha_m f_{md}$, distributed over an equivalent compression zone equal to βy_n , where y_n is the distance from extreme compression fibre to neutral axis and $\alpha_m = 0.85$ and $\beta = 0.8$, the design flexural capacity of the un-strengthened section is:

$$M_{Rd0}(N) = \frac{N}{2} \left(H - \frac{N}{t \alpha_m f_{md}} \right) = 92.8 \text{ kNm} .$$

For the un-strengthened masonry, it is initially assumed that flexural failure occurs when the ultimate strain of the masonry under compression is reached. In line with this assumption, the distance from extreme compression fibre to neutral axis is calculated with the Equation (A1.8) as follows:

$$y_n = \frac{N - E_f t_{2f} d_f \varepsilon_{mu} + \sqrt{N^2 + 2E_f t_{2f} d_f \varepsilon_{mu} (\alpha_m \beta t f_{md} d_f - N)}}{2\alpha_m \beta f_{md} t - E_f t_{2f} \varepsilon_{mu}} = 475.9 \text{ mm} .$$

In this case, the strengthening maximum strain is the following:

$$\varepsilon_f = \frac{\varepsilon_{mu}}{y_n} (d_f - y_n) = 6.43\% .$$

This value is greater than the strengthening design strain. Therefore, the section failure occurs when the strengthening design strain is reached. The distance from extreme compression fibre to neutral axis is calculated with the Equation (A1.10) as follows:

$$y_n = \frac{\varepsilon_{fd} \cdot E_f t_{2f} d_f + 2N}{2\alpha_m \beta f_{md} t + \varepsilon_{fd} \cdot E_f t_{2f}} = 467.3 \text{ mm} .$$

Finally, the design flexural capacity is calculated with Equation (A1.9) as follows:

$$M_{Rd}(N) = \frac{\alpha_m \beta f_{md} t y_n}{2} \cdot (H - \beta y_n) + \varepsilon_{fd} \cdot E_f t_{2f} \cdot \frac{d_f - y_n}{12} (2y_n + 4d_f - 3H) = 139.7 \text{ kNm} .$$

Figure 11.3 shows the comparison between the strength domain $M_{Rd0}(N)$ of the un-strengthened section and the strength domain $M_{Rd}(N)$ of the strengthened section.

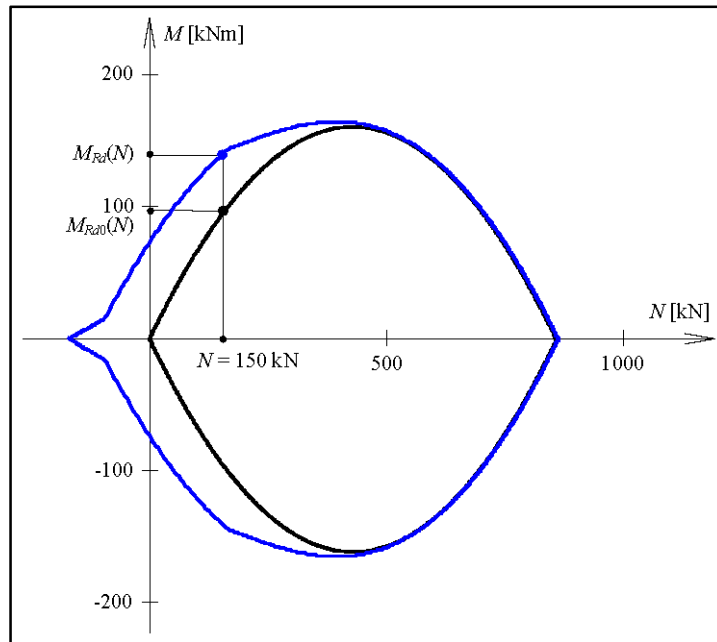


Figure 11.3 - Strength domains of the strengthened and un-strengthened sections. The domains are calculated according to a simplified approach with a uniform compressive stress of $\alpha_m f_{md}$, distributed over a distance equal to βy_n , where $\alpha_m = 0.85$ and $\beta = 0.8$.

Finally, Figure 11.4 shows the comparison between the domain $M_{Rd}(N)$ obtained with the masonry constitutive law of Figure 11.1 and the domain obtained with the application of the simplified approach with $\alpha_m = 0.85$ and $\beta = 0.8$.

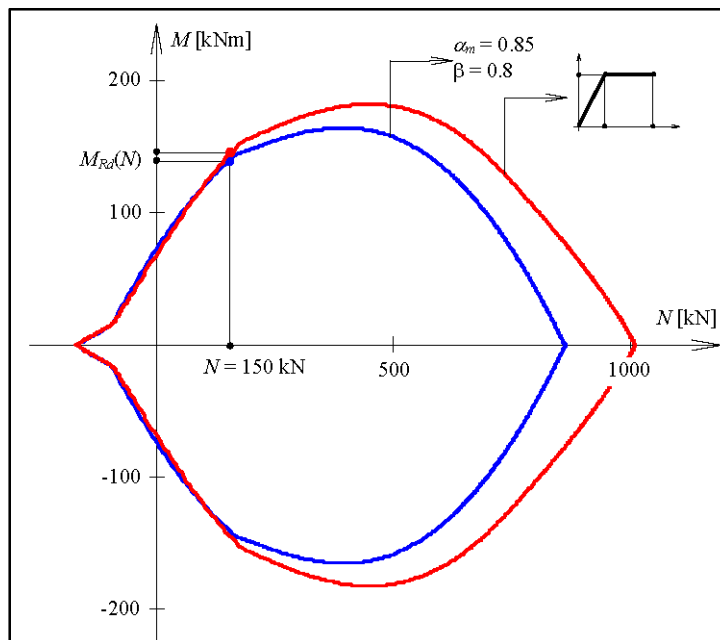


Figure 11.4 - Comparison between the domains $M_{Rd}(N)$ related to masonry constitutive law of Figure 11.1 and application of the simplified approach with $\alpha_m = 0.85$ and $\beta = 0.8$.

11.2 STRENGTHENING OF MASONRY PANELS FOR OUT-OF-PLANE LOADS

The safety of a masonry panel in an existing building subjected to out-of-plane loads is to be evaluated. This calculation is performed both without and with the FRCM strengthening system (*Ante-operam* and *post-operam conditions*, respectively). The strengthening system includes a balanced bi-directional carbon fabric applied on both sides of the panel with lime mortar. The combined axial and bending load acting on the masonry panel and the corresponding design bending moment M_{Sd} is compared with the corresponding design flexural capacity M_{Rd} associated with a specified axial load. The calculation is performed for two different values of axial loads N_{Sd} , equal to 110 kN/m and 290 kN/m, respectively. They represent the loading conditions of the centre section of a panel located at the top and the base of a building, respectively.

Furthermore, the shear check both at the top and the base of the building is performed, where the shear load V_{Sd} is equal to 27 kN/m.

All the quantities, if not expressly specified, refer to a masonry strip having unitary depth.

Characteristics of the panel section

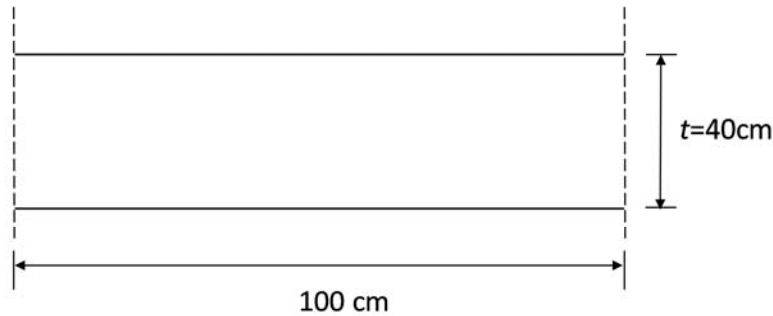


Figure 11.5 – Wall cross section.

- Thickness: $t = 40$ cm
- Level of knowledge LC2 $\rightarrow FC = 1.2$
- Partial factor for the seismic design of masonry structures: $\gamma_M = 2$
- Design compressive strain of the masonry: $\epsilon_{mu} = 0.35\%$
- Masonry elastic modulus: $E_m = 2000$ MPa
- Average compressive strength of the masonry: $f_{mu} = 4.8$ MPa
- Design compressive strength of the masonry: $f_{md} = \frac{f_{mu}}{FC \cdot \gamma_M} = \frac{4,8}{1,2 \cdot 2} = 2$ MPa
- Design axial load acting on the panel at the top of the building: $N_{Sd,top} = 110$ kN/m
- Design axial load acting on the panel at the base of the building: $N_{Sd,base} = 290$ kN/m
- Design bending moment acting on the panel at the top of the building: $M_{Sd,top} = 23.2$ kN m/m
- Design bending moment acting on the panel at the base of the building: $M_{Sd,base} = 33.7$ kN m/m
- Design shear on both panels: $V_{Sd} = 27$ kN/m

Symbols

In addition to the symbols used in the other sections of this document (see § 3.1), in the current example further symbols are introduced to guarantee a more fluid reading and a greater compaction of the formulas. They are listed below:

F_m the resultant of the masonry compression stresses (in the compressed section)

F_f the resultant of the tensile stresses in the strengthening system

Un-strengthened panel (ante-operam condition)

For the masonry, a constant distribution of the compressive stress, i.e. a *stress-block*, equal to $0.85 f_{md}$ is assumed. The depth of this distribution is $0.7 y_n$, where y_n is the distance from extreme compression fibre to neutral axis. In this way, y_n can be calculated by setting the equilibrium at the horizontal translation ($F_m = N_{sd}$), as follows:

$$F_m = 0.85 f_{md} \cdot \beta \cdot y_n = N_{sd} \cdot$$

- At the top: $0.85 \cdot 2 \cdot 0.7 \cdot y_n = 110 \rightarrow y_n = 92 \text{ mm} = 9 \text{ cm}$

- At the base: $0.85 \cdot 2 \cdot 0.7 \cdot y_n = 290 \rightarrow y_n = 243 \text{ mm} = 24 \text{ cm}$

After having calculated the position of the neutral axis, the flexural capacity of the non-strengthened section (M_{0d}) is evaluated with respect to the horizontal axis passing through the geometric centre of the masonry section:

$$M_{0d} = N_{sd} \left(\frac{t}{2} - \beta \frac{y_n}{2} \right).$$

- At the top: $M_{0d,top} = 110 \left(\frac{0.4}{2} - 0.7 \frac{0.092}{2} \right) = 18.4 \text{ kNm/m} < M_{Sd,top} = 23.2 \text{ kNm/m}$

- At the base: $M_{0d,base} = 290 \left(\frac{0.4}{2} - 0.7 \frac{0.243}{2} \right) = 33.3 \text{ kNm/m} < M_{Sd,base} = 33.7 \text{ kNm/m}$

The verification is not satisfied for both panels at the top and the base of the building.

In order to increase the bending capacity of the panel, an FRCM strengthening system with carbon fabric is applied. It entirely covers one of the two sides of the wall and consists of a balanced bi-directional net with a pitch of 10mm x 10mm applied with a lime mortar.

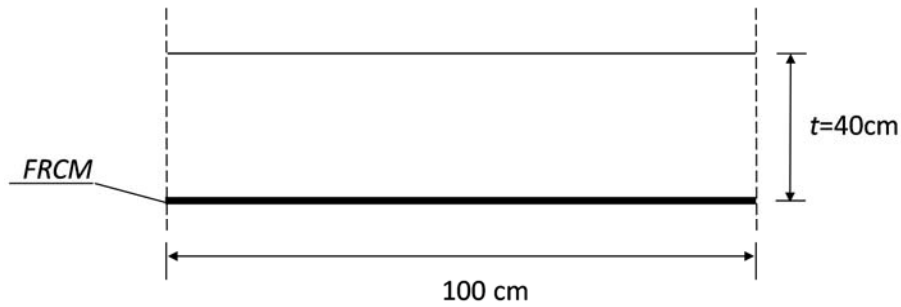
FRCM strengthening

Figure 11.6 – Strengthened section.

Strengthening system data declared in the manufacturer's technical data sheet

- Equivalent thickness of the net: $t_f = 0.047$ mm
- Elastic modulus: 240 GPa
- Fibre tensile strength: $f_{tu} = 4800$ MPa
- Fibre ultimate strain: 1.8%
- Compressive strength of the mortar: $f_{c,mat} > 20$ MPa (28gg)

Strengthening configuration

- Number of layers: $n_f = 1$
- Resistant area: $n_f \cdot t_f = 1 \cdot 0.047 = 47 \text{ mm}^2/\text{m}$

CVT data (qualification procedure)

- $E_f = 242.2$ GPa (elastic modulus of the dry fabric)
- $\sigma_{u,f} = 1601.3$ MPa (characteristic value of the ultimate stress of the dry fabric)
- $\varepsilon_{u,f} = 0.66\%$ (characteristic value of the ultimate strain of the dry fabric)
- $\sigma_u = 2233$ MPa (characteristic value of the ultimate stress of the FRCM strengthening)
- $\varepsilon_u = 0.91\%$ (average value of the ultimate strain of the FRCM strengthening)
- $\sigma_{lim,conv} = 1270$ MPa (characteristic value of the debonding capacity)
- $\varepsilon_{lim,conv} = 0.52\%$ (strain corresponding to $\sigma_{lim,conv}$ on the tensile curve of the dry fabric)

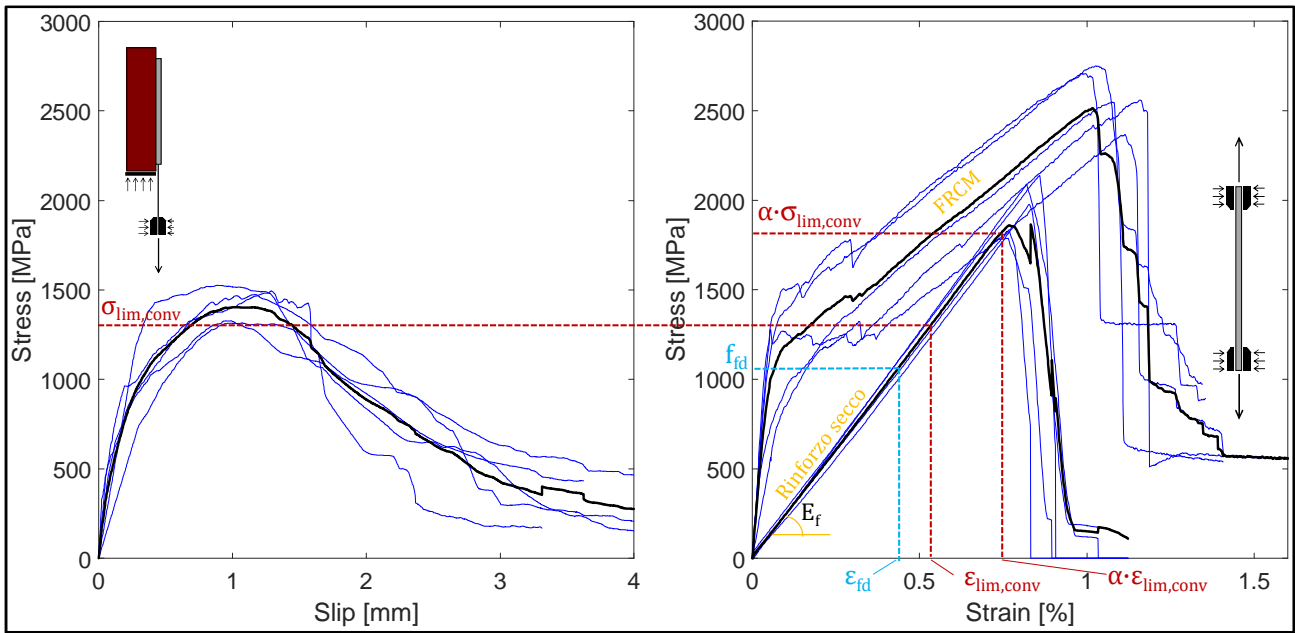


Figure 11.7 - Average stress-strain curve obtained from direct tensile tests on samples of FRCM and dry fabric.

The flexural contribution of the FRCM strengthening is taken into account multiplying the design strain, ϵ_{fd} , by the elastic modulus E_f . ϵ_{fd} is obtained amplifying the conventional strain of a factor α . If α is equal to 1.5:

$$\epsilon_{lim,conv}^{(\alpha)} = \alpha \cdot \epsilon_{lim,conv} = 1.5 \cdot 0.52\% = 0.78\% .$$

The maximum stress in the FRCM strengthening can be calculated by multiplying the design strain for the elastic modulus, as follows:

$$\sigma_{lim,conv}^{(\alpha)} = E_f \cdot \epsilon_{lim,conv}^{(\alpha)} = E_f \cdot \alpha \cdot \epsilon_{lim,conv} = 1889 \text{ MPa} < \sigma_u = 2233 \text{ MPa} .$$

The environmental conversion factor, η_a , in case of carbon fibres with internal exposure is equal to 0.9 (Table 3.1) (see § 3). For Ultimate Limit States (U.L.S.) the partial factor, γ_m , is equal to 1.5:

$$\epsilon_{fd} = \eta_a \frac{\alpha \cdot \epsilon_{lim,conv}}{\gamma_m} = 0.9 \cdot \frac{0.0078}{1.5} = 0.47\%$$

Strengthened panel (post-operam condition)

In this example, the failure of the section for the combined axial and flexural loads is due to one of the following behaviours:

- 1) Region 1: the failure of the section is due to masonry crushing under compressive loads (i.e. deformation in the masonry layer farther from the neutral axis equal to ϵ_{mu}); if this condition exists, the strain ϵ in the strengthening system shall not exceed the maximum design strain capacity of the strengthening (ϵ_{fd}).

- 2) Region 2: the failure of the section is due to tensile stresses in the strengthening system (according to the different types of strengthening, this can correspond to one of the six types of failures indicated in Section § 2.3); if this condition exists, the strain ε_m of the masonry layer farther from the neutral axis shall not exceed ε_{mu} .

For both failure regions and in the case of both strengthened and un-strengthened panels, a *stress-block* is assumed, i.e. a constant distribution of the compressive stress equal to $0.85f_{md}$ with a depth of $0.7y_n$, where y_n is the distance from extreme compression fibre to neutral axis.

Let

- F_m be the resultant of the masonry compression stresses, calculated with a *stress-block*
- F_f be the resultant of the tensile stresses in the strengthening system

After having hypothesized the failure region, the neutral axis position and the flexural capacity of the strengthened section are determined. The neutral axis and the flexural capacity are calculated by setting the equilibrium at horizontal translation ($F_m - F_f = N_{Sd}$) and the equilibrium at rotation around the horizontal axis through the geometric centre of the masonry section, respectively.

For both failure regions, the formulas for the calculation of the neutral axis position y_n , the resultant of the masonry compression stresses F_m , the resultant of the tensile stresses in the strengthening system F_f , the design flexural capacity of the strengthening system M_{ld} and the design flexural capacity of the strengthened section M_{Rd} are listed below:

- a) Region 1:

$$y_n = \frac{-(E_f \cdot \varepsilon_{mu} \cdot n_f \cdot t_f - N_{Sd}) + \sqrt{(E_f \cdot \varepsilon_{mu} \cdot n_f \cdot t_f - N_{Sd})^2 + 4 \cdot 0.85 \cdot f_{md} \cdot 0.7 \cdot E_f \cdot \varepsilon_{mu} \cdot n_f \cdot t_f \cdot t}}{2 \cdot 0.85 \cdot f_{md} \cdot 0.7}$$

$$F_m = 0.85 \cdot f_{md} \cdot 0.7 y_n$$

$$F_f = E_f \frac{\varepsilon_{mu}}{x} (t - y_n) n_f \cdot t_f$$

$$M_{ld} = F_m \left(\frac{t}{2} - \frac{0.7 y_n}{2} \right) + F_f \frac{t}{2}$$

$$M_{Rd} = M_{0d} + 0.5(M_{ld} - M_{0d})$$

- b) Region 2:

$$y_n = \frac{n_f t_f E_f \varepsilon_{fd} + N_{Sd}}{0.85 f_{md} \cdot 0.7}$$

$$F_m = 0.85 \cdot f_{md} \cdot 0.7 y_n$$

$$F_f = n_f t_f E_f \varepsilon_{fd}$$

$$M_{ld} = F_m \left(\frac{t}{2} - \frac{0.7 y_n}{2} \right) + F_f \frac{t}{2}$$

$$M_{Rd} = M_{0d} + 0.5(M_{ld} - M_{0d})$$

- At the top:

if the section failure is due to the tensile stresses in the strengthening system (region 2) it is:

$$y_n = \frac{47 \cdot 1138 + 110000}{0.85 \cdot 2 \cdot 0.7 \cdot 1000} = 137 \text{ mm} = 14 \text{ cm}$$

$$F_m = 0.85 \cdot 2 \cdot 0.7 \cdot 137 \cdot 1000 = 163030 \text{ N/m} = 163 \text{ kN/m}$$

$$F_f = 47 \cdot 242200 \cdot 0.0047 = 53486 \text{ N/m} = 53 \text{ kN/m}$$

$$M_{ld} = 163 \left(\frac{0.4}{2} - 0.7 \cdot \frac{0.14}{2} \right) + 53 \cdot \frac{0.4}{2} = 35 \text{ kNm/m}$$

$$M_{Rd} = 18.4 + 0.5(35 - 18.4) = 26.7 \text{ kNm/m} \geq M_{Sd,top} = 23.2 \text{ kNm/m}$$

The condition for verification of the panel located at the top of the building is therefore satisfied

- At the base:

If the section failure is due to masonry crushing under compressive loads (region 1):

$$y_n = \frac{-(242200 \cdot 0.0035 \cdot 47 - 290000) + \sqrt{(242200 \cdot 0.0035 \cdot 47 - 290000)^2 + 4 \cdot 0.85 \cdot 2 \cdot 0.7 \cdot 1000 \cdot 242200 \cdot 0.0035 \cdot 47 \cdot 400}}{2 \cdot 0.85 \cdot 2 \cdot 0.7 \cdot 1000} =$$

$$= 261 \text{ mm} = 26 \text{ cm}$$

$$F_m = 0.85 \cdot 2 \cdot 0.7 \cdot 261 \cdot 1000 = 310590 \text{ N/m} = 311 \text{ kN/m}$$

$$F_f = 242200 \frac{0.0035}{261} (400 - 261) 47 = 21218 \text{ N/m} = 21 \text{ kN/m}$$

$$M_{ld} = 311 \left(\frac{0.4}{2} - \frac{0.7 \cdot 0.26}{2} \right) + 21 \frac{0.4}{2} = 38 \text{ kNm/m}$$

$$M_{Rd} = 33.3 + 0.5(38 - 33.3) = 35.7 \text{ kNm/m} \geq M_{Sd,base} = 33.7 \text{ kNm/m}$$

The condition for verification of the panel located at the base of the building is therefore satisfied

Finally, the validity of the hypotheses performed regarding the region of failure shall be verified as follows:

- At the top:

$$\varepsilon_m = \varepsilon_{fd} \frac{y_n}{t - y_n} = 0.0047 \frac{137}{400 - 137} = 0.24\% < \varepsilon_{mu} = 0.35\%$$

The hypothesis for the panel at the top of the building is verified

- At the base:

$$\varepsilon_f = \varepsilon_{mu} \frac{t - y_n}{y_n} = 0.0035 \frac{400 - 261}{261} = 0.19\% < \varepsilon_{fd} = 0.47\%$$

The hypothesis for the panel at the base of the building is verified

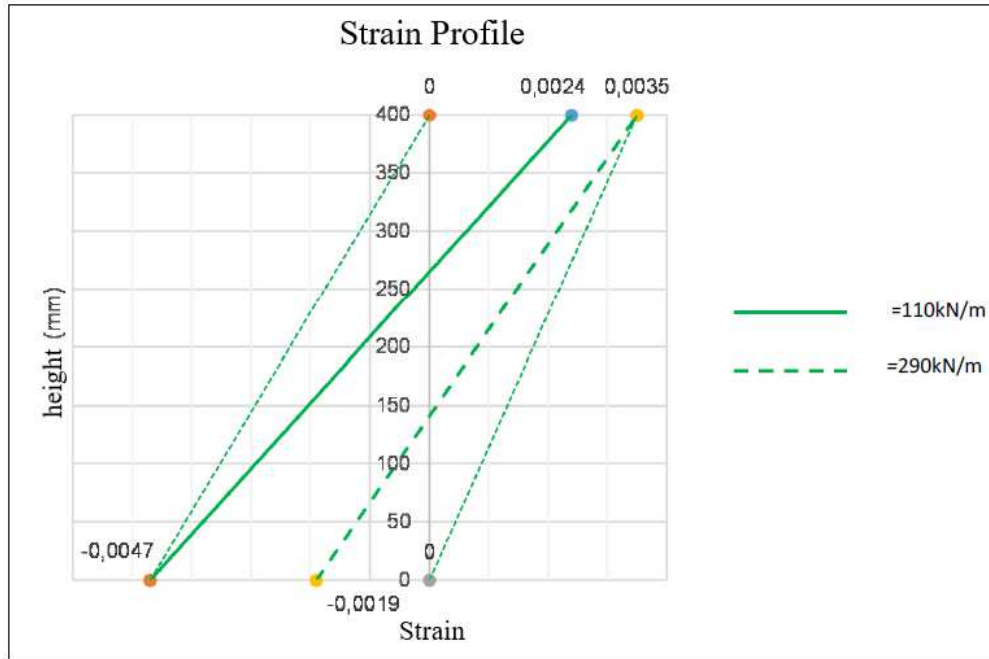


Figure 11.8 – Diagram of the strains in the two panels.

Furthermore, the design shear load, V_{sd} , in the simultaneous loading condition, shall not exceed the shear capacity:

$$V_{Rd,m} = y_n \cdot f_{vd}$$

where f_{vd} is the shear capacity of the un-strengthened masonry, evaluated according to current standards as a function of the average normal stress σ_n , calculated as the ratio of the resultant of the masonry compression stresses, F_m , and the area between the extreme fibre and the neutral axis.

According to the Italian code, the design shear capacity f_{vd} is calculate as follows:

$$f_{vd} = \frac{1}{\gamma_m} \cdot \left(\frac{\tau_0}{FC} + 0.4 \cdot \sigma_n \right)$$

where the average shear capacity of the masonry τ_0 is equal to 0.08 MPa.

Therefore it is:

- At the top:

$$\sigma_n = \frac{163}{137} = 1.18 \text{ MPa}$$

$$f_{vd} = \frac{1}{2} \cdot \left(\frac{0.08}{1.2} + 0.4 \cdot 1.18 \right) = 0.27 \text{ MPa}$$

$$V_{Rd,m} = 137 \cdot 0.27 \cdot 1000 = 36990 \text{ N/m} = 37 \text{ kN/m} \geq V_{sd} = 27 \text{ kN/m}$$

- At the base:

$$\sigma_n = \frac{311}{261} = 1.19 \text{ MPa}$$

$$f_{vd} = \frac{1}{2} \cdot \left(\frac{0.08}{1.2} + 0.4 \cdot 1.19 \right) = 0.27 \text{ MPa}$$

$$V_{Rd,m} = 261 \cdot 0.27 \cdot 1000 = 70470 \text{ N/m} = 70 \text{ kN/m} \geq V_{sd} = 27 \text{ kN/m}$$

The end debonding of the strengthening system shall also be verified. This verification is considered satisfied if, in the absence of suitable mechanical devices, the tensile stress of the strengthening system at a distance from the edges equal to the anchorage, is not greater than $E_f \cdot \varepsilon_{fd}$. This value is calculated without amplifying $\varepsilon_{lim,conv}$, in any way and from which ε_{fd} is derived through the Equation (3.1) (See § 3).

In this example, this check is performed verifying that the flexural capacity of the panel for end debonding failure is greater than the design bending moment acting at a distance from the panel edges equal to the anchorage length which is assumed to be equal to 30 cm. The hypotheses of end debonding failure is verified by checking that the compressed masonry strain is smaller than ε_{mu} .

$$\varepsilon_{fd} = \eta_a \frac{\varepsilon_{lim,conv}}{\gamma_m} = 0.9 \frac{0.0052}{1.5} = 0.312 \% .$$

- At the top:

If the section failure occurs for tensile stress in the strengthening system (end debonding) it is:

$$y_n = \frac{47 \cdot 242200 \cdot 0.00312 + 110000}{0.85 \cdot 2 \cdot 0.7 \cdot 1000} = 122 \text{ mm} = 12 \text{ cm},$$

$$\varepsilon_m = \varepsilon_{fd} \frac{y_n}{t - y_n} = 0.00312 \frac{122}{400 - 122} = 0.14\% < \varepsilon_{mu} = 0.35\% .$$

The hypothesis performed for the panel at the top of the building is verified. Therefore, the end debonding failure of the strengthening system shall be verified checking that $M_{Rd} \geq M_{sd}$, where M_{sd} is equal to 7 kNm/m:

$$F_m = 0.85 \cdot 2 \cdot 0.7 \cdot 122 \cdot 1000 = 145180 \text{ N/m} = 145 \text{ kN/m}$$

$$F_f = 47 \cdot 242200 \cdot 0.00312 = 35532 \text{ N/m} = 35 \text{ kN/m}$$

$$M_{ld} = 145 \left(\frac{0.4}{2} - 0.7 \frac{0.12}{2} \right) + 35 \frac{0.4}{2} = 30 \text{ kNm/m}$$

$$M_{Rd} = 18.4 + 0.5(30 - 18.4) = 24,2 \text{ kNm/m} \geq M_{sd,top} = 7 \text{ kNm/m}$$

The verification of the panel for end debonding is therefore satisfied

- At the base:

If the section failure occurs for tensile stress in the strengthening system (end debonding) it is:

$$y_n = \frac{47 \cdot 242200 \cdot 0.00312 + 290000}{0.85 \cdot 2 \cdot 0.7 \cdot 1000} = 274 \text{ mm} = 27 \text{ cm}$$

$$\varepsilon_m = \varepsilon_{fd} \frac{y_n}{t - y_n} = 0.00312 \frac{274}{400 - 274} = 0.67\% > \varepsilon_{mu} = 0.35\%$$

The hypothesis made for the panel at the top of the building is verified. Therefore, the end debonding failure is avoided.

11.3 CONFINEMENT OF MASONRY COLUMNS

11.3.1 Example 1

In the example, it is required to verify the axial capacity of a column that is part of a clay brick masonry building (mass density equal to about 1800 kg/m^3) with the following geometric and mechanical characteristics:

$b = 250 \text{ mm}$	width of the cross-section
$h = 250 \text{ mm}$	height of the cross-section
$D = \sqrt{b^2 + h^2} = 353.55 \text{ mm}$	diagonal of the cross-section
$H = 3000 \text{ mm}$	height of the column
$A_m = b \cdot h = 6.25 \cdot 10^4 \text{ mm}^2$	area of the cross-section
$f_{md} = 2.67 \text{ MPa}$	design compression strength of the masonry
$g_m = 1800 \frac{\text{kg}}{\text{m}^3}$	mass density of the masonry
$N_{sd} = 180 \text{ kN}$	axial load

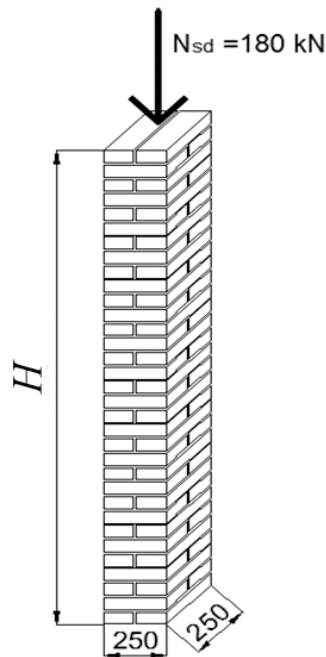


Figure 11.9 - Column subjected to normal centred load.

The safety verification of the unreinforced column is not satisfied, in fact:

$N_{Rm,d} = A_m \cdot f_{md} = 166.67 \text{ kN}$ is the design capacity value of the column

$$N_{sd} \leq N_{Rm,d}$$

Therefore, the axial capacity is improved by confining the column with a FRCM system consisting of a glass fibre open grid and a lime-based matrix. The edges are rounded and the FRCM reinforcement has the following characteristics:

$r_c = 30$ mm	corner rounding radius
$E_f = 95000$ MPa	longitudinal elastic modulus of the open grid
$t_f = 0.03$ mm	equivalent thickness of the open grid
$\varepsilon_{uf} = 0.0164$	open grid ultimate deformation
$\gamma_m = 1.5$	partial safety factor of the open grid
$\eta_a = 0.8$	environmental conversion factor (outdoor)
$t_{mat} = 10$ mm	matrix thickness of the single layer of FRCM
$f_{c,mat} = 10$ MPa	design compression strength of the FRCM matrix
$n_f = 1$	number of FRCM layers

Calculation of the effective confining pressure

$$\rho_{mat} = \frac{4n_f t_{mat}}{D} = 0.11 \quad \text{geometric percentage of FRCM matrix}$$

$$k_H = 1 - \left[\frac{(b - 2r_c)^2 + (h - 2r_c)^2}{3A_m} \right] = 0.61 \quad \text{horizontal efficiency factor}$$

$$k_{mat} = 1.81 \left(\rho_{mat} \frac{f_{c,mat}}{f_{md}} \right)^2 = 0.33 \quad \text{efficiency coefficient of the FRCM matrix}$$

$$\varepsilon_{ud,rid} = \min \left(k_{mat} \eta_a \frac{\varepsilon_{uf}}{\gamma_m} ; 0.004 \right) = 2.85 \cdot 10^{-3} \quad \text{design strain of the FRCM}$$

$$f_1 = \frac{2n_f t_f E_f \varepsilon_{ud,rid}}{D} = 0.05 \text{ MPa} \quad \text{confining pressure}$$

$$f_{l,eff} = k_H \cdot f_1 = 0.03 \text{ MPa} \quad \text{effective confining pressure}$$

calculation of the compressive strength of the confined masonry

$$k' = \frac{g_m}{1000} = 1.8 \quad \text{coefficient of strength increase}$$

$$f_{mcd} = f_m \left[1 + k' \left(\frac{f_{l,eff}}{f_{md}} \right)^{0.5} \right] = 3.16 \text{ MPa} \quad \text{design strength of the column confined with FRCM}$$

calculation of the axial capacity of the confined column

$$N_{Rmc,d} = A_m \cdot f_{mcd} = 197.55 \text{ kN from which}$$

$$N_{sd} \leq N_{Rmc,d} \text{ , thus the safety verification is satisfied}$$

11.3.2 Example 2

The purpose of the example is to calculate the increase in the load bearing capacity of a circular cross-section column made of natural stone masonry, by about 30% with FRCM confinement while minimizing the thickness of the reinforcement.

Geometric and mechanical data of the column to be confined

$g_m = 1700 \frac{\text{kg}}{\text{m}^3}$	mass density of the masonry
$D = 400 \text{ mm}$	diameter of the cross-section
$A_m = \frac{\pi \cdot D^2}{4} = 125663.7 \text{ mm}^2$	area of the cross-section
$f_{md} = 4.17 \text{ MPa}$	masonry compression design strength

Calculation of the axial capacity of the unconfined column

$N_{Rmd} = A_m \cdot f_{md} = 523.6 \text{ kN}$	actual axial capacity
$in = 1.30$	increase in capacity
$N_{Rmc,d} = N_{Rmd} \cdot in = 654.5 \text{ kN}$	design capacity target

In order to increase the compressive strength of the column, it is decided to confine it with a FRCM system made of basalt fibre net and lime-based matrix.

Reinforcement characteristics

$f_{c,mat} = 13 \text{ MPa}$	characteristic compressive strength of the FRCM composite matrix
$n_f = 1$	number of net layer
$t_f = 0.089 \text{ mm}$	equivalent thickness of the net
$E_f = 85 \text{ GPa}$	mean longitudinal elastic modulus of the net
$\varepsilon_{uf} = 0.02$	ultimate tensile strain of the net

Design of the thickness

In order to minimize the thickness of the composite, the minimum percentage of reinforcement is determined so that the final design deformation of the net is equal to 0.004.

$\eta_a = 0.80$	environmental conversion factor (outdoor)
$\gamma_m = 1.5$	partial safety factor of the net
$k_{mat,min} = \frac{0.004 \cdot \gamma_m}{\eta_a \cdot \varepsilon_{uf}} = 0.375$	minimum value of k_{mat}
$\rho_{mat,min} = \frac{f_{md}}{f_{cmat}} \sqrt{\frac{k_{mat,min}}{1.81}} = 0.146$	minimum percentage of FRCM matrix
$t_{mat,min} = \frac{\rho_{mat,min} \cdot D}{4} = 14.6 \text{ mm}$	minimum thickness of the FRCM matrix

$t_{\text{mat}} = 15 \text{ mm}$ design thickness of the FRCM matrix

Calculation of the effective confining pressure

$k_h = 1$ horizontal efficiency coefficient

$\rho_{\text{mat}} = \frac{(4 \cdot t_{\text{mat}})}{D} = 0.15$ geometric percentage of FRCM matrix

$k_{\text{mat}} = 1.81 \cdot \left[\rho_{\text{mat}} \cdot \left(\frac{f_{\text{cmat}}}{f_{\text{md}}} \right) \right]^2 = 0.396$ efficiency coefficient of the FRCM matrix

$\varepsilon_{\text{ud,rid}} = \min \left(0.004, k_{\text{mat}} \cdot \eta_a \cdot \frac{\varepsilon_{\text{uf}}}{\gamma_m} \right) = 0.004$ design deformation of the FRCM

$f_1 = \frac{2 \cdot n_f \cdot t_f \cdot E_f \cdot \varepsilon_{\text{ud,rid}}}{D} = 0.1513 \text{ MPa}$ confining pressure

$f_{\text{leff}} = k_H \cdot f_1 = 0.1513 \text{ MPa}$ effective confining pressure

calculation of the compressive strength of the confined masonry

$k = \frac{g_m}{1000 \frac{\text{kg}}{\text{m}^3}} = 1.7$ coefficient of strength increase

$f_{\text{mcd}} = f_{\text{md}} \left[1 + k \left(\frac{f_{\text{leff}}}{f_{\text{md}}} \right)^{0.5} \right] = 5.52 \text{ MPa}$ design compressive strength of the column confined with FRCM

Calculation of the axial capacity of the confined column

$N_{\text{Rmc,d1}} = A_m \cdot f_{\text{mcd}} = 693.22 \text{ kN}$

Thus, an increase of 32% is obtained, as required.

11.4 STRENGTHENING OF AN RC BEAM

11.4.1 Design of the flexural strengthening

A shallow beam supported by three square columns with edge 30 cm is considered. The beam and steel reinforcement geometry are depicted in Figure 11.10.

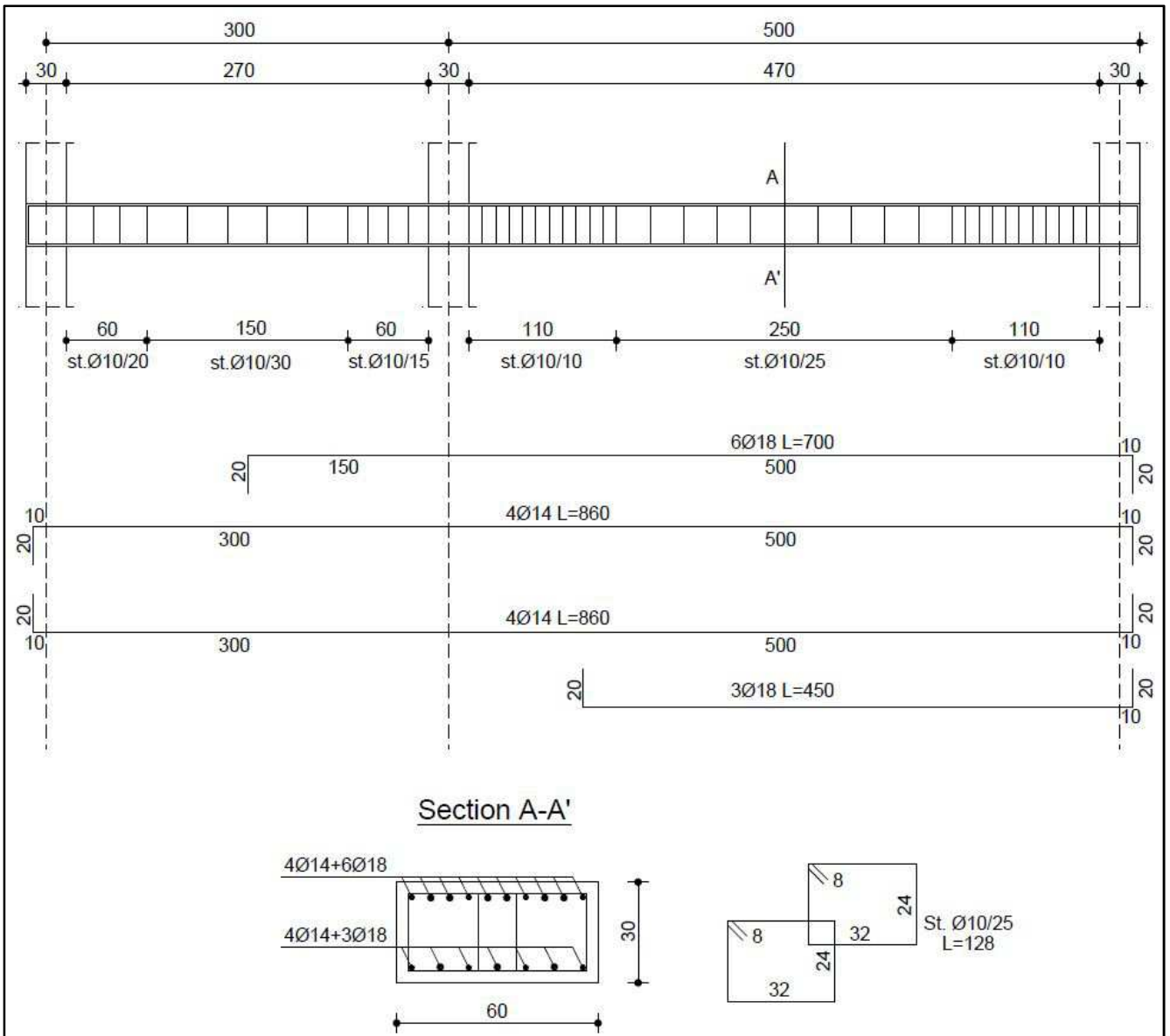


Figure 11.10 - Steel bars location for the beam considered.

The (measured) material properties are:

- Concrete mean cylindrical compressive strength: $f_{cm} = 20$ MPa
- Steel mean tensile strength: $f_{ym} = 380$ MPa

Applying a confidence factor $FC = 1.35$, the design values of the material properties are:

- Concrete design cylindrical compressive strength: $f_{cd} = f_{cm} / (FC \cdot \gamma_c) = 14.8$ MPa
- Steel design tensile strength: $f_{yd} = f_{ym} / (FC \cdot \gamma_s) = 281$ MPa

f_{cd} and f_{yd} were obtained by assuming partial safety coefficients of $\gamma_s = 1.0$ and $\gamma_c = 1.0$, respectively, associated with ductile members. The distances between the centroid of the lower and upper steel bars and the cross-section compressed edge are $d = 270$ mm and $d' = 30$ mm, respectively.

At the ultimate limit state, the following uniformly distributed load is applied to the beam:

- structural permanent load: $q_1 = 20.00 \text{ kN/m}$
- variable load: $q_2 = 25.00 \text{ kN/m}$

The maximum values of the acting bending moment along the beam, M_{Ed} , which were obtained neglecting the flexural stiffness of the central column, and the corresponding values of the resisting bending moment, M_{Rd} , are reported in Table 11.1. The following relationship shall be verified:

$$M_{Ed} \leq M_{Rd}$$

Span [m]	Section	M_{Ed} [kNm]	A_s [mm ²]	A'_s [mm ²]	M_{Rd} [kNm]	$M_{Ed} \leq M_{Rd}$
3.0	Left support	-30.2	616	616	-45.1	OK
3.0	Mid-span	31.0	616	616	45.1	OK
3.0-5.0	Central support	-115.6	616	2143	-141.8	OK
5.0	Mid-span	91.7	1379	2143	96.1	OK
5.0	Right support	-113.1	1379	2143	-141.8	OK

Table 11.1 – Values of M_{Ed} and M_{Rd} for the beam considered.

where A_s and A'_s are the lower and upper steel bar areas. The resisting bending moment M_{Rd} reported in Table 11.1 was conservatively computed neglecting the contribution of the compressed steel.

Due to a change in the use of the building, the variable load applied to the beam has increased by 20%:

- structural permanent load: $q_1 = 20.00 \text{ kN/m}$
- variable load: $q_2 = 30.00 \text{ kN/m}$

Under these loads, the maximum applied bending moment increases:

Span [m]	Section	M_{Ed} [kNm]	A_s [mm ²]	A'_s [mm ²]	M_{Rd} [kNm]	$M_{Ed} \leq M_{Rd}$
3.0	Left support	-34.9	616	616	-45.1	OK
3.0	Mid-span	35.7	616	616	45.1	OK
3.0-5.0	Central support	-129.2	616	2143	-141.8	OK
5.0	Mid-span	102.7	1379	2143	96.1	NO
5.0	Right support	-126.8	1379	2143	-141.8	OK

Table 11.2 – Values of M_{Ed} and M_{Rd} after the applied load increase.

The resisting bending moment M_{Rd} reported in Table 11.2, which was conservatively calculated neglecting the contribution of the compressed steel, is lower than the maximum acting bending moment for the 5 m span portion of the beam: $M_{Ed} = 102.7 \text{ kNm} > M_{Rd} = 96.1 \text{ kNm}$.

Therefore, a carbon FRCM composite is applied along the deficient beam portion across the entire cross-section width. The carbon FRCM has the following properties:

- Width of the carbon FRCM $b_f = 600$ mm
- Equivalent thickness $t_f = 0.055$ mm
- Textile elastic modulus $E_f = 220$ GPa
- Characteristic conventional limit stress $\sigma_{\text{lim,conv}} = 1214$ MPa
- Textile characteristic ultimate tensile strength $\sigma_{\text{uf}} = 2005$ MPa

The design value of the conventional limit stress $\sigma_{\text{lim,conv,d}}$ and of the textile ultimate tensile strength $\sigma_{\text{uf,d}}$ are obtained with Eq. (3.1) considering internal exposure for carbon fibres:

$$\sigma_{\text{lim,conv,d}} = \eta \frac{\sigma_{\text{lim,conv}}}{\gamma_m} = 0.90 \frac{1214}{1.5} = 728 \text{ MPa}$$

$$\sigma_{\text{uf,d}} = \eta \frac{\sigma_{\text{uf}}}{\gamma_m} = 0.90 \frac{2005}{1.5} = 1203 \text{ MPa}$$

The design values of the corresponding conventional limit strain $\varepsilon_{\text{lim,conv,d}}$ and textile ultimate tensile strain $\varepsilon_{\text{uf,d}}$ are:

$$\varepsilon_{\text{lim,conv,d}} = \frac{\sigma_{\text{lim,conv,d}}}{E_f} = \frac{728}{220000} = 0.0033$$

$$\varepsilon_{\text{uf,d}} = \frac{\sigma_{\text{uf,d}}}{E_f} = \frac{1203}{220000} = 0.0055$$

The design values of the conventional limit stress $\sigma_{\text{lim,conv,d}}^{(\alpha)}$ and strain $\varepsilon_{\text{lim,conv,d}}^{(\alpha)}$ for intermediate failure can be obtained multiplying $\sigma_{\text{lim,conv,d}}$ and $\varepsilon_{\text{lim,conv,d}}$ for $\alpha = 1.5$, respectively:

$$\sigma_{\text{lim,conv,d}}^{(\alpha)} = \alpha \cdot \sigma_{\text{lim,conv,d}} = 1.5 \cdot 728 = 1092 \text{ MPa}$$

$$\varepsilon_{\text{lim,conv,d}}^{(\alpha)} = \alpha \cdot \varepsilon_{\text{lim,conv,d}} = 1.5 \cdot 0.0033 = 0.0050$$

The maximum composite strain is then:

$$\varepsilon_{f,d} = \min \{ \varepsilon_{\text{lim,conv,d}}^{(\alpha)}, \varepsilon_{\text{uf,d}} \} = 0.0050$$

Before applying the FRCM strengthening, all non-structural loads are removed from the beam. Therefore, the structural permanent load $q_1 = 20.00$ kN/m induces a maximum bending moment along the 5 m span of $M_0 = 36.3$ kNm. The strain ε_0 of the tension side of concrete induced by M_0 can be approximated as:

$$\varepsilon_0 = \frac{M_0}{0.9 \cdot d \cdot E_s \cdot A_s} = \frac{36.3}{0.9 \cdot 0.27 \cdot 210 \cdot 1379} = 0.0005$$

where $E_s = 210\text{GPa}$ is the steel elastic modulus. The actual value of ε_0 , which can be obtained enforcing the cross-section rotational equilibrium, is $\varepsilon_0 = 0.0006$.

As a first attempt, debonding failure is assumed. The strains in the composite ε_f , in the compressed concrete ε_c , in the upper steel bars ε_s , and in the lower steel bars ε'_s are:

$$\begin{aligned}\varepsilon_f &= \varepsilon_{f,d} \\ \varepsilon_c &= (\varepsilon_{f,d} + \varepsilon_0) \frac{x}{h_f - x} \leq \varepsilon_{cu} \\ \varepsilon_s &= (\varepsilon_{f,d} + \varepsilon_0) \frac{d - x}{h_f - x} \\ \varepsilon'_s &= (\varepsilon_{f,d} + \varepsilon_0) \frac{x - d'}{h_f - x}\end{aligned}$$

where x is the distance between the neutral axis and the compressed edge and $h_f = 304\text{mm}$ is the distance between the centroid of the composite and the compressed edge, which was calculated accounting for the FRCM thickness recommended by the manufacturer, equal to 8 mm.

Imposing the translational and rotational cross-section equilibrium, the distance x and the corresponding resisting bending moment of the strengthened section $M_{Rd,f}$ can be obtained, respectively:

$$\begin{aligned}x &= \frac{A'_s \cdot \sigma'_s - A_s \cdot \sigma_s - t_f \cdot b_f \cdot E_f \cdot \varepsilon_{f,d}}{f_{cd} \cdot k_1 \cdot b} \\ M_{Rd,f} &= f_{cd} \cdot k_1 \cdot x \cdot b (d - k_2 \cdot x) + A'_s \cdot \sigma'_s (d - d') + t_f \cdot b_f \cdot E_f \cdot \varepsilon_{f,d} (h_f - d)\end{aligned}$$

where the coefficients k_1 and k_2 express the resultant of the compressive stresses and its distance from the compressed edge with respect to $f_{cd} \cdot x \cdot b$ and x , respectively.

Therefore, considering $\varepsilon_0 = 0.0006$ and enforcing the cross-section equilibrium (the contribution of the compressed steel is conservatively neglected), the resisting bending moment is:

$$\begin{aligned}\varepsilon_f &= \varepsilon_{f,d} = 0.0050 \\ \varepsilon_c &= 0.0018 < \varepsilon_{cu} = 0.0035 \\ \varepsilon_s &= 0.0048 \\ \varepsilon'_s &= 0.0012 \\ x &= 75 \text{ mm} \\ M_{Rd,f} &= 104.0 \text{ kNm}\end{aligned}$$

Since the strain at the concrete compressed edge obeys the inequality $\varepsilon_c < \varepsilon_{cu}$, the hypothesis of debonding failure is verified. Furthermore, since $M_{Rd,f} > M_{Ed} = 102.7 \text{ kNm}$, the beam is verified with respect to intermediate failure under the increased applied loads.

In order to prevent the end debonding failure, the stress in the composite at a distance equal to the composite anchorage length from the end of the composite shall be lower than the design conventional limit stress $\sigma_{lim,conv,d}$. The carbon FRCM, which has an anchorage length equal to 300 mm, is applied for a length of 470 cm. The FRCM is subjected to compressive stresses at a distance of 300 mm from the composite ends. Therefore, end debonding failure is verified.

11.4.2 Design of the shear strengthening

According to current regulations the acting shear force V_{Ed} shall be lower than the beam shear strength V_{Rd} along the entire length of the beam:

$$V_{Ed} \leq V_{Rd} = \min\{V_{Rd,s}, V_{Rd,c}\}$$

where $V_{Rd,s}$ and $V_{Rd,c}$ are the steel and concrete contributions to the shear capacity, respectively:

$$V_{Rd,s} = 0.9 \cdot d \cdot \frac{A_{sw}}{s} \cdot f_{ywd} (\cot \alpha + \cot \theta) \sin \alpha$$

$$V_{Rd,c} = 0.9 \cdot d \cdot b \cdot \alpha_c \cdot 0.5 \cdot f_{cd} (\cot \alpha + \cot \theta) / (1 + \cot^2 \theta)$$

where A_{sw} and s are the area and spacing of the steel stirrups, whereas $f_{ywd} = f_{ym} / (FC \cdot \gamma_s) = 245 \text{ MPa}$ and $f_{cd} = f_{cm} / (FC \cdot \gamma_c) = 9.9 \text{ MPa}$ are the stirrup design tensile strength and concrete design compressive strength, respectively, calculated assuming $\gamma_s = 1.15$ and $\gamma_c = 1.5$ for brittle members.

Conservatively, an inclination angle $\theta = 45^\circ$ of the concrete compressed strut is assumed, whereas the inclination of the steel stirrups is $\alpha = 90^\circ$. Due to the change in the use of the building, the acting shear force V_{Ed} at the edge of the columns and the corresponding beam shear strength V_{Rd} are (Table 11.3):

Span [m]	Section	V_{Ed} [kN]	A_{sw} [mm ²]	s [mm]	$V_{Rd,s}$ [kN]	$V_{Rd,c}$ [kN]	V_{Rd} [kN]	$V_{Ed} \leq V_{Rd}$
3.0	Left support	88.9	314	200	93.4	360.0	93.4	OK
3.0	Right support	135.6	314	150	124.6	360.0	124.6	NO
5.0	Left support	168.7	314	100	186.9	360.0	186.9	OK
5.0	Right support	169.9	314	100	186.9	360.0	186.9	OK

Table 11.3 - Values of V_{Ed} and V_{Rd} after the applied load increase.

Table 11.3 shows that the shear force acting on the right support of the 3 m span beam portion is higher than the corresponding shear strength.

Therefore, a U-wrapped carbon FRCM composite is applied to the 3 m span portion. The FRCM has the following properties:

- Equivalent thickness $t_f = 0.070 \text{ mm}$
- Textile elastic modulus $E_f = 220 \text{ GPa}$
- Characteristic conventional limit stress $\sigma_{lim,conv} = 1150 \text{ MPa}$
- Design conventional limit stress $\sigma_{lim,conv,d} = 690 \text{ MPa}$
- Anchorage length $l_{Ed} = 300 \text{ mm}$

Unless further investigations are performed, the design value of the FRCM composite effective stress, f_{fed} , is obtained from bond tests and, in particular, from $\sigma_{lim,conv}$. The strengthening is applied continuously with the fibres inclined of $\beta = 45^\circ$ with respect to the beam longitudinal axis. The maximum bond length L_{max} is:

$$L_{max} = \frac{\min\{0.9 \cdot d, h_w\}}{\sin \beta} = 344 \text{ mm}$$

Since $l_{ed} < L_{max}$, the effective tensile stress f_{fed} is:

$$f_{fed} = \sigma_d \left(1 - \frac{1}{3} \frac{l_{ed}}{L_{max}} \right) = 489.2 \text{ MPa}$$

The FRCM composite contribution to the shear capacity is:

$$V_{Rd,f} = \frac{1}{\gamma_{Rd}} \cdot 0.9 \cdot d \cdot f_{fed} \cdot 2t_f \cdot (\cot \theta + \cot \beta) \cdot \sin^2 \beta = 11.10 \text{ kN}$$

where the partial safety factor for shear strengthening is $\gamma_{Rd} = 1.5$.

The shear strength of the strengthened portion of the beam is:

$$V_{Rd} = \min \{ V_{Rd,s} + V_{Rd,f}, V_{Rd,c} \} = 135.8 \text{ kN}$$

Since $V_{Rd} > V_{Ed} = 135.6 \text{ kN}$, the cross-section is verified.

11.5 CONFINEMENT OF A REINFORCED CONCRETE COLUMN

The axial capacity is to be verified for a circular cross-section column, subjected to pure compression, that is part of a reinforced concrete building with geometrical and mechanical characteristics as follows:

$D = 300 \text{ mm}$	diameter of the cross-section
$H = 2700 \text{ mm}$	height of the column
$A_c = \pi \left(\frac{D}{2} \right)^2 = 7.07 \cdot 10^4 \text{ mm}^2$	area of the cross-section
$FC = 1.2$	confidence factor (LC2)
$f_{cm} = 20 \text{ MPa}$	mean compression strength of the unconfined concrete
$\gamma_c = 1.5$	safety factor of the concrete
$f_{cd} = \frac{f_{cm}}{FC \cdot \gamma_c} = 11.11 \text{ MPa}$	design compression strength of the concrete
$\phi = 14 \text{ mm}$	diameter of the steel longitudinal reinforcement
$n = 4$	number of steel bars
$A_s = n\pi \left(\frac{\phi}{2} \right)^2 = 615.75 \text{ mm}^2$	total area of the steel reinforcement
$f_{yd} = 232 \text{ MPa}$	design yielding strength of the steel reinforcement
$N_{sd} = 1000 \text{ kN}$	design axial load

The safety verification of the unreinforced column is not satisfied, in fact:

$N_{Rc,d} = A_c \cdot f_{cd} + A_s \cdot f_{yd} = 928.25 \text{ kN}$ is the design capacity of the column

$$N_{sd} \leq N_{Rm,d}$$

It was decided to confine the column by means of FRCM system consisting of carbon fibre net and cement-based matrix. The FRCM reinforcement has the following characteristics:

$E_f = 245000 \text{ MPa}$	longitudinal elastic modulus of the net
$t_f = 0.047 \text{ mm}$	equivalent thickness of the net
$\varepsilon_{uf} = 0.0081$	ultimate tensile strain of the net
$\gamma_m = 1.5$	safety factor of the net
$\eta_a = 0.9$	environmental conversion factor (indoor)
$t_{mat} = 10 \text{ mm}$	matrix thickness of the single layer of FRCM
$f_{c,mat} = 30 \text{ MPa}$	design compression strength of the FRCM-matrix
$n_f = 2$	number of FRCM-layers

Calculation of the effective confinement pressure

$$\rho_{mat} = \frac{4n_f t_{mat}}{D} = 0.27 \quad \text{geometric percentage of FRCM matrix}$$

$$k_H = 1 \quad \text{horizontal efficiency coefficient}$$

$$k_{mat} = 0.217 \left(\rho_{mat} \frac{f_{c,mat}}{f_{cd}} \right)^{\frac{3}{2}} = 0.16 \quad \text{efficiency coefficient of the FRCM matrix}$$

$$\varepsilon_{ud,rid} = \min \left(k_{mat} \eta_a \frac{\varepsilon_{uf}}{\gamma_m} ; 0.004 \right) = 7.6 \cdot 10^{-4} \quad \text{design strain of the FRCM composite}$$

$$f_1 = \frac{2n_f t_f E_f \varepsilon_{ud,rid}}{D} = 0.12 \text{ MPa} \quad \text{confining pressure}$$

$$f_{l,eff} = k_H \cdot f_1 = 0.12 \text{ MPa} \quad \text{effective confining pressure}$$

calculation of the compressive strength of confined masonry

$$f_{ccd} = f_{cd} + 2.6 f_{cd} \left(\frac{f_{l,eff}}{f_{cd}} \right)^{\frac{2}{3}} = 12.5 \text{ MPa} \quad \text{design compression strength of the confined column}$$

calculation of the axial capacity of the confined masonry

$$N_{Rmc,d} = A_m \cdot f_{mcd} = 1.03 \cdot 10^3 \text{ kN}, \text{ thus } N_{sd} \leq N_{Rmc,d}$$

12 APPENDIX 1: ON THE IN-PLANE AXIAL-MOMENT RESISTANCE CALCULATION

Following the assumptions of paragraph 4.2 and Figure 4.1, the different situations that can arise are specified below.

In the case of failure for reaching the maximum strain in compression ε_{mu} ($\varepsilon_m = \varepsilon_{mu}$ in Figure A1.1), and with the neutral axis within the section, the resistance moment can be calculated as follows:

$$M_{Rd}(N_{Sd}) = f_{md} \frac{t y_n}{2} \left[H(1-k) - y_n(1-k)^2 + k \left(\frac{H}{2} - y_n + \frac{2}{3} k y_n \right) \right] + \frac{\varepsilon_{mu}}{y_n} E_f t_{2f} \frac{(d_f - y_n)^2}{12} (2y_n + 4d_f - 3H), \quad (A1.1)$$

where $k = \bar{\varepsilon}_m / \varepsilon_{mu}$, $t_{2f} = 2 \cdot t_f$ and y_n the neutral axis depth, given by:

$$y_n = \frac{N_{Sd} - E_f t_{2f} d_f \varepsilon_{mu} + \sqrt{N_{Sd}^2 + E_f t_{2f} d_f \varepsilon_{mu} [(2-k) t d_f f_{md} - 2N_{Sd}]}}{t f_{md} (2-k) - E_f t_{2f} \varepsilon_{mu}}. \quad (A1.2)$$

In the case of failure of the strengthening for reaching the maximum strain ε_{fd} ($\varepsilon_f = \varepsilon_{fd}$ in Figure A1.1) and with the neutral axis within the section, if the maximum strain ε_m of the masonry satisfies $\bar{\varepsilon}_m \leq \varepsilon_m \leq \varepsilon_{mu}$, the design moment resistance is:

$$M_{Rd}(N_{Sd}) = \frac{t f_{md}}{12} \left[2d_f y_n \xi (2\xi + 3) + 3H [y_n (2 + \xi) - \xi d_f] - 2y_n^2 (\xi^2 + 3 + 3\xi) - 2\xi^2 d_f^2 \right] + \varepsilon_{fd} E_f t_{2f} \frac{d_f - y_n}{12} (2y_n + 4d_f - 3H), \quad (A1.3)$$

where $\xi = \bar{\varepsilon}_m / \varepsilon_{fd}$ and y_n the neutral axis depth, given by:

$$y_n = \frac{2N_{Sd} + t \xi f_{md} d_f + E_f t_{2f} d_f \varepsilon_{fd}}{t f_{md} (2 + \xi) + E_f t_{2f} \varepsilon_{fd}}. \quad (A1.4)$$

In the case of failure of the strengthening due to reaching the maximum strain ε_{fd} ($\varepsilon_f = \varepsilon_{fd}$ in Figure A1.1) and with the neutral axis within the section, if the maximum strain ε_m of the masonry satisfies $\varepsilon_m \leq \bar{\varepsilon}_m$, the design moment resistance is:

$$M_{Rd}(N_{Sd}) = \frac{tE_m \varepsilon_{fd}}{12} \cdot \frac{y_n^2}{d - y_n} \cdot (3H - 2y_n) + \varepsilon_{fd} E_f t_{2f} \frac{d_f - y_n}{12} (2y_n + 4d_f - 3H), \quad (A1.5)$$

where $E_m = f_{md} / \bar{\varepsilon}_m$ elastic modulus of the masonry y_n the neutral axis depth, given by:

$$y_n = \frac{N_{Sd} + E_f t_{2f} d_f \varepsilon_{fd} - \sqrt{N_{Sd}^2 + E_m \varepsilon_{fd} d_f t \cdot (E_f t_{2f} d_f \varepsilon_{fd} + 2N_{Sd})}}{\varepsilon_{fd} (E_f t_{2f} - tE_m)}. \quad (A1.6)$$

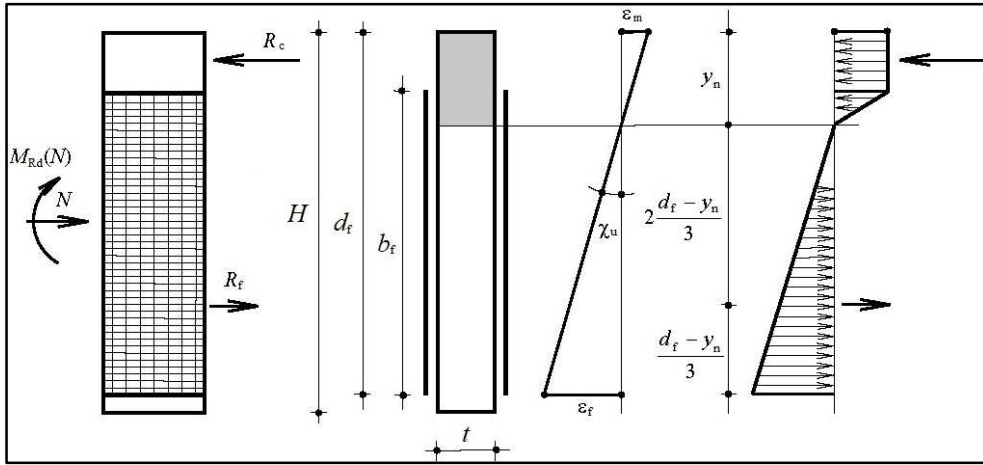


Figure A1.1 - Diagram for assessing the design moment resistance of a section reinforced with FRCM.

In a simplified way, the design moment resistance can be evaluated by assuming a constant compression diagram of the stresses equal to $\alpha_m f_{md}$, extended to a depth equal to βy_n , with y_n the neutral axis depth. $\alpha_m = 0,85$ and $0,6 \leq \beta \leq 0,8$ are assumed. Using this approach, with reference to the diagram of Figure A1.2, the cases that may occur are as follows.

In the case of failure for reaching the maximum strain in compression ε_{mu} ($\varepsilon_m = \varepsilon_{mu}$ in Figure A1.2) and with the neutral axis within the section, the design moment resistance is:

$$M_{Rd}(N_{Sd}) = \frac{\alpha_m \beta f_{md} t y_n}{2} \cdot (H - \beta y_n) + \frac{\varepsilon_{mu}}{y_n} \cdot \frac{(d_f - y_n)^2}{12} \cdot E_f t_{2f} \cdot (2y_n + 4d_f - 3H), \quad (A1.7)$$

where y_n the neutral axis depth is given by:

$$y_n = \frac{N_{Sd} - E_f t_{2f} d_f \varepsilon_{mu} + \sqrt{N_{Sd}^2 + 2E_f t_{2f} d_f \varepsilon_{mu} (\alpha_m \beta f_{md} d_f - N_{Sd})}}{2\alpha_m \beta f_{md} t - E_f t_{2f} \varepsilon_{mu}} \quad (A1.8)$$

In the case of failure of the strengthening for reaching the maximum strain ε_{fd} ($\varepsilon_f = \varepsilon_{fd}$ in Figure A1.2) and with the neutral axis within the section, the design moment resistance is:

$$M_{Rd}(N_{Sd}) = \frac{\alpha_m \beta f_{md} t y_n}{2} \cdot (H - \beta y_n) + \varepsilon_{fd} \cdot E_f t_{2f} \cdot \frac{d_f - y_n}{12} (2y_n + 4d_f - 3H), \quad (A1.9)$$

where y_n the neutral axis depth is given by:

$$y_n = \frac{\varepsilon_{fd} \cdot E_f t_{2f} d_f + 2N_{Sd}}{2\alpha_m \beta f_{md} t + \varepsilon_{fd} \cdot E_f t_{2f}}, \quad (A1.10)$$

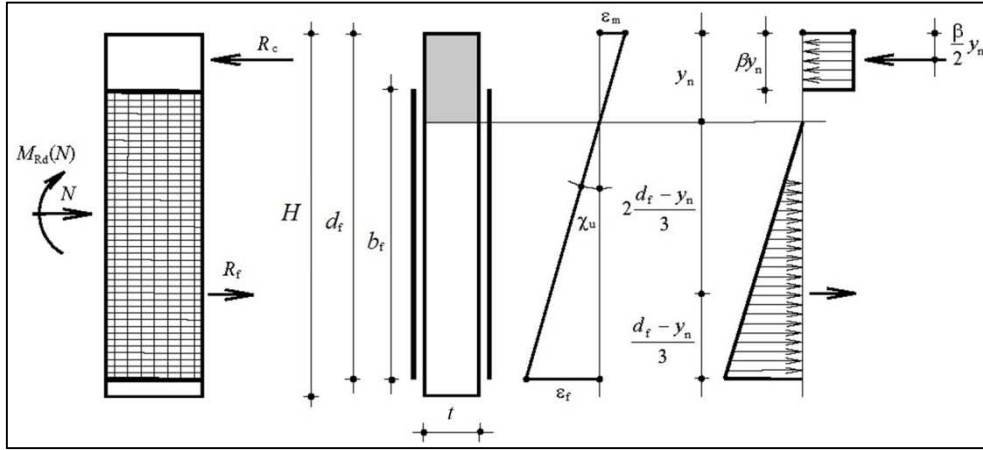


Figure A1.2 - Diagram for assessing the design moment resistance of a section reinforced with FRCM with constant compression stresses in the masonry.

The other symbols used in (A1.1 – A1.10) are defined in Figure A1.1 and Figure A1.2. In particular:

- H is the length of the wall (height of the section);
- t is the thickness of the wall (section width);
- t_{2f} is the total equivalent thickness of the fibres applied on the two faces;
- d_f is the distance between the extreme fibre in compression and the most distant strengthening fibre;
- N_{Sd} is the applied axial load (it can be assumed equal to zero in the case of spandrels).

In the case of strengthening arranged in stripes, the design moment resistance can be evaluated in a similar way, neglecting the stripes arranged in the compressed area.

If the spacing p_f of the stripes of width b_f (Figure A1.3) is sufficiently small with respect to the height of the section, the design moment resistance can be determined with the formulas reported above replacing the thickness with the equivalent thickness:

$$t_{f,eq} = \frac{t_{2f} b_f}{i_f}, \quad (A1.11)$$

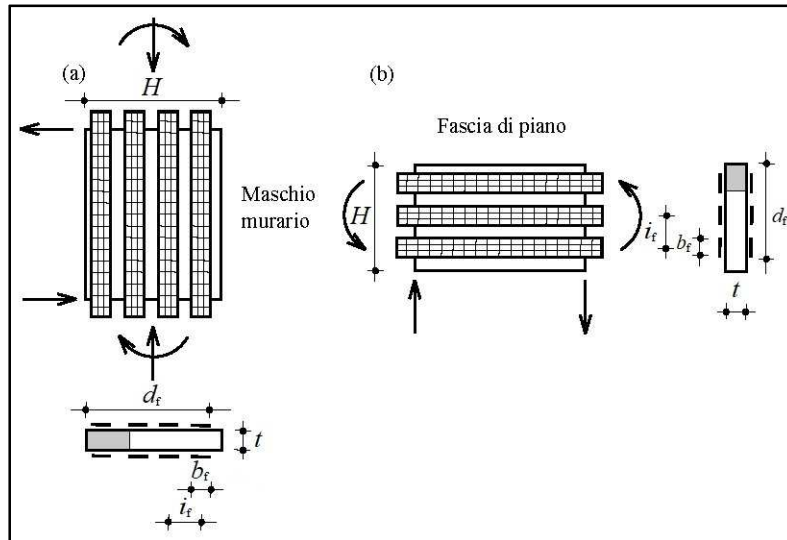


Figure A1.3 – In-plane panel strengthening with FRCM strips.

13 APPENDIX 2: ASSESSMENT OF SOLIDARITY BETWEEN REINFORCEMENT AND STRUCTURE IN THE CASE OF CURVED SUPPORT

The capacity assessment of the reinforcement under the applied loads, when the reinforcement is applied to a concave structural element (Figure A2.1.a), is based on the equilibrium of an arch reinforcement element (Figure A2.1.b).

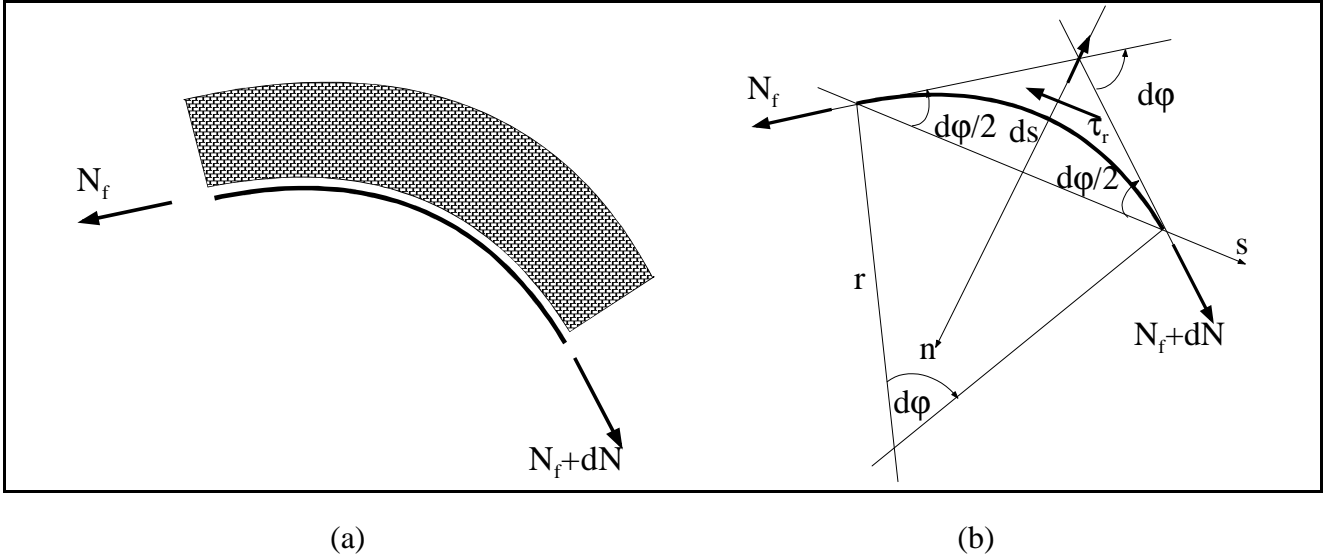


Figure A2.1- (a) Intrados reinforcement; (b) Equilibrium pattern of reinforcement.

With reference to a curved surface, it is noted that, due to the curvature, in addition to a longitudinal interaction between reinforcement and support, a radial tension is also created orthogonal to the connection surface (*bond surface*) and therefore it results in a (variable) traction at the interface between the curvilinear reinforcement and the support deriving from the combined effect of normal and shear stress.

Therefore, the mechanism associated to the rupture (debonding) due to the combined effect of the normal stress with curvature and of the variable normal stress in the curvilinear FRCM reinforcement has to be verified.

With reference to Figure A2.1b, for the generic curvilinear elementary segment of length ds , the conditions of radial equilibrium are expressed, along the secant direction "s" (parallel to the chord subtended by the mean line):

$$-N \cos \frac{d\varphi}{2} - \tau ds + (N + dN) \cos \frac{d\varphi}{2} = 0,$$

and along the direction "n" orthogonal (to the chord subtended by the mean line):

$$-N \sin \frac{d\varphi}{2} + \sigma ds - (N + dN) \sin \frac{d\varphi}{2} = 0.$$

Considering the infinitesimal size of the curvature angle relevant to the element ($d\varphi \ll 1$), it is:

$$\begin{cases} -N \cos \frac{d\varphi}{2} - \tau ds + (N + dN) \cos \frac{d\varphi}{2} = 0 \\ \tau ds = dN \end{cases}$$

$$\begin{cases} -N \sin \frac{d\varphi}{2} + \sigma ds - (N + dN) \sin \frac{d\varphi}{2} = 0 \\ -Nd\varphi - dN \frac{d\varphi}{2} + \sigma ds = 0 \\ -Nd\varphi + \sigma ds = 0 \end{cases}$$

Finally, the interface between the reinforcement and the masonry element will be subject to a longitudinal shear action τ_r and to an orthogonal release action σ_r :

$$\begin{cases} \sigma_r = \frac{1}{b} N_f \frac{d\varphi}{ds} = \frac{N_f}{br} \\ \tau_r = \frac{1}{b} \frac{dN}{ds} \end{cases} \quad (\text{A2.1})$$

where b is the width of the reinforcement, r represents the radius of curvature and N_f is the force applied on the filaments of the reinforcement under the considered load condition, inferred from the overall equilibrium of the structural system.

Combining normal and shear stresses (Figure A2.2):

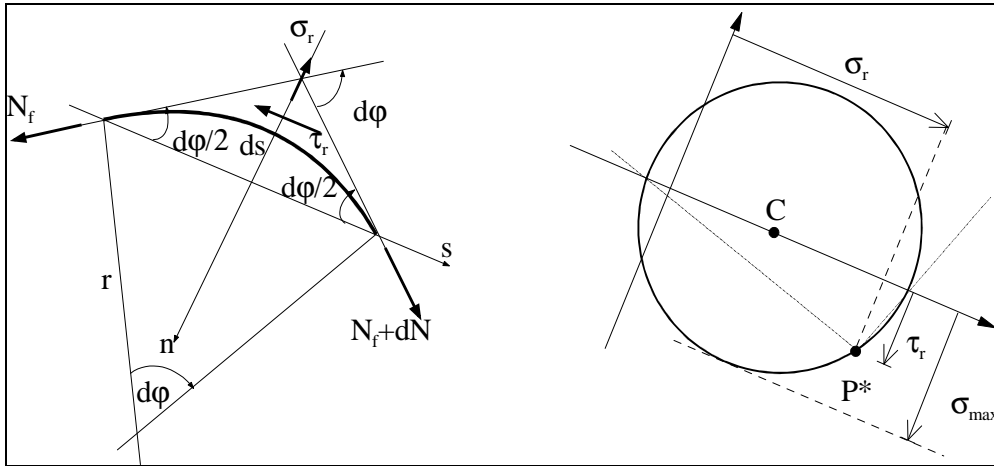


Figure A2.2 - Shear stress τ_r combined with normal stress σ_r .

it is:

$$\sigma_{\max} = \frac{\sigma_r}{2} + \sqrt{\frac{\sigma_r^2}{4} + \tau^2} \quad (\text{A2.2})$$

and it shall be verified that:

$$\sigma_{\max} \leq \frac{\sigma_{rt}}{\gamma_{rt}}, \quad (\text{A2.3})$$

where σ_{rt} represents the minimum tensile strength between the corresponding characteristic values of the matrix and of the support, and γ_{rt} is the partial factor defined in paragraph 4.5.

If by contrast the reinforcement is applied to the extrados (convex arch element), the component σ_r (which in this case would result in compression and therefore not destabilizing) can be neglected, and therefore the verification can be performed in the following terms:

$$\tau_r \leq \frac{\sigma_{rt}}{\gamma_{rt}}. \quad (\text{A2.4})$$